MASTER COPY KEEP THIS COPY FOR REPRODUCTION PURPOSES

REPORT DOCUMENTATION PAGE

Form Approved
OMB No. 0704-0188

1. AGENCY USE ONLY (Leave blank)	2. REPORT DATE	3. REPORT TYPE AND DATES COVERED
	May 1996	Final 1 Sep 95 - 31 Aug 96

4. TITLE AND SUBTITLE

Fourth International Workshop on Computational Electronics

5. FUNDING NUMBERS

DAAH04-95-1-0501

6. AUTHOR(S)

David K. Ferry (principal investigator)

7. PERFORMING ORGANIZATION NAME(S) AND ADDRESS(ES)

Arizona State University
Tempe, AZ 85281

8. PERFORMING ORGANIZATION REPORT NUMBER

9. SPONSORING / MONITORING AGENCY NAME(S) AND ADDRESS(ES)

U.S. Army Research Office
P.O. Box 12211
Research Triangle Park, NC 27709-2211

10. SPONSORING / MONITORING AGENCY REPORT NUMBER

ARO 34525.1-EL-CF

11. SUPPLEMENTARY NOTES

The views, opinions and/or findings contained in this report are those of the author(s) and should not be construed as an official Department of the Army position, policy, or decision, unless so designated by other documentation.

12a. DISTRIBUTION / AVAILABILITY STATEMENT

Approved for public release; distribution unlimited.

12b. DISTRIBUTION CODE

13. ABSTRACT *(Maximum 200 words)*

The International Workshop on Computational Electronics was held in Tempe, Arizona, on October 30 - November 2, 1995.

The workshop is intended to be an international forum for the discussion of the current trends and the future directions of computational electronics. The IWCE attempts to bring together engineers, physicists, computational scientists, and applied mathematicians in the area of simulation and modeling.

14. SUBJECT TERMS

15. NUMBER OF PAGES

16. PRICE CODE

17. SECURITY CLASSIFICATION OF REPORT	18. SECURITY CLASSIFICATION OF THIS PAGE	19. SECURITY CLASSIFICATION OF ABSTRACT	20. LIMITATION OF ABSTRACT
UNCLASSIFIED	UNCLASSIFIED	UNCLASSIFIED	UL

DISCLAIMER NOTICE

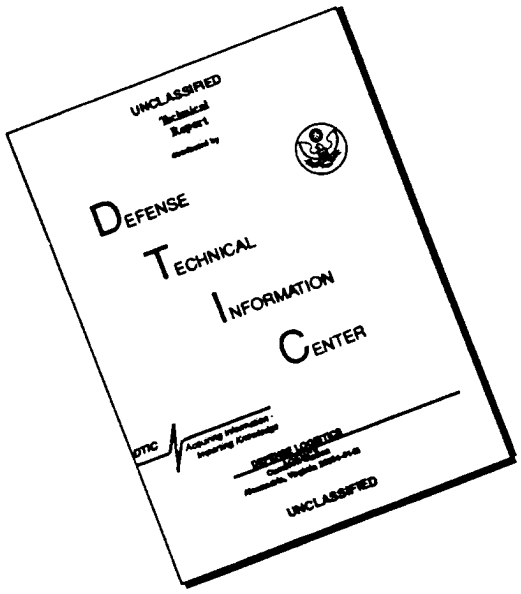

THIS DOCUMENT IS BEST QUALITY AVAILABLE. THE COPY FURNISHED TO DTIC CONTAINED A SIGNIFICANT NUMBER OF PAGES WHICH DO NOT REPRODUCE LEGIBLY.

Final Report

Fourth International Workshop on Computational Electronics

30 October - 2 November 1995

Supported by

National Science Foundation
Office of Naval Research
Army Research Office

The International Workshop on Computational Electronics was held in Tempe, Arizona, on October 30 - November 2, 1995. This workshop was the fourth in a series and was held under the auspices of the *National Center for Computational Electronics* at the University of Illinois (K. Hess, Director). Previous conferences have been held in Urbana, Leeds (UK), and Portland. In general, the series of workshops covers all aspects of advanced simulation and modeling of electronic transport in semiconductors and semiconductor devices, particularly those aspects that utilize intensive computational and/or visualization resources.

The workshop is intended to be an international forum for the discussion of the current trends and the future directions of computational electronics. The IWCE attempts to bring together engineers, physicists, computational scientists, and applied mathematicians in the area of simulation and modeling. The major topics of this past year's workshop continued to be:

- Advances in two- and three-dimensional simulations utilizing standard techniques such as drift-diffusion and hydrodynamic equations.
- Particle simulation methods such as ensemble Monte Carlo, molecular dynamics, and cellular automata.
- Simulation of optical processes, optoelectronic and electro-optic devices which e.g. need the incorporation of Maxwell's equations.\
- Quantum transport and quantum devices.
- High performance computing techniques for computational electronics, including parallelization, vectorization, and improved numerical algorithms.

A major subsidiary theme for this past year's workshop was *process modeling and simulation*. To accentuate this theme, a special session was held with several invited papers addressing this topic. This focused upon both feature-scale and reactor-scale process modeling and simulation.

Site

The IWCE was held at the Radisson Tempe Mission Palms Hotel in downtown Tempe, Arizona. This hotel is a few minutes walk from Arizona State University, and is only a few minutes from Phoenix's Sky Harbor International Airport.

Program/Organizing Committee

The Program and Organizing Committee was composed of internationally known scientists in the disciplinary areas covered by the conference. This year's committee is:

- David K. Ferry, Arizona State University, Chair
- Karl Hess, University of Illinois, Director, NCCE
- Chris Ringhofer, Arizona State University, Local Arrangements
- Carl Gardner, Arizona State University, Publications
- Robert Dutton, Stanford University
- Massimo Fischetti, IBM Watson Research Center
- Stephen Goodnick, Oregon State University
- Chihiro Hamaguchi, Osaka University

- Joseph Jerome, Northwestern University
- Peter Markowich, University of Berlin
- Hiroshi Mizuta, Hitachi Central Research Lab.
- Massimo Rudan, Bologna University
- R. Kent Smith, A.T.&T. Bell Laboratories
- Chris Snowden, Leeds University

In addition to the Program/Organizing Committee, the IWCE benefits from the guidance and insight of an international advisory committee, which is composed of:

- Herb Bennett, National Institutes of Science and Technology
- Larry Cooper, Office of Naval Research
- William Coughran, A.T.&T. Bell Laboratories
- Wolfgang Fichtner, ETH, Zurich
- William Frensley, University of Texas at Dallas
- M. Fukuma, NEC Corporation
- Harold Grubin, SRA, Inc.
- Gerald Iafrate, Army Research Office
- Thomas Kerkhoven, University of Illinois
- Steve Laux, IBM Watson Research Center
- Thomas C. McGill, California Institute of Technology
- Mark Pinto, A.T.&T. Bell Laboratories
- Al Tasch, University of Texas

- Peter Vogl, Walter Schottky Institut
- Naoki Yokoyama

Invited Speakers

Approximately 10 invited speakers were selected to preface the major topics described earlier, including the special session on process modeling and simulation. These invited speakers will be drawn from internationally recognized experts in the field, and will help to provide an introduction to the contributed papers in each session.

Student Support

One of the most important aspects of the IWCE is the opportunity for graduate students pursuing research in this area to discuss their work with internationally recognized participants in the workshop. This was aided by approximately 12 student stipends to help defray the cost of attendance at the workshop by the students. The availability of this support was advertised in the second announcement and call for papers, and preference was given to students who presented papers at the workshop.

Proceedings

The proceedings of the 4th IWCE will be published as a regular issue of *VLSI Design*. This will be an issue of approximately 300 pages, as all manuscripts will be contained in a single issue. Papers will be submitted at the beginning of the workshop with regular refereeing occuring during the workshop.

Conference Results

In the following pages, the program of the workshop is presented. That is followed by a list of the attendees to the workshop.

Next Workshop

The Fifth workshop is scheduled for May-June 1997, and will be held at the University of Notre Dame, Notre Dame, Indiana. It will be organized by Prof. Wolfgang Porod.

Program

MA1. Quantum Kinetic Transport under High Electric Fields, *Nobuyuki Sano and Akira Yoshii, N7TLSI Laboratories, 3-1 Morinisato-Wakamiwa, Atsugi-shi, Kanagawa 243-01, Japan.* As the device size continues to shrink, various quantum effects are expected to play an important role in determining the device characteristics. Among others, the dynamical quantum effects such as collisional broadening (CB) and intracollisional field effect (ICFE) inevitably come into play in conventional ultrasmall devices.[1] A clear understanding of these effects usually requires extensive numerical computations and is an indispensable matter from the view point of not only fundamental physics but also of device applications. In the present talk, we will give a brief review of the dynamical quantum effects (CB and ICFE) under high electric fields and show our recent results of Monte Carlo calculations of electron transport for 3-, 2-, and 1-D electron gases. We derive the quantum kinetic (Barker-Ferry) transport equation from the reduced density matrix of electrons by employing the projection operator approach. It is shown that both CB and ICFE are closely related to the finite collision duration time with phonons, i.e., the finite life-time of the electron yields the broadening of the spectral density (CB) and the energy gain (loss) from (to) the external electric field during collision duration skews as well as broadens the spectral density (ICFE). It is also demonstrated that ICFE is insignificant in bulk up to extremely large electric fields (several hundreds kV/cm), whereas it becomes more and more important even under moderate electric field strengths as the dimensionality of the structure is reduced. This is because ICFE is most effective when the momentum transfer of the electron due to the scattering with phonons is directed to the electric field and the momentum transfer is strictly restricted to reduced dimensions in lower dimensional structures. More specifically, in the case of a 1-D rectangular quantum wire in GaAs under the extreme quantum limit, the total electron-phonon scattering rate becomes asymmetric, as shown in Fig. 1, with respect to the direction of the electron propagation. The double peak structure near the threshold energy ($\mathcal{E}$ = 36 meV) for phonon emission is ascribed to the shift of the energy detuning due to ICFE. Namely, when the electron travels in the opposite (same) direction to the electric field, the electron gains (loses) energy from (to) the electric field during collision duration and the phonon energy is effectively reduced (increased). The change of the effective phonon energy is about 4 meV for F = 500 V/cm and even greater than the damping factor (~ 2.5 meV) often assumed for CB.[2] Figure 2 shows the electric field dependence of the drift velocity obtained from the Monte Carlo simulations for T = 300 K. It should be noted that the drift velocity is greatly reduced when ICFE is taken into account in 1-D quantum wires. In short, extensive numerical computations are successfully employed to extract a significance of the dynamical quantum effects in low dimensional electron gases. Especially, ICFE would become crucial in the analyses of electron transport when the dimensionality of the structure comes into play.

---

[1] J. R. Barker and D. K. Ferry, Phys. Rev. Lett. 42, 1779 (1979); L. Reggiani, P. Lugli, and A-P. Jauho, J. Appl. Phys. 64, 3072 (1988).
[2] S. Briggs, B. A. Mason, and J. P. Leburton, Phys. Rev. B 40, 12001 (1989); J. P. Leburton and D. Jovanovic, Semicond. Sci. Technol. 7, B202 (1992).

MA2. A Generalized Tunneling Formula for Quantum Device Modeling, *R. Lake[a], G. Klimeck[b], R. C. Bowen[b], D. Jovanovic[a], P. Sotirelis[a], and W. R.Frensley[b]; [a]Corporate R&D, Texas Instruments Incorporated, Dallas, TX 75235, [b]Eric Jonsson School of Engineering, University of Texas at Dallas, Richardson, TX 75083-0688.* We have developed novel theory and numerical algorithms to create a general purpose quantum device simulator which includes the effects of charging, scattering (alloy disorder, interface roughness, acoustic phonon, and polar optical phonon), and a number of bandstructure models (2, 4, 8, and 10 band with nearest and next nearest neighbor coupling). The most novel and useful invention resulting from this effort is a generalized tunneling formula based on generalized boundary

conditions. Tlle boundary conditions give a unified treatment of emitter quasi-bound states and emitter continuum states, and they treat thermalization amd scattering induced broadening in the leads with no more effort than the standard coherent tunneling approaches [1]. The single-band version of the theory is briefly clescribed in references [2, 3, 4] and single-based numerical results based on the theory are described in references [4, 5]. We will describe both the single-band and multi-band versions of the theory and we will give both single-band and multi-band numerical examples of device simulations using the theory.

[1] D. Landheer and G. C. Aers, Superlattices and Microstructures 7, 17 (1990).

[2] R. Lake, in Proceedings of the Third Internataonal Workshop on Computational Electronics (Portland, OR, May 18-20, 1994), p. 239 .

[3] R. Lake, in Quantum Transport in Ultrasmall Devices, edited by D. K. Ferry, H. L. Grubin, and C. Jacoboni (Plenum Press, New York, 1995), pp. 521-524.

[4] G. Klimeck, R.. Lake, R. C. Bowen, W. R. Frensley, and T. Moise Quantum Device Simulation with a Generalized Tunneling Formula, (preprint, April 1995) .

[5] G. Klimeck, R. Lake, R. C. Bowen, W. R. Frensley, and D. Blanks, in the 1995 53rd Annual Device Research Conference Digest, p. 52, Charlottesville, VA, June 19-21, 1995.

MA3. Monte Carlo Simulation of HEMT Using Self-Consistent Method, *H. Ueno, S.Yamakawa and C. Hamaguchi, Dept. of Electronic Engineering, Faculty of Engineering, Osaka University, Suita City, Osaka 565, Japan; and K. Miyatsuji, Electronics Research Laboratory, Matsushita Electronics Corporation, Takatsuki City, Osaka 569, Japan.*: We report here Monte Carlo simulation of HEMT by using self-consistent method, where the real device structures are taken into account. The electronic states of 2DEG in the channel are calculated by solving Schrödinger equation and Poisson equation self-consistently, by taking the Γ, L and X valleys, where the electrons in the three valleys are assumed to be two-dimensional. The eigen states of 2DEG in the, Γ L and X valleys obtained by self-consistent calculations are used to evaluate the scattering rates. For the scattering of the electrons. we take account of the acoustic phonon, polar optical phonon, intervalley phonon and ionized impurity scatterings, where the nonparabolic energy structures are used. In our previous simulation of HEMT the electric field parallel to channel is treated as uniform, resulting in unnegligible error in drain current of saturation region. In the real device the sheet electron density in the channel is not homogeneous and the electric field along the channel is not uniform, higher near the drain. In the present simulation we take into account of the nonuniformity of the electric field due to the sheet electron density distribution. The electric field at each point of a real device is evaluated by calculating two-dimensional Poisson equation where the distribution of the electrons and the ionized impurities are taken into account. At high electric fields electrons are heated to form hot electrons which behave as three-dimensional electrons rather than 2DEG. In addition hot electrons make real space transfer between the GaAs layer and the AlGaAs barrier. These effects are taken into account by assuming that an electron with energy higher than the barrier after the scattering is three-dimensional. Such a three-dimensional electron is staying in the GaAs layer or is transferred into the AlGaAs layer depending on the wave vector of the electron. Simulation were carried out for a typical HEMT structure with sheet electron density 5 x 10^{11}cm^{-2} and Al content x = 0.3. Obtained results at 300K will be reported.

MA4. The Smooth Effective Potential for the Quantum Hydrodynamic Model, *Carl L. Gardner and Christian Ringhofer, Department of Mathematics,Arizona State University, Tempe, AZ 85287-1804.* An "extended" quantum hydrodynamic (QHD) model, valid for potentials with discontinuities, is derived in the Born approximation to the Bloch equation. The quantum potential appearing in the stress tensor *Pij* and energy density W is valid to all orders of $\hbar^2$ and to first order in βV, and involves both a smoothing integration of the classical potential over space and an averaging integration over temperature. At potential barriers in semiconductors, the new effective stress tensor and energy density are more tractable analytically and numerically than in the original $O(\hbar^2)$ QHD theory. By cancelling the leading singularity in the

classical potential at a barrier and leaving a residual smooth effective potential (with a lower potential height) in the barrier region, the effective stress tensor makes the barrier partially transparent to the particle flow and provides the mechanism for particle tunneling in the QHD model. Numerical comparisons demonstrate excellent agreement between the first three moments of the equilibrium full density matrix and the effective density matrix for the Bloch equation with a barrier potential for $\beta\Delta V \lesssim 1$, and good qualitative agreement for $\beta\Delta V \lesssim 10$. The moments of the $O(\hbar^2)$ density matrix are in severe quantitative and qualitative disagreement with the moments of the full density matrix. Mathematical results on the convergence of our iteration method for solving the Bloch equation and numerical simulations of a resonant tunneling diode comparing solutions of the extended and $O(\hbar^2)$ QHD equations are also presented.

MA5. Quantum Transport Simulation of the DOS Function, Self-Consistent Fields and Mobility in MOS Inversion Layers*, *Dragica Vasileska, Terry Eldrideg@, Paolo Bordone#, and David K. Ferry, Center for Solid State Electronics Research, Arizona State University, Ternpe,Az, 85287-6206.* We propose a simulation of the self-consistent fields and mobility in (100) Si-inversion layers for arbitrary inversion charge densities and temperatures. Green's functions are employed in obtaining the analytic expressions for the broadening of the states, real shift in the subband energies and conductivity. The initial potential energy profile is calculated numerically by a variational approach. The Poisson, Schrödinger and Dyson equation for the retarded Green's functions are solved independently for the corresponding unknowns and the self-consistency is achieved through the outer iterative loop, split up into two parts. First, the Schrödinger and Poisson equations are solved by assuming an ideal density of states (DOS) function. In the second loop, we use the real DOS function. The potential energy profile for the next iteration is calculated by using a combination of fixed- and extrapolated-convergence factor scheme. The exchangecorrelation corrections are calculated by using the density-functional formalism. The wavevectordependent matrix elements for the various scattering mechanisms (surface-roughness scattering, depletion layer and interface/oxide Coulomb scattering, acoustic and non-polar optical phonon scattering) are calculated within the self-consistent Born approximation. Screening is treated within the RPA. The diagonal polanzation function is used in the calculation of the screened matrix elements. The simulation results suggest that the proposed theoretical model gives mobilities which are in very good agreement with the experimental data.

---

* Work supported by the Office of Naval Research
@ McDonnel Douglass Helicopter Systems, 5000 E. McDowell Rd, Mesa, Az, 85215.
# Permanent address: Dipartimento di Fisica ed Instituto Nazionale di Fisica della Materia, Universita di Modena, Via Campi 213/A, 41100 Modena, Italy.

[1] D.K. Ferry, Phys. Rev. B 14, 5364 (1976).
[2] S. Takagi, M. Iwase, and A. Toriumi, IEDM Tech. Dig. 398 (1988).

MA6. Study of Interface Roughness Dependence of Electron Mobility in Si Inversion Layer using Monte Carlo Method, *S. Yamakawa, H. Ueno and C. Hamaguchi, Department of Electronic Engineering, Faculty of Engineering, Osaka University, Suita City, Osaka 565, Japan; K. Masaki, Anan College of Technology, Anan City, Tokashima 744, Japan; K. Miyatsuji, Electronics Research Laboratory, Matsushita Electronics Corporation, Takatsuki City, Osaka 569, Japan; U. Ravaioli, Department of Electrical and Computer Engneering, University of Illinois at Urbana-Champaign, Urbana, IL 61801.* We report the effect of interface roughness scattering on the electron mobility in MOSFET. Mobility of the two-dimensional electron gas (2DEG) in MOSFETs is one of the most important parameters from the viewpoint of device operation. Since a strong gate field results in confinement of electrons at the si/siO_2 interface in a MOSFET, with the formation of a 2DEG, the electron transport in the inversion layer is known to be different from the case of threedimensional carriers in bulk materials. So first we calculate the subband structures by solving Schrodinger equations and Poisson equations self-consistently. Since at strong normal fields the electrons are confined in a narrow region of the conduction channel near the interface, there is

considerable scattering due to roughness of the Si/SiO_2 interface, resulting in a reduction of the effective mobility. Electron mobility in the inversion layer of a MOSFET, formed on the (100) silicon surface, is calculated by using a Monte Carlo approach which takes into account size quantization, acoustic phonon scattering, intervalley phonon scattering and surface roughness scattering. Degeneracy is also considered because it is important at higher normal effective fields (high gate voltages). The main emphasis is placed on the influence of the specific autocovariance function, used to express the surface roughness, on the electron mobility. Here we compare the mobilities obtained using exponential and Gaussian autocovariance functions. It is found that the electron mobility calculated with roughness scattering rates based on the exponential function shows a good agreement with experiments. The effect of screening on the roughness scattering is also discussed.

MA7. Lattice Effects in the Complex Subband Dispersion of 2DEG Semiconductor Waveguide Structures Subject to a Perpendicular Magnetic Field*, *G. Edwards and D. K. Ferry, Center for Solid State Electronics Research, Arizona State University, Tempe, AZ, 85287-6206.* In modeling 2DEG magneto-transport experiments it is important to have knowledge of the electronic states subject to a magnetic field perpendicular to the plane of the 2DEG, and the waveguide confinement potential. The Schrödinger equation including the **B** field and the confinement potential can be solved by a discretization procedure and hence putting the wavefunction 'field' on a lattice. When the lattice constant is much smaller than the Fermi wavelength the lattice model should be able to reproduce the true continuum situation, for states up to the Fermi level. We present numerical results, within the lattice model, for the full edge state (magneto-electric states) complex subband dispersion of a rectangular waveguide, including both the real 'bands' and the complex evanescent 'bands'. The full complex dispersion is needed in treating a heterogeneous structure such as a ballistic cavity or disordered quantum wire, in a **B** field, when a rectangular waveguide section is used as a lead region to inject current. The waveguide states subject to the **B** field can be obtained analytically by perturbation theory or **WKB** theory. At a fairly fine degree of discretization the form of our numerical purely real subband solutions 'agree' well with the analytic real band solutions. However, far from the bandedges, our numerical evanescent solutions can have a different topology to the analytic evanescent solutions. We find that a very fine level of discretization is necessary to describe the evanescent states accurately, deep into the complex dispersion region .

* Work supported by NEDO under the Intemational Joint Research Program 'Nanostructures and Electron Waves Project'.

P1. Simulation of a Single Electron Tunnel Transistor with Inclusion of Inelastic Macroscopic Quantum Tunneling of Charge, *Christoph Wasshuber and Hans Kosina, Institute for Microelectronics, TU-Vienna, Gusshausstrasse 27-29/E360, A-1040 Wien, Austria.* Until now Single Electron Tunnel (SET) devices were simulated by either neglecting macroscopic quantum tunneling of charge (q-MQT) or approximating it. Thus, we simulated a SET transistor with the full non-approximative inclusion of inelastic q-MQT or cotunneling. A Monte Carlo method was used to simulate electrons that tunnel back and forth through the two tunnel junctions of the SET transistor and co-tunnel back and forth through both junctions simultaneously. In the coulomb blockade regime and at low temperature the q-MQT effect dominates the current through the transistor. The thermally agitated normal tunneling is orders of magnitude smaller. Resonances in the I-V characteristic were found. The resonant peaks decrease with increasing temperature. This resonance does not originate from the normal tunnel effect, like in the well known resonant tunneling in double barriers, but from the co-tunnel effect. Thus the simulation shows a new feature of the SET transistor, that can be helpful for particular measurements of, for example, the coulomb energy or related capacitances, or can be exploited in new devices. This resonance is not yet experimentally verified.

P2. Wireless Single-Electron Logic Biased by Alternating Electric Field, *Alexarlder N. Korotkov, Department of Physics, State University of New York at Stony Brook, NY 11794-3800.* Single-electron

effects in systems of small-capacitance tunnel junctions can possibly be used as the physical basis for a new generation of ultradense digital electronics.[1] Logic/memory based on single-electron transistors[1,2] and logic/memory which uses single electrons to represent digital information[1] have been discussed in the literature. In the present work a new type of single-electron logic is proposed.[3] The basic element is a short chain of islands which shows bistable polarization and affects the polarization of neighboring chains. In contrast to previous approaches wires are not used (which is a very favorable feature when considering nanometer-size circuits and possibly molecular structures), and the circuits are biased by an external electric field. The proposed logic has some similarity to circuits suggested for "ground state computing".[4] The principal difference is that we use a conventional dissipative method of switching elements (power is supplied by an alternating electric field) which makes the logic simple, robust, and relatively fast and allows the circuits consisting of arbitrary large number of gates. Monte-Carlo simulation of logic gates, propagation lines, and fan-out circuits for a particular geometry shows parameter margins of about 5%. This number depends on the chosen layout (positions and sizes of conducting islands) and can probably be increased up to 10-15%.

The work was supported by AFOSR and ONR/ARPA.

[1]. D. V. Averin and K. K. Likharev, in: Single Charge Tunneling, ed. by H. Grabert and M. Devoret (Plenum, New York, 1992), p. 311.
[2]. A. N. Korotkov, R. H. Chen, and K. K. Likharev, J. Appl. Phys. 78 (August 15, 1995).
[3] A. N. Korotkov, to be published.
[4]. P. D. Tougaw, C. S. Lent, and W. Porod, J. Appl. Phys. 74, 3558 (1993).

P3. Single-Electron Parametron, *Konstantin K. Likharev and Alexander N. Korotkov, Department of Physics, State University of New York at Stony Brook, NY 11794-3800.* Since 1987, several families of single-electron logic devices have been suggested[1]. In these devices, digital bits are presented by single electrons, which are manipulated using the Coulomb blockade effect. Most of the devices suggested earlier imply the use of long wires for delivery of the power supply to the logic gates. In this work we propose a new type of single-electron logic consisting of three-island elements biased by a rotating electric field which also plays the role of a global clock. At a certain phase of field rotation the cell becomes polarized by the transfer of a single electron from the central island to one of the edge islands. The symmetry of the situation is broken by the electric field created by earlier polarized neighboring cells. The idea is very similar to that used in ac and dc parametrons (see, e.g., Ref. 3 and references therein), so we call our basic cell the single-electron parametron. In contrast to the recently suggested "wireless single-electron logic"[2], the parametron is physically reversible. As a consequence, for example, the shift register based on these cells can dissipate power less than k_BT per element per switching. We have carried out extensive analytical calculations and numerical simulations of the single-electron parametron on both equivalent-circuit and geometrical-model levels. Results for parameter margins, power consumption and operation speed will be presented at the meeting.

The work was supported by AFOSR and ONR/ARPA.

[1]. D. V. Averin and K. K. Likharev, in: Single Charge Tunneling, ed. by H. Grabert and M. Devoret (Plenum, New York, 1992), p. 311.
[2] A. N. Korotkov, to be published.
[3]. K. K. Likharev, IEEE Trans. Magn. 13, 245 (1977).

P4. Parallel Computation for Electronic Waves in Quantum Corrals*, *Henry K. Harburyt and Wolfgang Porod#, University of Notre Dame, 'Science Computing Facilities, #Dept. of Electrical Engineering, Notre Dame, IN 46556.* Recent scanning tunneling microscopy (STM) studies on the (111)

faces of noble metals have directly imaged electronic surface-confined states. Dramatic standing-wave patterns have been observed in geometrically arranged "quantum corral" structures formed by Fe adatoms on Cu(111).[1,2] We solve for the local density of electronic states (LDOS) in these structures using a coherent elastic scattering theory. We seek solutions of the two-dimensional Schrödinger equation compatible with Sommerfeld radiation conditions[3,4] in these "leaky" confinement structures. We present direct comparisons of our calculations to the reported experimental differential conductance STM data which reveal excellent agreement with our elastic scattering theory. We also investigate possible "surface waveguides", similar to split-gate type structures, by modeling a wide-narrow-wide lateral adatom confinement structure for the Cu(111) surface. We implement non-reflecting boundary conditions which asymptotically satisfy the Sommerfeld radiation condition on the boundary using a local method based on the work of Bayliss and coworkers.[3,4] The large matrices generated by the discretization of realistic quantum corral structures require the use of sparse matrix methods. In addition, a parallel finite element solution was undertaken using the message passing interface standard (MPI) and the Portable, Extensible, Toolkit for Scientific Computation (PETSc) [5] for an efficient computational solution on both distributed and shared memory architectures.

This work has been supported by the Office of Naval Research and the Air Force Office of Scientific Research.

[1] M. F.Crommie, C. P. Lutz, and D. M. Eigler, Science 262, 218 (1993).
[2] E. J. Heller, M. F. Crommie, C. P. Lutz, and D. M. Eigler, Nature 369, 464 (1994).
[3] H. K. Harbury, W. Porod, R. K. Smith, Third International Workshop on Computational Electronics, Portland, OR (1994).
[4] A. Bayliss, M. Gunzburger, and E. Turkel, SIAM J. Appl. Math. 42 430 (1982).

P5. A Monte Carlo Study of Electron Transport in Silicon nMOSFET Inversion Layers, *W.-K. Shih, S. Jallepalli, C.-F. Yeap, M. Rashed, C.M. Maziar and A.F. Tasch, Jr., Microelectronics Research Center, The University of Texas at Austin, Austin, TX 78712.* Despite decades of research effort [l] problems associated with carrier transport in the inversion layers of silicon MOSFETs continue to capture the attention of the research community.[2-4] Today's advanced devices introduce further complications with the aggressive scaling of channel length that introduces pronounced non-local effects such as velocity overshoot.[4] In order to investigate and anticipate future device performance issues, simulation tools that rely on physically rather than empirically based models are required. We present here a single-particle Monte Carlo (MC) simulation on uniform silicon nMOSFET inversion layers within and beyond the ohmic regime for various substrate doping levels and gate biases. Inversion layer electrons, whose motion in the transverse direction is confined by the steep band bending in silicon, form a two-dimensional electron gas (2DEG.) Transport of the 2DEG is well described by a two-dimensional multi-subband BTE for the fields typical of the linear region. We obtain the subband structure of the 2DEG by self-consistently solving the effective-mass Schrödinger equation and the Poisson equation within UTMINIMOS [5]. an advanced device simulator that encompasses drift diffusion, hydrodynamic and MC models. The non-parabolic nature of the bulk band structure is included within a first-order perturbation in obtaining the subband structure, using a formalism that builds on the work ol Fischetti et al.[3] Scattering in the 2D system due to phonons and surface roughness is considered using the formalism developed by Price and Cheng [6], respectively, with selection rules for the intervalley phonon processes established by Ferry.[7] Degeneracy is also considered. The universal relationship between the effective mobility and the transverse effective field has been obtained (see Fig. I). Good agreement between the simulated and experimental low-field mobility has been achieved for both 300K and 77K. The simulated results are compared with the experimental work of Takagi [8] at 77K and with the UT mobility model [2] at 300K. The UT mobility model has been well characterized with a large number of devices of varying structures and industrial sources. As such it is used as the best representation of a large body of experimental work. The universal dependence of phonon-limited mobility on E_{eff} is readily observed in Fig. 2. The fractional population and the average mobility of electrons in the lowest primed (2-fold degenerate) and unprimed (4-fold

degenerate) subbands are illustrated in Fig. 3. At high lateral field, the electron drift velocity and energy distribution are illustrated in Figures 4 through 6. The calculated inversion layer saturation velocity is found to be independent of the transverse field and agrees well with experimental data as described by the UT mobility model. With different numbers of subbands included in the simulation, the extracted electron energy distribution indicates the necessity of including either more subbands or a classical simulation domain if the tail of the energy distribution is desired. In summary, we have developed a Monte Carlo simulation tool that accurately reproduces and explains the experimental universal mobility curve and high-field transport characteristics in uniform silicon nMOSFET inversion layers at different temperatures. The MC tool also provides access to important but experimentally unavailable microscopic information.

This work was supported, in part, by the Semiconductor Research Corporation (SRC), thc Texas Advanced Technology Program, Motorola and AMD.

[1] T. Ando et al., Rev. Mod. Phys., vol. 54, p. 437, 1982.
[2] H. Shin et al., Solid State Electron., vol. 34,. 6, p. 545, 1991.
[3] M. V. Fischetti et al., Phys. Rev. B, vol. 48, 4, p. 2244, 1993.
[4] F. Assaderaghi et al., IEDM Tech Dig., p. 479, 1994.
[5] C.-F. Yeap et al., NUPADS V, p. 15-18, 1994. X. L. Wang et. al., J. Appl. Phys., Vol. 73, 7, p.3339, 1993.
[6] P. J. Price. Anls. Phys. vol. 133, p. 217, 198I. Y. C. Cheng, Surf. Sci. vol. 27, p. 663, 1971.
[7] D K. Fcrry, Surf.Sci.,. vol. 57, p. 218, 1976.
[8] S. Takagi, et al.. IEEE Trans. on Elec. Devices, vol. 41,12, p. 2357, 1994.

P6. A Numerical Study of Rare Events in Single Electron Devices, *L. R. C. Fonseca, A. N. Korotkov, and K. K. Likharev; Department of Physics, State Uniuersity of Neun York at Stony Brook, NY 11794-3800.* During the past decade several devices based on correlated tunneling[1] of single electrons have been suggested and tested.[2,3] These devices may be used in various analog and digital systems, in particular as ultradense logic/memory units[1] and as fundamental standards of dc current.[4] However, tools for their computer-aided design which would account for all the most important physical phenomena have not been available until very recently. In my talk I will describe a new algorithm[5] suitable for studies of the dynamics of single electron devices presenting arbitrary combinations of small tunnel junctions, capacitances, and voltage sources. In contrast to Monte-Carlo schemes, the method is useful both to analyse the "classical" behavior of the system and for calculating small deviations from this behavior, due to the finite speed of applied signals, thermal activation, and cotunneling. I will show results from the analysis of errors in memory cells and current deviations in proposed dc current standards.[4] I will also discuss the effect of background charge on the behavior of these devices.

This work was supported by AFOSR, and CNPq-Brazil.

[1] D.V. Averin and K.K. Likharev in,Single Charge Tunnling,. ed. by H. Grabert ancl M. Devoret (Plenum, New York, 1992), p. 311.
[2] J.M. Martinis et al., Phys. Rev. Lett. 72, 904 (1994).
[3] P.D. Dresselhaus et al., Phys. Rev. Lett. 72, 3226 (1994).
[4] H. Pothier et al., Europhys. Lett. 17, 249 (1992).
[5] L.R.C. Fonseca et al., J. Appl. Phys. 79 (September 1, 1995).

P7. New Method for Computing Resonances and Transmission Properties for Quantum Devices, *V. Mandelshtam, T. Ravuri and H. S. Taylor; Department of Chemistry, University of Southern California, Los Angeles, CA 90089-0482.* Two relatively new methods, the Spectral Projection method and the Stabilization Method, of implementing scattering calculations are described, and are here applied to two devices. Both methods use essentially short range spectral projection operators to produce a complete set of solutions of the wave equation that need be valid only inside the interaction region. While the Spectral

Projection method is more generic than the Stabilization Method which is based on using the more difficult to compute spectral density operator, the latter becomes very efficient when narrow resonances exist. For problems of small size methods are practical in the sense that they involve only real, symmetric matrices resulting from Hamiltonians represented on £^{2} basis sets. For more challenging larger systems the Spectral Projection method lends itself to a very efficient time independent iterative procedure that obtains transmission results simultaneously at all energies. This procedure uses modified Chebyshev recursion relations to essentially expand the operator $\left(E-\hat{H}+\hat{\Gamma}\right)^{-1}$, where $\hat{\Gamma}$ is an absorbing optical potential that eliminates the need for large grids. This latter procedure requires minimal storage and the resulting series converges rapidly in a manner that is uniform in energy. For small systems resonances can be computed directly using stabilization. "Directly" means no S matrix or transmission coefficient is needed. For large systems the modified Chebyshev version of the spectral projection operator can be used to create a basis with which $\hat{H}+\hat{\Gamma}$ can be represented and diagonalized to yield a direct calculation of resonance energies. Large problems requiring up to several hundred thousand functions or grid points can be treated using this method.

P8. Quantum Contributions and Violations of the Classical Law of Mass Action, *H L. Grubin and T. R. Govindan; Scientific Research Associates, Inc., Glastonbury, Connecticut..* The law of mass action refers to the product of the concentration of reactants, where for a particular material the product is a function of temperature only. In the case of nondegenerate semiconductors this is represented by the product of electrons and holes:
$NP=N_i^2=N_cN_v exp\text{-}E_G/k_BT$. For degenerate material *NP* is a function of concentration as well as temperature. Since the work of Wigner it has been known that when there are strong concentration gradients the carrier density is no longer given by a simple Boltzmann like distribution. As discussed by Ancona and Iafrate, for non-degenerate semiconductors the density may be approximated by $N = N_c \exp^{-}\left[E_c(x)+(\hbar^2/6m)\nabla^2\sqrt{N}/\sqrt{N}\right]/k_BT$ where we have incorporated the quantum potential in the exponential. The quantum modification of the density suggests that the product of *NP* under thermodynamic equilibrium would depend on features other than temperature. Certainly this would be expected at heterostructure interfaces, even if effective mass variations are ignored. The question addressed in this paper is: **are significant variations in the product** *NP* to be expected in ostensibly classical structures such as a bipolar transistor. To answer this question we have solved the quantum Liouville equation (avoiding the use of the quantum potential): $i\hbar\frac{d\rho_{op}(t)}{dt}=\left[H(t),\rho_{op}(t)\right]$ under conditions of thermodynamic equilibrium. The equation was coupled to Poisson's equation and solved in the coordinate representation for two generically nondegenerate *classical* structures: *NIN* and *NPN* devices, where in all cases the I and P regions were each 50 nm in length. Devices of 200 nm and 400 nm were considered. Several calculations were performed for parameters appropriate to GaAs; parametric studies were also performed. In these studies the *N* region was doped to $10^{24}/m^3$, (which is too high to strictly satisfy the nondegeneracy condition). Calculations at lower densities will be discussed at the meeting. For the approximations and assumptions made, the results for the *NIN structures, were ordinary;* the departures from the law of mass action were negligible. However, for the *NPN* structures, *the results were extraordinary.* Even modest values of P (near $10^{24}/ m^3$) resulted in two orders of magnitude departures from the mass action law. These results which are quite new suggest that the use of the law of mass action, one of the most frequently used relationships in the design of devices needs to be re-examined. This issue will be addressed at the conference.

This work is supported by ONR & ARO.

P9. One-Dimensional Analysis of Subthreshold Characteristics of SOI-MOSFET Considering Quantum Mechanical Effects, *Rimon Ikeno, Hiroshi Ito & Kunihiro Asada, Dept. of Electronic Eng.,*

Fac. of Engineering, The University of Tokyo, 7-3-1 Hongo, Bunkyo-ku, Tokyo 113, Japan. We have been studying on substrate bias dependence of subthreshold characteristics of SOI MOSFETs. We have simulated subthreshold characteristics by solving simple 1-D Poisson's equation on SOI multi-layer structure (fig.1) and estimated the structural parameters of real devices. Here, we considered quantum mechanical effects in electron inversion layer of thin SOI MOSIFET, implementing self-consistent solver of Poisson and Schrödinger equation in the 1-D subthreshold simulator. Figure 2 shows an example of quantum mechanical results of band diagrams with electron distribution probability plots in SOI layer. In this case, structural device parameters are: T_{fox}=7nm,T_{sol}=30nm~~ T_{box}= 80nm and N_A=1.5 x $10^{17}cm^{-3}$. Figure 3 and 4 show simulation results of subthreshold I_d-V_{gs} characteristics of SOI MOSFET for 2-D, 1-D and 1-D with quantum mechanical effects. Here L is channel length and V_{BS} is substrate bias as parameters. Classical 2-D and 1-D curves show good agreement in subthreshold region in long devices, though they show discrepancy because of absence of drift term from 1-D simulation model. Classical and quantum simulation show a considerable amount of difference, which proves that quantum mechanical analysis estimates higher threshold voltage than the classical analysis. We calculated V_{th}-V_{gs} characteristics of SOI MOSFET (V_{th}(@I_d=l0nA/L=W=100μm), with classical and quantum mechanical simulator. Figure 5 shows the calculated curves with measured data. Device parameters used in each simulation are shown in table 1, with designed device parameters of real device. Those results indicate that quantum mechanical effects must be considered to obtain a good agreement with experimental data, based on the reasonable device parameters in thin SOI devices.

P10. Total Dielectric Function Approach to the Electron Boltzmann Equation for Scattering from a Coupled Mode System, *B.A. Sanborn, Arizona State University, Center for Solid State Electronics Research, Tempe, AZ 85287-6206.* The total dielectric function $\varepsilon_T(q,\omega)$lends itself to a simple and general rnethod for deriving the inelastic collision term in the electron Boltzmann equation for scattering from a coupled mode system.[1] Useful applications include scattering from plasmon-polar phonon hybrid modes in rnodulation doped semiconductor structures. In the Born approximation, the inelastic differential scattering rate W^{inel} can be expressed in terms of the *nonequilibri*um) $\varepsilon_T(q,\omega)$, including both electronic and ionic contributions. Within the random-phase approximation W^{inel} separates into an electron-electron interaction and an electron-phonon interaction including the phonon self-energy due to polarization of the electrons. The self-energy modifies phonon dispersion, so that hybrid modes appear in the electron-phonon collision term. An iterative method will be deseribed for exactly solving the Boltzmann equation for low fields including dynamically screened electron electron scattering and plasmonphonon coupling. Numerical results for mobility in n-type GaAs show that inelastic scattering from the coupled electron-phonon system dominates over acoustic mode scattering at 77 K for moderate doping, if mode coupling and electronelectron scattering are included.[2] New results to be presented include an investigation of electron scattering from coupled intrasubband-intersubband electronic excitations in modulation doped quantum wells.

---

[1] B.A. Sanborn, Phys. Rev. B 51, 14247 (1995).
[2] B.A. Sanborn, Phys. Rev. B 51, 14256 (1995).

P11. A Study of Transconductance Degradation in HEMT Using a Self-Consistent Boltzmann-Poisson-Schrödinger Solver, *R. Khoie, Department of Electrical and Computer Engineering, University of Nevada, Las Vegas, Las Vegas, NV 89154.* Recent advances in III-V compound semiconductor growth techniques have pushed the cutoff frequency of high electron mobility transistors well into the 300 GHz range. Nguyen, et. al. [1] have reported design and fabrication of a 50-nm self-aligned-gate pseudomorphic AlInAs/GaInAs HEMT with a maximum transconductance of 1740 mS/mm and a cutoff frequency of 340 GHz. These impressive high-frequency parameters have been measured at very low gate bias voltages. In fact, as the gate bias voltage of the device is increased, both transconductance and the cut-off frequency of the device start decreasing rather sharply, as shown in Fig. 1.[1]-[2] Similar results have been reported by others.[3][4] The high transconductance in HEMT devices is obtained mainly by scaling down the channel

length of the device to 500A°.[5]-[6] Further reduction in the gate length results in degradation of the transconductance and decrease in the cut-off frequency. Kizilyalli, et. al.[7] have performed a Monte Carlo study of short channel effects in a submicrometer AlGaAs/GaAs HEMT, and suggested that the high-frequency performance of the device can be improved by scaling the gate length down to a minimum of about 0.1 μm, beyond which the device transconductance is degraded rather rapidly. They discussed reasons for observed degradation of the transconductance of ultra-small gate length HEMT's, citing poor charge control in the channel, and sharp reduction in the output resistance of the device as the main sources of transconductance degradation. We previously reported a *two-subband self-consistent Boltzmann-Poisson-Schrödinger* solver for high electron mobility transistor in which we self-consistently solved the two higher moments of Boltzmann equation, along with Poisson and Schrödinger equations.[8] We further incorporated an additional self-consistency by calculating field-dependent, energy-dependent intersubband and intrasubband scattering rates due to ionized impurities and polar optical phonons. In this work, we have used our Boltzmann-Poisson-Schrödinger solver and studied the effects of the intersubband and intrasubband scatterings of electrons, on the transconductance of a single quantum well HEMT device. The results of our simulations (shown in Fig. 2) exhibit the same pattern reported by [1] and [2]. The transconductance increases with gate voltage at low gate voltages, and then decreases as the gate voltage is further increased. Without the energy-dependent field-dependent scattering rates, the transconductance decreases linearly with increasing gate voltage. We concluded that the degradation of transconductance of the device with applied gate bias is attributed to the intersubband and intrasubband scattering mechanisms due to polar-optical phonons and ionized impurities.

[1] L.D. Nguyen, et al., IEEE Trans. on Electron Devices, Vol. 39, 9, pp. 1007-2014, 1992.
[2] Y.H. Wang, et al., Solid State Electronics, Vol. 37, 2, pp. 237-241, 1994.
[3] R. Plana, et al., IEEE Trans. on Electron Devices, Vol. 40, 5, pp. 852-858, 1993.
[4] S.K. Sargood, et al., IEEE J. of Quantum Electronics, Vol. QE-29, pp. 136-149, 1993.
[5] J.K. Abrokwah, et al., IEEE Trans. on Electron Devices, Vol. 40, pp. 278-284, 1993.
[6] Y. Zhao, et al., IEEE Trans. on Electron Devices, Vol. 40, 1067-1070, 1993.
[7] I.C. Kizilyalli, et al., IEEE Trans. on Electron Devices, Vol. 40, 4, pp. 234-249, 1993.
[8] R. Khoie, et al., Proceedings of the International Workshop on Computational Electronics, Edited by K. Hess, U. Ravioli, and R. Dutton, pp. 181-184, 1992.

P12. Advanced Macroscopic Device Simulation of InGaAs/InP Based Avalanche Photodiodes, *Joseph Parks and Kevin F. Brennan, School of Electrical and Computer Engineering, Georgia Tech, Atlanta, GA 30332--0250; and Larry Tarof, Bell Northern Research, P.O. Box 3511 Station C, Ottawa, Canada, K1Y4H7.* In this paper, we analyze, based on two-dimensional drift-diffusion and hydrodynamic simulations, how variations in the structural components of an InGaAs/InP separate absorption, grading, charge, and multiplication avalanche photodiode alter the device performance. The model is employed in conjunction with experimental measurements to enhance the understanding of the device performance. Excellent agreement between the calculated results and experimental measurements of the breakdown voltage, dark current, mesa punch-through voltage, photoresponse and gain are obtained. We examine specifically how variations in the doping concentrations, doping profiles, and layer thicknesses alter the device terminal characterisitics. In this way, the model can be used to predict how processing variations influence the overall workings of advanced, state-of-the-art avalanche photodiodes.

PL1. Self-Consistent Scattering Calculation of Resonant Tunneling Diode Characteristics, *J.P. Sun and G.I. Haddad, Center for High Frequency Microelectronics, Dept. of Electrical Engineering and Computer Science, University of Michigan, Ann Arbor, MI. 48109-2122.* We perform a self-consistent calculation of resonant tunneling diode (RTD) I-V characteristics including optical phonon scattering. The self-consistency is botained by solving the Schrödinger equation and Poisson's equation iteratively with the Thomas-Fermi approximation used for the device contact regions. For evaluation of phonon-assisted current density, the optical phonon scattering in the quantum well is modeled using the optical model potential. The calculated transmissions and electron wavefunctions illustrate the optical model and effects

of the phonon scattering on the current transport. The I-V characteristics we obtain from the model calculation are in good agreement with experimental results. This work manifests the importance of including both self-consistency and optical phonon scattering in modeling realistic RTD structures.

PL2. Microscopic Theory for Transconductivity, *A.-P. Jauho[a],M. Bonsager[a], K. Flensberg[a,b], B. Y.-K. Hu[a], and J. Kinaret[c], [a]MIC, Technical University of Denmark, DK-2800 Lyngby, Denmark; [b]DFM, A. Engelundsvej 1, DK-2800 Lyngby, Denmark (permanent address); [c]Chalmers University of Technology, Goteborg, S-41296 Sweden.* Measurements of momentum transfer between two closely spaced mesoscopic electronic systems, which couple via Coulomb interaction but where tunneling is inhibited, have proven to be a fruitful method of extracting information about interactions in mesoscopic systems.[1] Theoretical analyses reported so far have been based on the semiclassical Boltzmann theory [2], memory functions [3], or momentum balance equations.[4] None of these methods possesses the full rigor of a diagrammatic Green function theory, and inclusion of higher order interaction terms necessarily involves some phenomenology. We report a fully microscopic theory for transconductivity σ_{12} , or, equivalently, momentum transfer rate between the system constituents. Our main formal result expresses the transconductivity in terms of two fluctuation diagrams, which are topologically related, but not equivalent to, the Azlamazov-Larkin and Maki-Thompson diagrams known for superconductivity. We have evaluated the general expression in a number of special cases. Our new results include: (i) Semiclassical clean limit, when Boltzmann results [2] are recovered; (ii) Dirty systems with a constant relaxation time, which reproduces the memory function results [3], however, for energy dependent relaxation times the final result is not expressible in terms of standard density-response functions, and the recently reported plasmon enhancement of the drag rate [5] reflects the details of the underlying scattering mechanisms; (iii) At $T = 0$ the frequency dependent transfer rate can be computed; (iv) Weak localization corrections can be evaluated, and we find that $\Delta\sigma_{12}^{WL}\alpha\Delta\sigma_1^{WL} + \Delta\sigma_2^{WL}$; (v) The magnetic field dependence of σ_{12} is computed, and we can prove previous conjectures that in the clean limit the density-response function can be replaced by its magnetic-field dependent generalization. $\sigma_{12}(B)$ is strongly enhanced over its zero field value, and it displays strong features, which can be understood in terms of a competition between density-of-states and screening effects.

[1] T.-J. Gramila, et al., Phys Rev. Lett. Vol. 66, 1216 (1991).
[2] A.-P. Jauho and H. Smith, Phys. Rev. B, Vol. 47, 4420 (1993).
[3] L. Zheng and A.H. MacDonald, Phys. Rev. B, Vol. 48, 8203 (1993).
[4] H.C. Tso, et al., Phys. Rev. Lett. Vol. 68, 2516 (1992).
[5] K. Flensberg and B. Y.-K. Hu, Phys. Rev. Lett, Vol. 73, 3572 (1994).

P13. Beating in the RHEED Intensity Oscillations During Surfactant Mediated GaAs Molecular Beam Epitaxy: Process Physics and Modeling, *Vamsee K.Pamula and R.Venkatasubramanian, Department of Electrical and Computer Engineering, University of Nevada, Las Vegas. Las Vegas, NV 89154.* In a recent work, it was shown that beating in the reflection high energy electron diffraction (RHEED) intensity oscillations can be obtained during MBE growth of *GaAs* when the surfactant, *Sn is* employed.[1] It is also observed that the strength of beating is dependent on the *Sn* monolayer coverage [1] with strong beating observed for 0.4 monolayer coverage of *Sn.* Moreover, the period of oscillation decreases with *Sn* coverage even though the actual growth rate measured by high resolution transmission electron spectroscopy is the same. The origin of these oscillations and its dependence on *Sn* coverage have not been fully explained. In this work, we have developed a rate equation model of growth allowing elementary kinetic processes such as adsorption and migration. In the adsorption model, two types of possibilities are considered depending on the surface of adsorption, i.e., *GaAs* and *Sn.* In addition to the normal adsorption process considered for the *GaAs* surface, the *Ga* atoms arriving on the *Sn* surface are allowed to incorporate by direct exchange process, the area covered by the *Sn is* assumed to grow at a slower rate compared to the rest of the area. Results of RHEED intensity are computed as a function of time based on the kinematic theory of diffraction assuming that the electron beams reflected from the *Sn*

covered area and the rest of the area are incoherent. This is justified if the *Sn* island size is comparable to the coherent length of the electron beam. The results of RHEED intensity oscillations for various monolaver coverages of *Sn* were obtained for substrate temperature of 600°C and compared with experimental data.[1] The agreement is excellent suggesting that the proposed model of growth is a plausible one for *Sn* mediated *GaAs* MBE growth.

---

[1] G.S.Petrich, A.M.Dabiran, J.E.MacDonald and P.I.Cohen, J.Vac.Sci.Technol., B 9, pp 2150-2153, (1991).

P14. Plasma Process Modelin for Integrated Circuits Manufacturing, *M. Meyyappan and T. R. Govindan, Scientific Research Associates, P. O. Box 1058, Glastonbury, CT 06033.* Plasma processing of semiconductors is widely used in integrated circuits (IC) manufacturing; plasma based deposition of dielectrics and etching are two key steps in device fabrication. At the microscopic level, prediction of deposition and etch profile shapes is of much importance. There are several programs such as EVOLVE and SPEEDIE to address these needs. These programs need information on neutral and ionic species flux, ion energy, etc. In order to obtain such data, one needs to model the process at the reactor level. The reactor level model also provides other valuable information on deposition/etch rates and uniformity across the wafer. In this work we discuss the reactor model development work at SRA. The reactor model consists of discharge physics, chemistry, fluid flow and heat transfer. We solve the governing species conservation equations for neutral and ionic species, flow and energy equations in a complex manner. Homogenous and heterogenous chemistry are included. Our code includes discharge physics and power coupling modules suitable for rf capacitively coupled reactors and high density ECR and ICP reactors. Plasma reactor simulations in two-dimensions are computationally intensive due to the coupling of physics and chemistry and the large number of species. Therefore, we have also developed a 0-d model (well-mixed reactor model) and a 1-d model (in the flow direction). These lower order models take much less computer time than 2-d simulations and provide valuable information (except on uniformity issues) for use with Eopographic simulation codes. Results from these three codes are discussed and compared.

MP1. Derivation of an Energy-Transport Model from the Boltzmann Equation, *P. Degond and N. Ben Abdallah, MIP, (CNRS UMR 9974), University of Toulouse.* An energy-transport model is rigorously derived from the Boltzmann Transport Equation of semiconductors under the hypothesis that the energy gain or loss of the electrons by the phonon collisions is weak. Retaining at leading order electron-electron collisions and elastic collisions (i.e., impurity scattering and the "elastic part" of phonon collisions), a rigorous diffusion limit of the Boltzmann equation can be carried over, which leads to a set of diffusion equations for the electron density and temperature. The derivation is given in both the degenerate and non-degenerate case.

MP2. Topologically Rectangular Grids in the Parallel Simulation of Semiconductor Devices, *A. Asenov*, A.R. Brown, S. Roy, and J.R. Barker, Department of Electronics and Electrical Engineering, University of Glasgow, Glasgow, G12 8QQ, Scotland, UK.* Topologically rectangular two (2D) and three dimensional (3D) grids are particularly attractive for the parallel simulation of semiconductor devices, because they can be easily partitioned onto processor arrays, enhancing the scalability and portability of code. Cartesian finite difference grids are inherently topologically rectangular, preserving the number of nodes along the horizontal and vertical grid lines. However, topologically rectangular finite element grids can also be designed for a wide range of simulation problems. Fig. 1 represents an example of a 3D topologically rectangular grid based on distorted bricks, used for the triangulation of a spherical solution domain. Such a grid preserves the number of condensation points in each one of the three index directions i,j,k as in a Cartesian 3D grid. The spherical solution domain can be mapped into a cube by isoparametric transformations mapping each of the distorted bricks into unit cubes. There are significant advantages in speed-up and efficiency when such topologically rectangular grids are partitioned on mesh connected arrays of processors instead of on pipelines. For 3D grids this is illustrated in Fig. 2 where the speed-up of

a linear equation solver is shown as a function of problem size for a pipeline, 2D and 3D array of processors. This figure, based on detailed performance theory [1], also shows some of the problems arising from the 'naive' rectilinear partitioning of the grid. Here we report on the different aspects of the implementation of topologically rectangular grids in the simulation of semiconductor devices. As an illustration we will use the the finite element 3D simulation of cellular power IGBTs. The schematic view of an individual cell of an IGBT is illustrated in Fig. 3. The complex shape and the doping distribution in the device requires a 3D finite element discretization. This, together with the computational complexity in the simulation of power devices, makes the problem a distinguished candidate for parallel processing. We use spatial decomposition of the simulation domain over arrays of processors. The basic idea of decomposing a 3D device over a 2D array of processors is illustrated in Fig.4. Compared to the most frequently used pipeline, the use of a 2D array of processors minimises the inter-processor communications by reducing the ratio between the bulk and the surface of the partition subdomains. A universal communication harness, designed in PARIX, provides all necessary global and local communications and improves the portability of our approach. A generalised approach to the generation of topologically rectangular grids has been developed. In the IGBT case, because of the symmetry only one quarter of the device has been discretized. The grid conforms to the shape of the gate and the metallurgical *pn* junctions. Fig. 5 illustrates the top view of the IGBT grid and its partition over a 3x3 array of processors. A simulated annealing procedure is further used to optimise the grid partitioning. The final partitioning after the annealing is illustrated in Fig.6. For parallel matrix generation and assembly we use a node based procedure. The partition sub-domain is scanned node by node. For all elements which condense in a given node only the contributions to this particular node are calculated. This leads to almost 100% efficiency when the numbers of grid points are equal in each partition sub-domain (Fig.7). A Coloured One Step Block Newton-SOR scheme has been adopted for the Poisson equation. As an example the electric field distribution in an example IGBT simulation is given in Fig. 8. The applied voltages are V_G = 0V and V_A = 600V, respectively.

---

[1] Asenov, A., et al. Speed-up of scalable iterative linear solvers implemented on array of transputers, Parallel Computing, 21, (1995) 669-682.

MP3. Moment Closure Hierarchies from Kinetic Theories, *C. David Levermore, Department of Mathematics, University of Arizona, Tucson, AZ 85721.* We seek models that properly capture the macroscopic regime when the mean free path is much smaller than the macroscopic length scales, while in the transition regime give values for physical fluxes (and other quantities) that are hopefully of the correct order of magnitude, and are at least consistent with the nonnegativity of the particle density. By doing so, such models may provide a bridge over the transition regime that may be useful in the construction of hybrid macroscopic/kinetic simulations. This paper presents a systematic *nonperturbative* derivation of a hierarchy of closed systems of moment equations corresponding to any classical kinetic theory. In the context of gas dynamics the first member of the hierarchy is the Euler system, which is based on Maxwellian velocity distributions, while the second member is based on non-isotropic Gaussian velocity distributions. In the context of semiconductors, one obtains generalizations of so-called hydrodynamic rnodels. The closure proceeds in two steps. The first ensures that every member of the hierarchy is hyperbolic and has an entropy. This implies that, unlike for many traditional approaches, the resulting equations are formally well-posed. The second step involves modifying the collisional terms so that members of the hierarchy beyond the second also recover the correct dissipative behavior—the Navier-Stokes equations for gas dynamics and the drift difusion equation for semiconductors. This is done through the introduction of generalizecl BGK type collision operators. The simplest such system for gas dynamics in three spatial dimensions is a "14-moment" closure, which also recovers the behavior of the Grad "13-moment" system when the velocity distributions lie near local Maxwellians. The closure procedure can be applied to a general class of kinetic theories.

MP4. Three-Dimensional S-Matrix Simulation of Single-Electron Resonant Tunnelling through Random Ionised Donor States, *Hiroshi Mizuta, Central Research Laboratory, Hitachi, Ltd., Kokubunji, Tokyo 185, Japan.* Laterally-confined resonant tunnelling diodes (LCRTDs) exhibit an interesting interplay phenomenon of 3D quantisation, Coulomb blockade and impurity-induced tunnelling depending on the structural parameters. This work specially focuses on the single-electron resonant tunnelling (RT) in LCRTDs assisted by a few ionised donors in an unintentionally doped GaAs quantum dot. The 3D multi-mode scattering matrix (S-matrix) theory [1] is adopted for this purpose newly introducing the random scattering potential caused by ionised donors in the quantum dot. By comparing simulated current-voltage characteristics with experimental data [2], it is manifested for the first time that the observed current staircase results from background donors and so reflects the random configuration of the donors in the quantum dot. In the present simulation the 3D Schrödinger equation is numerically solved with scattering boundary conditions for an AlAs(4.2nm)/GaAs(5.6nm)/AlAs(4.2nm) LCRTD with various configurations of a few ionised donors. The S-matrix and hence transmission probability is calculated based on the 2D lateral eigenstates, and the tunnelling current is evaluated in the global coherent tunnelling scheme. With a few ionised donors being placed in the dot, the calculated energy-dependence of the total transmission rate clearly shows new peaks and, in addition, the resonant energies are dependent on the donor configuration. Visualised electron probability density reveals that these resonances originate in RT via single-donor-induced localised states. This new type of RT leads to current steps of order 0.1 nA near the current threshold which is quantitatively in good agreement with the experimental results.

[1] H. Mizuta, C. Goodings, M. Wagner and S. Ho, J. Phys.: Condens. Matter 4, 8783, 1992.
[2] C. Goodings, H. Mizuta, J. R. A. Cleaver and H. Ahmed, J. Appl. Phys. 76, 1276, 1994.

MP5. Hierarchy of Full Band Structure Models for Monte Carlo Simulation, *Umberto Ravaioli, Beckman Institute, University of Illinois at UrbanaChampaign, Urbana, IL 61801.* Monte Carlo methods which include the numerical band structure of semiconductor materials, provide an accurate physical picture of hot carrier transport. These methods find direct applications in transport calculations and device simulation, and are also useful for interpretation of experiments and calibration of other models based on simplified band structures. Main drawbacks of Monte Carlo approaches are the computational cost and the numerical noise. When details of the numerical band structure are utilized, it is very important to understand which aspects of the physics are relevant in order to design efficient simulation approaches that adequately resolve the behavior of carrier high energy tails. This talk will discuss the various hiererachy levels that are possible when the full band structure is considered. At the highest level, the scatterings are treated using complete k-k' transition rates, which entail extremely memory intensive computational applications. At the lowest level, the scattering anisotropy is neglected and the scattering rate is considered to be a constant average value on energy isosurfaces of the bandstructure. This model is more practical for device simulation, and examples will be presented which show how reasonable speed and efficiency can be obtained for practical applications on workstations. In between the two extremes, it is possible to design intermediate models which preserve some essential features of both. A model which has been recently implemented subdivides the momentum space into a set of equivalent valleys, using as a guideline the deformation potential variations evaluated inside the Brillouin zone from k-k' transition calculations. Within each valley, a specific deformation potential is selected for the phonon scattering rates, and the transport is treated as in the isotropic case for more efficient computations. At all levels of the band structure hierarchy of models, there are similar issues of numerical noise, related to the sampling of real and momentum space that the Monte Carlo method necessarily performs with a relatively small number of particles. The last part of the talk will address computationally efficient approaches based on the assignment of variable weights to the simulated particles, in conjunction with careful gather-scatter procedures to split particles of large weight and combine particles of small weight. Such methods can be designed to reduce the variance of statistical noise and may provide better efficiency and a broader range of applications when full band structure approaches are applied to probe the physics of hot carrier energy tails and rare events in device simulation.

P15. Energy Grid Generation for Resolving and Integrating Ultra-Fine Resonances in Quantum Device Simulation, *Gerhard Klimeck[a], Roger Lake[b], R. Chris Bowen[a], Chenjing L. Fernando[a], and William R. Frensley[a]; [a]Eric Jonsson School of Engineering, University of Texas at Dallas, Richardson, TX 75083-0688; [b]Corporate R&SD, Texas Instruments Incorporated, Dallas, TX 75235.* We describe the crucial algorithm which allows us to efficiently include scattering from alloy disorder, interface roughness, acoustic phonons, and polar optical phonons in single band and multi-band quantum device simulations. Such calculations require the integration of electron density and current density distributions over a range of 1 eV while, at the same time, resolving resonances on the order of 1 μeV. To perform this task using a limited number of energy nodes (≈ 200) requires an extremely well optimized energy grid. Typical [1] adaptive integration schemes place nodes by trial and error, checking for the relative error due to the introduction of additional nodes, because the "location" of the spectral features is initially unknown. Resonance finding algorithms for single band [2] and multi band [3] tight binding models have been developed and implemented. We have developed a general energy grid generator that utilizes the information of the resonance energies and life times of the states, the conduction band edges and the thermal distribution of the carriers in the contacts. The grid minimizes the absolute error in the integration of the spectral features avoiding the placement of nodes in energy ranges without significant integral contribution. Also the grid is constructed such that the integral contributions from segment to segment are about the same size and therefore minimizes the numerical round-off errors. We will describe the algorithm and present device simulations which include the scattering mechanisms listed above.

[1] W. H. Press, S. A. Teukolsky, W. T. Vetterling, and B. P. Flannery, Numerical Recipes in C, The Art of Scientific Computing, 2 ed. (Cambridge University Press, Cambridge, 1992).
[2] C. L. Fernando and W. R. Frensley, J. Appl. Phys. 76, 2881 (1994).
[3] R. C. Bowen, W. R. Frensley, G. Klimeck, and R. K. Lake, Phys. Rev. B (1995).

P16. Gridding and Discretization For Divergence Form (Semiconductor-Like) PDEs, *Donald J. Rose, Hai Shao, Ming-Yaq Kao; Department of Computer Science, Duke University, Durham, NC 27708.* In this presentation we will discuss gridding and discretization for a PDE (or PDE system) of the form (in 2D) $-\nabla \cdot j + f = 0$, (1) where $j = (j_1, j_2)^T$, and j and f are specified as $j_k = j_k(x, y, u_x, u_y, u), k = 1,2$, (2) $f = f(x, y, u_x, u_y, u)$, (3). For example, j could take the specific form $j = a\nabla u + \beta u$, (4) where a is a scalar function and $\beta = (\beta_1, \beta_2)^T$. Note that (4) arises in the continuity equations of the drift-diffusion semiconductor equations; here $\beta = \mu \mathrm{E}, \mu$, a mobility and E the electric field. Our approach to discretization (in 2D) will be to use the "box method" (finite volume and finite box methods using Voronoi boxes at a set of appropriate grid points in the region specifying the PDE. By using the divergence theorem, this transforms (1) to the operational equation $-\oint_{\partial Bi} j \cdot n \, ds + \oint_{\mathrm{B}} f = 0$, (5) where $\mathrm{B}i$ is a box containing grid point ρ_i with boundary $\partial \mathrm{B}_i$. After approximating the integrals in (5) on each box B_i associated with the unknown u_i, we obtain the coupled system of nonlinear (or linear) algebraic equations representing the discretization. The transient extension of equation (1), $\frac{du}{dt} - \nabla \cdot j + f = 0$, where j and f are defined as in (2) and (3), is easily handled. Hence most of our exposition in the presentation will deal with the PDE in the form of (1)-(3). Our intention in the presentation will be to consider increasingly more general cases of j as in (2) to make the exposition tractable and oriented to an engineering viewpoint. For example, the case of (4) for a and β being constants is interesting and instructive even in 1D. The case when a in (4) is replaced by a 2 x 2 (constant) matrix motivates much of the discretization algebra. In order to discretize (5), we need to approximate the integrals. We will derive a discretization based on the *constant j assumption,* namely, that j is constant pairwise on the lines of the Delaunay triangles dual to box β_i. This allows us to approximate $j \bullet n$ and to assemble the parts of the line integral which, in turn, relates the variable u_i, to the other u_k corresponding to Delaunay neighbors, say p_k, of the box mesh point p_i. We will show that the constant j discretization *is*

a natural generalization of the Scharfetter-Gummel discretization used in semiconductor modeling. When j is linear, as in (4), the constant j discretization produces a linear system to solve with interesting matrix properties. We will discuss these matrix properties and their algorithmic significance. We will also examine the relation between such matrix properties and the boxes and triangles. The generalization to nonlinear j of the more general form (2) will also be examined.

P17. A New Method to Recover Vectorial Electric Fields and Current Densities from Unstructured Meshes, *Daniel C. Kerr and Isaak D. Mayergoyz, Dept. of Electrical Engineering, University of Maryland, College Park, MD 20742.* In the numerical simulation of semiconductor devices, the vectorial electric field and current density field are required throughout the domain of simulation to compute various physical models, such as mobility, impact ionization, and Joule heating. In finite-box simulations, the discretization and solution do not uniquely define the fields off of the edges joining the nodes. The fields must be reconstructed from the projections of electric field or current density along the edges. The existing recovery methods, the method of corner averages [1], and the method of least-squares fitting, are *ad hoc* means to average the data. With 3-D device simulation becoming more common, a mathematically sound recovery method is needed. This paper describes a new recovery method, which is based on the edge elements of the finite-element theory. The method of edge-elements directly interpolates vectorial values defined on the edges of an element into the interior of the element. The vectorial interpolant J^k of the edge values F*ij* into the interior of element of element *k* is $J^k = \sum_{ij \in \mathcal{E}^k} F_{ij} e_{ij}$, where e_{ij} is the basis function of edge *ij* and E^k is the set of edges of the element. The edge basis function is defined in terms of the scalar finite-element shape function and d_{ij} is the length of edge *ij*. Reconstruction of the field using edge elements yields a non-constant vector function defined on the element which has the following properties: (1) the projection of the edge-element reconstruction on each edge reproduces the original data, and (2) the tangential components of the field are continuous from one element to the next. A simple modification of the basis functions is needed when the edge-element method is applied to non-simplex elements. In this form, edge elements are suitable for 2- and 3-D nonsimplex elements. The original and modified 2-D edge-elements in standard position are listed in Table 1. This element-averaged J^k, which can be used in device simulators, is also listed.

Work is supported by the Semiconductor Research Corporation contract SJ-377.

[1] S. E. Laux and R. G. Byrnes, IBM J. Res. Develop.. vol. 29. no. 3, pp. 289-301, 1985.
[2] D. C. Kerr and I. D. Mayergoyz, to appear, 1995.

P18. Parallel Spectral Multilevel Solution of the Augmented Drift-Diffusion Equations, *M.B. Davis and G.F. Carey, ASE and EM Dept., University of Texas at Austin.* Semiconductor devices in the sub-micron range exhibit non-local electric field effects such as velocity overshoot. Standard field-dependent mobility models in the drift-diffusion equations do not model such effects since calculation of the mobility is dependent only on the local value of the electric field. These non-local effects can be captured by augmenting the carrier mobility with a term proportional to the local rate of change of the electric field. We present results for an augmented mobility model with sensitivity studies for the augmentation coefficient. Comparison studies to other augmented mobility models, hydrodynamic and Monte Carlo results are also presented. Spectral *(p)* finite elements are used to discretize the equations in a decoupled Gummel algorithm, and the multilevel solution strategy uses projections between bases of different degree (level). Hierarchic bases are particularly well suited since the element matrices and vectors are nested and the projections easily defined and performed. The projection methods for p-multilevel are particularly important and are developed and analyzed for Lagrange and hierarchic bases. The element-by-element (EBE) parallelization is natural for the finite element method, and if basis degree is used to specify the multigrid level, an EBE strategy is natural for the multilevel technique as well. Algorithm scalability and effIciency is analyzed and tested.

P19. Distributed Algorithms for Three-Dimensional Semiconductor Device Simulations, *Mei-Kei Ieong and Ting-wei Tang, Department of Electrical and Computer Engineering, University of Massachusetts, Amherst, MA 01003.* The parallel simulation of semiconductor devices has attracted much attention in recent years. In [1] [2], various massively parallel algorithms for the solution of linear equations arising from three-dimensional semiconductor device simulations using direct and iterative methods have been studied. In [3], stationary iterative methods (such as Gauss-Seidel and Successive Over Relaxation) were used on an array of transputers to solve two-dimensional simulation problems. A speedup of 14.3 on 16 transputers has been reported. Because of the higher performance-to-cost ratio, the coarse grain parallelism is a very good alternative for semiconductor device simulations. In [4], an optimum speedup of three on a network of four workstations for a two-dimensional device simulation using various domain decomposition methods has been reported.

In this work, we study the *coarse grained parallelism* using a cluster of DECstations at the University of Massachusetts. The performance of two iterative methods, JNGS and PBICGSTAB, are investigated. The JNGS method for approximating the solution of nonlinear semiconductor equations is naturally parallel. The nonlinear problem is solved in a point-wise fashion and therefore a global Jacobian matrix is not necessary; consequently a tremendous saving in memory can be expected. However, the convergence rate of this method begins to deteriorate as the number of domains increases. On the other hand, PBICGSTAB method is simply a parallel version of the BICGSTAB algorithm to solve the linearlized semiconductor equations. This method together with a good preconditioner is robust and has been reported to be capable for solving extremely ill-conditioned problems. We have simulated a three-dimensional submicron N-MOSFET. The current density vector shown in Fig.1 clearly indicates the three dimensional feature of the result. Table 1 shows the performance of the JNGS algorithm applied to the solution of the 3-D MOSFET simulation, with gate bias of 2.0 volts and drain bias of 0.001 volts on a cluster of DECstation5000. The cluster is simultaneously shared by other users and some fluctuation in the performance has been observed. Yet, a near ideal speedup is clearly indicated. Most importantly, very large problems that cannot be handled by a workstation previously can now be solved by using a network of workstations in a relatively short time. However, as the drain voltage is increased, the number of iterations required to solve the problem also increases. The deterioration of the convergence rate is due to a larger coupling between Poisson's and continuity equations at high drain bias. In this case, the BICGSTAB method is preferred. A comprehensive comparison between the two methods will be reported.

---

[1] Donald Webber et al. IEEE TCAD, Vol.10, pp.1201-1209. Sept. 1991.
[2] Eric Tomacruz and Alberto Sangiovanni-Vincentelli, Supercomputing 94, pp 24-33, 1994.
[3] C.S. Tsang-Ping,. D.M. Barry and C.M. Snowden, The Proc. of the IWCE, pp. 266-269, 1994.
[4] Peter E. Bjorstad, W.M. Coughran, Jr. and Eric Grosse, The Proc. of Decomposition Method 7, 1993.

P20. Quadrilateral Finite Element Monte Carlo Simulation of Complex Shape Compound FETs, *S. Babiker, A. Asenov*, J. R. Barker and S. P. Beaumont, Nanoelectronics Research Centre, Department of Electronics and Electrical Engineering, University of Glasgow, Glasgow G12-8QQ, UK.* The ensemble Monte Carlo simulation approach plays a particularly important role in the simulation of compound FETs where both steady-state and transient device behaviour are governed by velocity overshoot effects. However, in almost all ensemble Monte Carlo studies of MESFETs and HEMTs, planar or rectangular solution domains are considered. This is usually dictated by the rectangular finite-difference grid used for the discretization of Poisson's equation. In addition, the surface potential pinning effects are normally neglected. In contrast, all modern sub micrometer compound FETs are single or double recess devices with complicated recess geometry. Very often the length of the free recess region is comparable to the length of the gate. Device parasitics like access resistances and coupling capacitances are strongly dependent on the shape and surface conditions of the recess. These parasitics are critical to the device characteristics, limiting in many cases the device performance and the advantages of device miniaturization. To be used not only in qualitative research but in the practical design of real sub micrometer FETs, Monte Carlo simulation codes should combine the extensive transport capabilities with a precise description of the device geometry and proper handling of surface effects. The use of finite

elements as a discretization approach offers the necessary flexibility. Here we report on a new Monte Carlo (MC) module incorporated in our Heterojunction 2D Finite element FET simulator H2F [1,2]. For the first time this module combines a precise finite-element description of device geometry, with realistic particle simulation of the non-equilibrium hot carrier transport in ultra-short recess gate compound FETs. Quadrilateral finite elements are used for the discretization of the solution domain. The grid is generated by deformation of originally rectangular sub-domains. The Galerkin method with linear isoparametric mapping has been adopted to approximate Poisson's equation. An efficient bi-conjugate gradient method is used to solve the resulting system of equations. The motion of particles within the solution domain is based on a unified modular approach. A single quadrilateral element is the building block of the MC module where the trajectory of each particle is traced, both in momentum and real spaces. Each quadrilateral finite element contains a single material and has a uniform doping distribution and local scattering table attached to it. The boundaries between the elements may be homo-, hetero-interface, contact or line of symmetry, and particles reaching the boundary are transferred or reflected according to the local transition probability. Using a Single Programme Multiple Data (SPMD) parallel approach, we are running H2F and its MC module in parallel on a Parsytec 64 Supercluster and Parsytec X'plorer. This makes it possible to use the MC simulations for practical design work, generating the necessary I-V characteristics in parallel. The capabilities of the new finite element MC module are illustrated in example simulations of two compound FETs fabricated in the Nanoelectronics Research Centre of Glasgow University. Fig. 1 represents the SEM cross sectional view and the H2F simulation domain of a 200 nm MESFET with 55 nm offset between the gate and recess edge. Fig. 2 represents the SEM cross sectional view and the H2F simulation domain of a 200 nm gate length pseudomorphic HEMT fabricated virtually without offset between the gate and the recess edges. The role of the surface potential pinning is illustrated in Fig. 2 *a,b* where the longitudinal component of the electric field and the average electron velocity in the channel, with and without surface potential pinning, are plotted for the MESFET from Fig. 1. In the transient simulation of both devices terahertz oscillations were observed. The switching behaviour of the pseudomorphic HEMT is illustrated in Fig. 4 for different doping concentrations in the cap. The Fourier transform of the currents from Fig. 4 is given in Fig. 5.

[1] A. Asenov, D. Reid, J. Barker, N. Cameron, S. Beaumont, Proc. of International Workshop on Computational Electronics, Leeds University Press, 45-49, 1993.
[2] A. Asenov, D. Reid, J. Barker, N. Cameron and S. Beaumont, in Simulation of Seminconductor Devices and Processes, eds. S. Selberherr, H. Stippel, E. Strasser, 265-268, 1993.

P21. 2D Finite Element Method Simulation of Lateral Resonant Tunneling Devices, *Zhi-an Shao, Wolfgang Porod, and Craig S. Lent, Department of Electrical Engineering, University of Notre Dame, Notre Dame, IN 46556.* We numerically investigate device applications of lateral resonant tunneling structures which consist of a transmission channel with attached resonators. In our previous studies, we have found that the transmission amplitude possesses resonance/anti-resonance features in quantum waveguide systems with resonantly-coupled cavities.[1] Here, we explore the utility of this transmission feature in negative differential resistance device applications. We solve the 2D effective-mass Schrödinger equation with current-carrying boundary condition [2] by the finite element method. We first calculate the transmission probabilities of two lateral resonant tunneling devices at different biases, then we calculate the I-V characteristics at finite temperature. We show that negative differential resistance with high current peak-to-valley ratio can be engineered in 2D lateral resonant tunneling structure through appropriate placement of the transmission resonance/anti-resonance feature on the real-energy axis (or the zero-pole pair in the complex-energy plane). The experimental realization of these two devices at low temperature is also discussed.

[1] W. Porod, Z. Shao, and C.S. Lent, Applied Physics Letters 61, 1350 (1992); W. Porod, Z. Shao, and C.S. Lent, Physical Review B 48, 8495-8498 (1993); Z. Shao, W. Porod, and C.S. Lent, Physical Review B 49, 7453-7465 (1994).
[2] C. S. Lent and D. J. Kirkner, J. Appl. Phys. 67, 6353-6359 (1990).

P22.A Lattice Boltzmann Method for Extended Hydrodynamical Models of Electron Transport in Semiconductors, *S.Succi, EXEC-IBM, Roma, Italy, and P.Vergari, Dept. of Mathematics, University of Catania, Italy.* Lattice Gas (LG) and Lactice Boltzmann (LB) methods have been much in use in the recent years to simulate a wide host of fluid-dynamic flows, ranging from creeping flows in porous media and multiphase flows with surface tension, to homogeneous incompressible fully developed turbulent flows, to name but a few. Although originally targeted to 'plain' hydrodynamics as described by the Navier-Stokes equations, the LB method lends itself to a number of remarkable extensions which permit us to handle generalized hydrodynamic flows including passive scalar transport, Rayleigh-Benard convection, magnetohydrodynamics and others. In this paper, we shall report on some preliminary efforts to construct an LB model able to describe the generalized hydrodynamic equations governing the dynamics of relatively hot charge-carrier in semiconductor devices. The basic question behind this effort is whether a generalized LB scheme can be devised which can capture the higher order moments of the 'true' Boltzmann equation, so as to capture physical effects beyond the reach of the drift-diffusion approximation. Preliminary computations indicate that indeed such a model can be found under appropriate assumptions on the nature of the local thermal equilibrium of the charge-carriers. Further theoretical and numerical investigation is definitely required to make quantitative assessments of the present model versus existing techniques.

P23. Second Order Newton Iteration Method and Its Application to MOS Compact Modeling and Circuit Simulation, *Zhiping Yu and Robert W. Dutton, AEL 204, Center for Integrated Systems, Stanford University, Stanford, CA 94305.* A novel second order Newton iteration scheme has been developed. Different from other higher order methods [1] it not only exhibits the cubic convergence rate but also preserves the linear (thus robust) nature of the conventional Newton method. The second order derivative is used to correct the slope of the tangent in such a way that the curvature of the curve is naturally incorporated in the iteration. The extra computational effort in evaluating the second order derivative is partially compensated by reduction of the iteration times, and more importantly by providing a better initial guess when the function parameters are changed. The applications of the proposed scheme to the charge-sheet MOS compact modeling [2] and prediction of region crossing in the fast circuit simulation [3] are demonstrated. It is expected that the wide recognition of this technique will provide a vital alternative in solving nonlinear problems and in particular for obtaining an approximate solution in the closed form. The algorithm for the scheme is as follows. Given a system of nonlinear equations, $\mathbf{f(x,p)=0}$, $\mathbf{f,x,0}\in\Re^N,\mathbf{p}\in\Re^M$ (1) where bold symbols represent vectors and x is the basic variable(s) such as the surface potential in the charge-sheet model and p is the parameter(s) such as the applied bias. Assuming for now $M = N = 1$, the conventional Newton-Raphson method updates the solution as follows, $x^{i+1}=x^i+\Delta x^i,\quad \Delta x^i=-f(x^i)/f_x(x^i)$ (2) where i is the iteration count and f_x is the first derivative. The proposed scheme modifies the update using the second order derivative, f_{xx}, in the following way (the details of derivation will be provided in a full length paper) $\Delta x=-\dfrac{f}{f_x}\left(1+\dfrac{1}{2}\dfrac{f}{f_x^2}f_{xx}\right)$(3).

It essentially changes the slope of the tangent to better reflect the curvature of the function at solution x^i. Because Eq. (3) still represents a straight line, the scheme is robust. Moreover, this scheme can readily be applied to the projection of the initial guess when p changes. The following expression is for the change in x due to change in p for the same function value.

$$\Delta x=-\frac{f_p\Delta p+\frac{1}{2}f_{pp}\Delta^2 p}{f_x+f_{xp}\Delta p}\left[1+\frac{f_p\Delta p+\frac{1}{2}f_{pp}\Delta^2 p}{(f_x+f_{xp}\Delta p)^2}f_{xx}\right]$$

In view of the critical role of initial guess in Newton iteration, the extra effort is worthwhile to ensure the solution be found with the iteration. The example on charge-sheet MOS modeling shown on the next page confirms the merit and effectiveness of this method. The iteration times can be cut as much as one half.

MP6. Testing Hydrodynamical Models on the Characteristics of One-Dimensional Submicrometer Structure, *A .M. Anile*, 0. Muscato*, S.Rinaudo#, P. Vergari*, *Dip. of Mathematics, University of Catania, Italy, #S.G.S. Thompson, Catania, Italy.* Recent advances in technology leads to increasing high speed performance of submicrometer electron devices by the scaling of both process and geometry. In order to aid the design of these devices it is necessary to utilize powerful numerical simulation tools. In an industrial environment the simulation codes based on the Drift-Diffusion models have been widely used. However the striking dimension of the devices causes the Drift-Diffusion based simulators to become less accurate. Then it is necessary to utilize more refined models (including higher order moments of the distribution function) in order to correctly predict the behaviour of these devices. Short of a direct Monte Carlo simulation (which requires prohibitively large computational cost in an industrial setting) hydrodynamical models have been considered as viable simulation tools. Several hydrodynamical models have been considered in the literature with various degree of sophistication and completeness ([2]- [3]- [5]- [6]- [8]). For a given device structure the various hydrodynamical models can give widely different results for the velocity and energy profiles according to the various assumptions made in the model (the crucial parameter seems to be heat conductivity of the electron gas). However the different velocity or energy profiles are hardly accessible to experimental detec ion. Therefore it is mandatory to discriminate among the various hydrodynamical models on the basis of their results on the output characteristics of the electron device which are measurable (I-V curves). We have analyzed two classes of hydrodynamical models:

• bfields hydrodynamical models and hfields drift-diffusion model [1] a general purpose two-dimensional device simulator developed at the Bologna University to perform a large kind of analysis like steady-state, small signal and transient. It resolves the semiconductor equations supporting the most important physical effects using a large range of models. Default parameters are used both *in the* drift-diffusion version and in the hydrodynamical version ($\tau p, \tau \omega$, heat conductivity phenomenologically represented by the Weidermann-Frau law with c=-2.1 (arbitrarily)).

• Self-consistent extended hydrodynamical models with relaxation times determined from Monte Carlo simulations (homogeneous and non-homogeneous). Heat conductivity consistently represented:

-Linearized Fourier law and Non Linear (gradient dependent) heat conductivity. There are no free parameters because all of them are consistently determined from Monte Carlo simulations. The results are shown in the accompanying figure. We plan to manufacture an electron device in order to validate the different models.

---

[1] G.Baccarani,G. Guerrieri,P. Ciampolini, and M. Rudan, HFIELDS: a Highly Flexible 2D Semiconductor-Device Analysis Program Proceeding of the Fourth International Conference on the Numerical Analysis of Semiconductor Devices and Integrated Circuits (NASECODE IV) pp. 3-12, June, 1985.

[2] K. Blotekjaer, IEEE Trans.Electron Devices 17, 38 (1970).

[3] G. Baccarani,M.R. Wonderman, Solid State Electron 29, 970 (1982).

[4] R. Thoma, A. Edmunds, B. Meinerzhagen, H.J. Peifer, W. Engl, IEEE Trans.Electron Devices 38, 1343 (1991).

[5] A. Gnudi, F. Odeh, M. Rudan, Eur.Trans.Telecommun. 1, 307 (1990).

[6] T.J. Bordolon, X.L. Wang, C.M. Maziar, A.F. Tasch, Solid-State Electron 34, 617 (1991).

[7] S.C. Lee, T.W. Tang, Solid-State Electron 35, 56138 (1992).

[8] A.M. Anile, S. Pennisi, Phys. Rev. B 46, 13186 (1992).

[9] A.M. Anile, S. Pennisi, Continuum Mech. Thermodyn. 4, 187 (1992).

[10] T. Tang, S. Ramaswamy, J. Nam, IEEE Trans.Electron Devices 40, 1469 (1993).

MP7. Monte Carlo Analysis of Anisotropy in the Iransport Relaxation Times for the Hydrodynamic Model, *R Brunetti*, M.C. Vecchi#, and M. Rudan# , *Dipartimento di Fisica, Universitá di Modena, Via Campi 213/A, 1-41100 Modena, Italy; #Dipartimento di Elettronica, Universitá di Bologna, Viale Risorgimento 2, I-40136, Bologna, Italy.* The purpose of this paper is an investigation of the anisotropy features of the relaxation times used in the hydrodynamic model. This method in fact considers the moments of rank 0 *tbrough* 3 *of* the Boltzmann Transport Equation (BTE), constituting a set of two second-order nonlinear PDEs in the real space. Its solution provides, in addition to the concentration of carriers, their mean velocity, energy, and energy flux. In *the* derivation of the model it is possible to incorporate the effects of the collisions into a set of generalized relaxation times for the moments of rank 1, 2, and 3, this yielding three tensors of rank 2, 4, and 6, respectively. The rank *is* then decreased by taking the trace of the corresponding PDEs [1], thus obtaining, with no loss of generality, the following expressions for the generalized relaxation times:

$$\int_B \varepsilon(k)\frac{f-f}{\tau}d^3k = \tau_w^{-1} n(w-w^{eq}), \quad (1)$$

$$\int_B u(k)\frac{f-\tilde{f}}{\tau}d^3k = \hat{\tau}_p^{-1} n\upsilon, \quad \int_B u(k)\varepsilon(k)\frac{f-\tilde{f}}{\tau}d^3k = \hat{\tau}_q^{-1}\, n\mathbf{P}. \quad (2)$$

In the above, f is the distribution function and $n = \int_B f d^3k$ the electron concentration. The inverse total scattering rate τ and the scattering-out are defined by $1/r = \int_B H(k,k')d^3k'$ and $\tilde{f}/\tau = \int_B f(k')\mathrm{H}(k',k)d^3k'$. Quantities $\omega, \upsilon, and \mathrm{P}$ are the mean energy, velocity, and energy flux of the electrons, respectively. In practice, tensors $\hat{\tau}_p^{-1}$ *and* $\hat{\tau}_p^{-1}$ are supposed to reduce to scalars. However, in a non-equilibrium condition the existence of an electric field breaking the cubic symmetry of the crystal *is* expected to reflect into some degree of anisotropy of the distribution function, whose moments over k would then acquire a tensor nature. It is therefore of interest to investigate the validity of the approximation above, and to this purpose it is necessary to determine a full solution of the BTE, incorporating those features of the band structure that are relevant to determine the anisotropy effects. A Monte Carlo simulator for electron transport in Si [2] has been used, accounting for the full 3D electron dynamics in the *k space* for a homogeneous system and including all six ellipsoidal nonparabolic valleys, as described in [2]. The generalized relaxation times $\tau\omega, \tau_{p33} and \tau_{e33}$ were calculated directly from Eqs. (1) and (2), since the average quantities are different from zero. All components o£ τ_p and τ_q have also been independently evaluated by means of a set of microscopic correlation functions, as described in [3]. This procedure allows one to evaluate also the tensor components involving directions orthogonal to the field direction. Numerical results were obtained at T = 300 and T = 77 K as functions of the electric field strength and direction.

[1] M. Rudan, A. Gnudi, W. Quade, in *Process and Device Modeling for Microelectronics*, Elsevier, 1993.
[2] R. Brunetti, C. Jacoboni, F. Nava, L. Reggiani, J. Appl. Phys. 52 (11), 6713, 1981.
[3] R. Thoma, K.P. Westerholz, H.J. Peifer, W.L. Engl, Semicond. Sci. Technol. 7, B328, 1992.

MP8. Monte Carlo Simulation of Hole Transport in Strained $Si_{1-x}Ge_x$ and of Electron Transport in Strained Si*, *Gabriele F. Formicone and David K. Ferry, Center for Solid State Electronics Research, Arizona State University, Tempe, Az, 85287-6206.* Monte Carlo simulations are used to study the transport properties of holes in a strained $Si_{1-x}Ge_x$ layer and of electrons in a strained Si layer. Mobility enhancement ratio (effective mobility in strained channel over effective mobility in unstrained channel) is extracted for both holes and electrons and compared with available experimental data.[1] Using an electric field pattern computed by Medici simulation for pMOS and nMOS SiGe based devices as the input for our Monte Carlo simulation, we also study the carrier drift velocity profile vs. the distance along the channel. The physical

model employed for the conduction and valence bands structure in strained Si and strained $Si_{1-x}Ge_x$ is taken from Rieger and Vogl.[2] Surface roughness scattering is treated according to Ferry.[3] Preliminary results show that electron mobility enhancement ratio saturates at a Ge concentration equal to 0.15-0.20. This is due to the fact that the energy splitting between the two lowered valleys and the four raised valleys becomes greater than the intervalley optical phonon energy, suppressing intervalley scattering between them.

*Work supported by Motorola.

[1] J. Hoyt, private communication.
[2] M.M. Rieger and P. Vogl, "Electronic band parameters in strained Si1-xGex alloys on Si1-yGey substrates," Phys. Rev. B 48, pp. 14276-14287, 1993.
[3] David K. Ferry, "Semiconductors," Macmillan, pp. 232-236, 1991.

P24. Time-Dependent Solution of a Full Hydrodynamic Model Including Convective Terms and Viscous Effect, *Deyin Xu[+] Ting-wei Tang[+] and Sergei S. Kucherenko[++]; [+] Dept of Electrical and Computer Engineering, University of Massachusetts, Amherst, MA 01003; [++] Dept. of High Energy Density Phvsics, Moscow Engineering Physics Institute, Moscow, Russia.* Over the past decade the hydrodynamic transport model has been extensivelv used in the simulation of submicron semiconductor devices in order to more accurately predict the nonequilibrium and non-local phenomena occurring in these devices. Most of these simulations, however, are limited to either steady-state solution and/or use of a simplified hydrodynamic transport model. Recently, we have developed a svstem of hydrodynamic transport equations based on the first three moments of the Boltzmann transport equation (BTE) calibrated by Monte Carlo data[1]. This transport model differs from the conventional ones in that the first-order moment of the BTE is taken w.r.t.. velocity $(\vec{v})$ rather than momentum $(\hbar\vec{k})$. Thus, the average velocity $\vec{V}$ is treated as one of state variables along with ψ, n and W. The resulting velocity "transport" equation involves a second-order tenser, $\hat{A} = <\vec{v}\vec{v}>$, which replaces the energy tensor $\hat{U} = <\vec{v}\hbar\vec{k}>$ in the conventional momentum transport equation. In one dimension, $\hat{A}$ is modeled as [1] A = VV(1 + 2.85(2aW)$-\eta\tau_v\frac{dV}{dx}) + \frac{W_0}{m_c}a(W)$, where the third term represents the bulk viscosity and $\eta \approx 2$ [1], [2].

To solve this system of transport equations, we used the second upwind for spatial discretization[3]. For time stepping scheme, we used Bank's TR-BDF2 composite method[4]. As an application, we simulated various N[+]—N—N[+] structures, one of which is shown in Fig. 1. The study shows that the steady-state is established within a few picoseconds after all external voltage is suddenly applied at $t = 0$. Figs. 2, 3, 4 and 5 show time evolution of the electric field, the electron velocity, the average energy and the current density, respectively. Note that the electric field changes suddenly from its initial value to a constant value of $E = 33.3KV/cm$ at $t = 0+$. The average energy increases smoothly with time from its thermal equilibrium value to the final distribution (Fig. 4). However, the velocity has a rapid overshoot (Fig. 3) at around 0.1ps near the N[+] — N junction and then gradually relaxes to a much lower steady-state value. About the same time, the current density also exhibits a similar surge (Fig. 5). This surge of current density is interpreted as onset of a free electron plasma oscillation. After approximately one quarter of plasma oscillation, however, the relaxation process due to collisions with impurities, photons, etc. dominates. In Fig. 6, the steady-state velocity distribution with and without the viscous term are compared. As expected, the viscous term has a dissipative effect and substantially suppresses the velocity overshoot near the N[+] — N junction which results in a better agreement with the M.C. data. We are now extending this work to the simulation of narrow-base BJT's in which the viscous effect is expected to play a more important role.

[1] Deyin Xu, M.S. Thesis, University of Massachusetts/Amherst, May 1995.

[2] Ting-Wei Tang. and Joonwoo Nam, Proceedings of the Third International Workshop on Computational Electronics, May 1994.
[3] Carl L. Gardner, Proceedings of the International Workshop on Computational Electronics, August 1993.
[4] Bandolph E. Bank, William M. Coughran, Jr., Wolfgang Fichtner, Eric H. Grosse, Donald J. Rose, and R. Kent Smith, IEEE Trans. Computer-Aided Design, CAD-4, No. 4, Oct. 1985.

P25. Non-Parabolic Inhomogeneous Hydrodynamic Models for Semiconductor Device Simulation, *Arlvnn W. Smith and Kevin F. Brennan, School of Electrical and Computer Engineering, Georgia Institute of Technology, Atlanta, GA 30332-0269.* In this paper, we discuss different hydrodynamic model formulations suitable for the simulation of inhomogeneous semiconductor devices without using the parabolic band approximation. The most common model for the inclusion of non-parabolicity utilizes the Kane dispersion law $(\hbar k)^2/2m = W(1+aW)$. An alternative choice to the Kane dispersion model is the power law relation of Cassi and Ricco, $(\hbar k)^2/2m = xW^y$. Generalized particle and energy flux equations, without any assumption of the distribution function, are presented based on the two choices of the dispersion relation. The physical significance of the band non-parabolicity is discussed as well as the advantages/disadvantages and approximations of the two non-parabolic models. To properly account for band non-parabolicity the field term must contain a non-parabolicity factor in the particle flux equation. This is true for both non-parabolic formulations independent of the distribution function chosen and has been commonly neglected. Accounting for non-parabolicity in the field and inhomogeneous material terms in the hydrodynamic model using the Kane dispersion law severely restricts the energy range over which the model is valid. The valid energy range is a factor of 2 to 3 times smaller than is commonly assumed for the Kane formulation due to the binomial expansion used in the derivation of these terms. Finally, closed form particle and energy flux equations, derived assuming a heated Fermi-Dirac distribution, are presented in a form suitable for implementation in device simulators. Extensions of the model to more accurately describe both the distribution function and band structure will also be discussed.

P26. Hydrodynamic Device Modeling with Band Nonparabolicity, *J. Cai and H.L. Cu, Department of Physics and Engineering Physics, Stevens Institute of Technology, Hoboken, New Jersey 07030.* We present a semiconductor device model based on a set of quantum mechanically derived hydrodynamic balance equations capable of dealing with arbitrary electronic energy band structures. Compared with the hydrodynamic balance equations for parabolic energy bands, the main difference is the introduction of a variable, ensemble-averaged, inverse effective mass tensor, which modifies the momentum balance equation directly and the other balance equations indirectly. As in the parabolic-band case, the momentum and energy relaxation rates are cast in the form of electric field dependent frictional force and energy transfer functions, with full account of electron-electron interaction effects, such as dynamical screening, and these functions are calculated using the electronic dielectric function, which is normally treated within the random phase approximation. However, these calculations are now modified with the introduction of the ensemble-averaged inverse effective mass tensor to treat the arbitrary energy band dependence on the crystal momentum. Device modeling issues such as discretization and optimization are addressed here. The device model is applied to a semiconductor with a Kane-type conduction band to demonstrate the usefulness of the new approach. We compare with other works dealing with Kane nonparabolicity and whenever possible, show explicitly deviations from parabolic expressions and results. Numerical simulations using this model is carried out for a submicron ballistic diode structure, using the Kane model conduction band, and the results are compared with those for the same device but under the parabolic-band approximation.

P27. Computation of the Spectral Density of Noise in Bulk Silicon Based on the Solution of the Boltzmann Transport Equation, *Alfredo J. Piazza and Can E. Korman, Department of Electrical Engineering and Computer Science, The George Washington University, Washington, DC 20052.* The

paper presents numerical simulation results for the spectral density of noise due to current fluctuations in bulk silicon based on a new semiconductor noise model [1]. The mathematical framework of the noise model is the machinery of stochastic differential equations (SDE). In semiclassical transport theory, the differential equations which describe the motion of an electron in a semiconductor can be interpreted as stochastic differential equations which are driven by inhomogeneous randomly weighted Poisson processes. These processes model the random scattering of electrons in momentum space due to interband and intraband scattering. The solution of such differential equations is a Markov process which can be characterized by a transition probability density function and satisfies the Kolmogorov-Feller equation. In the case of semiclassical transport, this equation is identical to the linear Boltzmann transport equation. Based on this formalism, the key computations for the evaluation of the autocovariance function of current fluctuations are reduced to the transient solution of the Boltzmann transport equation (BTE) with special initial conditions. The key feature which differentiates this model from other microscopic noise models is that this approach is strictly within the framework of semiclassical transport. Consequently, this approach directly connects the noise characteristics with the properties of the inhomogeneous randomly weighted Poisson processes which describe the physics of scattering in the semiclassical transport model. The solution method for the solution of the BTE is based on the Legendre polynomial method. The stationary solution is represented by the zero and first order Legendre polynomials, while the transient solution is represented by the zero, first and second order Legendre polynomials, due to the particular form of the initial condition. The paper describes in some detail, the numerical algorithm for the solution of the transient BTE and the numerical results for the spectral density of current fluctuations. The numerical results presented in this paper are for bulk silicon under static electric fields where the noise is due to acoustic and optical phonon scattering.

---

[1] C.E. Korman and I.D. Mayergoyz, "A Semiconductor Noise Model for Semiclassical Transport," in preparation.

P28. Hydrodynamic Device Modeling with New State Variables Specially Chosen for a Block Gummel Iterative Approach, *Wenchao Liang, Daniel C. Kerr, Neil Goldsman, and Isaak D. Mayergoyz, Dept. of Electrical Engineering, University of Maryland, College Park, MD 20742.* We report on a new numerical method for solving the HD equations which is specially tailored for use with a block-Gummel iterative method. The motivation for using the Gummed method for this 2D simulator is to establish a basis for future 3D calculations, where memory limitations inhibit use of full Newton solvers. With this approach, instead of using standard variables $\{\phi, n, p, T_e, T_p\}$, we define new state variables $\{\phi, u, \upsilon, g_n, g_p\}$. These new variables have the following attributes: (i) The new variables facillitate tailoring the HD equations specifically for use with a Gummel iterative method; (ii) The new variables yield transformed HD equations so that the left-hand side of each equation is linear with respect to a new state variable with which this equation is identified; (iii) The transformed equations yield well-conditioned coefficient matrices upon discretization; (iv) The new variables help resolve the fast spatial variation in carrier concentration and carrier temperature which occurs in semiconductor devices. These attributes were realized by developing mappings, from the standard variables to the new ones, which facilitate expressing each of the HD equations in forms which are linear, and either self-adjoint, or very close to it. This approach yielded the following relations between the new $\{\phi, u, \upsilon, g_n, g_p\}$ and the original variables $\{\phi, n\, p, Te, TP\}$:.

$$n = n_1 e^{\phi / V_T} \frac{T_L}{T_n} u; \qquad \rho = n_1 e^{-\phi / V_T} \frac{T_L}{T_p} \upsilon$$

$$T_n = T_L \left[e^{\phi / V_T} u \right]^{5/4} g_n; \qquad T_p = T_L \left[e^{-\phi / V_T} \upsilon \right]^{5/4} g_p$$

A new Scharfetter-Gummel-type discretization was developed for each of the transformed linear HD equations. The SG discretization yields a discrete system with coefficient matrices which are well conditioned, thereby helping to avoid numerical problems associated with their solution. The coordinated use of the new variables, the Gummel iterative approach, and the SG discretization yields a robust

approach to solving the HD equations. We demonstrate the new approach by applying it to a realistic 0.35 μm 2-D LDD MOSFET structure. The following page gives some example results including the predicted LDD device I-V characteristics.

P29. Modelling of Hot Acoustic Phonon Propagation in Two Dimensional Layers, *N. A. Bannov, V. V. Mitin, and F. T. Vasko, Department of Electrical and Computer Engineering, Wayne State University, Detroit, MI 48202.* Acoustic modes in layered structures differ substantially from modes in bulk material. We have obtained the quantum kinetic equation for confined acoustic phonons interacting with 2D electron gas and solved it for the case of phonon transport in a layered structure. We use the Wigner distribution function, $N_m(\mathbf{q}_\parallel,\mathbf{r}_\parallel)$, to describe the phonon syb-system; here m is a discrete index for mode number, $\mathbf{q}_\parallel$ and $\mathbf{r}_\parallel$ are the in-plane phonon wave vector and coordinate. The kinetic equation for $N_m(\mathbf{q}_\parallel,\mathbf{r}_\parallel)$, have the following form $\left(\frac{\partial}{\partial t}+\mathbf{S}_{m,q}\frac{\partial}{\partial \mathbf{r}_\parallel}\right)N_m(q_\parallel,r_\parallel)=T_m(q_\parallel,r_\parallel)$, where $\mathbf{S}_{m,q}$, is the renormalised due to electron-phonon interactions phonon group velocity, $T_m(q_\parallel,r_\parallel)$ is a collision integral responsible for decay of phonon modes. We have obtained explicit expressions for $T_m(q_\parallel,r_\parallel)$ and $\mathbf{S}_{m,q}$ for the case of a deformation potential interaction of 2D phonons with 2D electrons. The renormalization of the acoustic wave velocity and characteristic decay time have substantially different dependence on m and $\mathbf{q}_\parallel$ for $aq_\parallel<<1$ and for $aq_\parallel>>1$, where a is a width of the quantum well. We have numerically solved the kinetic equation for the thermal pulse propagation along a layer. Due to existence of several confined acoustic modes in layered structures, and complicated dispersion relation for confined phonons, the arrival time for different phonons varies significantly. This fact may be used for probing electron-phonon interaction in layered structures by time-of-flight technique.

P30. Numerical Simulation of Heat Removal from Low Dimensional Nanostructures,*V. V. Mitin, N. A. Bannov, R. Mickevicius, and G. Paulavicius , Department of Electrical and Computer Engineering, Wayne State University, Detroit, MI 48202.* Heat removal from active elements of high performance ultralarge integrated circuits is one of the major technical problems in developing new generations of IC. We have investigated the acoustic phonon radiation due to electron-acoustic phonon interaction in double barrier quantum wells and quantum wires. The electron and phonon density matrices are governed by coupled kinetic equations which have been solved numerically by the Monte Carlo technique. The effect of hot electrons on the radiation pattern of emitted phonons has been taken into account. We have calculated the angular and energy spectrum of nonequilibrium acoustic phonons radiated from low dimensional structures. A major peculiarity of acoustic phonon emission is a violation of the conservation law for the phonon wave vector component which is perpendicular to the direction of spatial confinement. Due to this violation the characteristic energies of the emitted acoustic phonons greatly exceed the energies of acoustic phonons emitted in bulk materials and are order of several *meV*. Nevertheless, such phonons propagate ballistically over macroscopic distances and have been detected experimentally. Except for the case of a strongly degenerate electron gas, the along-structure wave vectors of acoustic phonons emitted by electrons in nanostructures are smaller than the transverse wave vectors. Therefore the acoustic phonons carry energy primary in the direction normal to the nanostructure. We have demonstrated that due to large acoustic-phonon energies and strong scattering in nanostructures the heat removal by ballistic fluxes of acoustic phonons is extremely efficient.

P31. A Hot-Hole Transport Model Based on Spherical Harmonics Expansion of the Anisotropic Bandstructure, *M. Harrer, H. Kosina, Institute for Microelectronics, Vienna Technical University, Gusshausstrasse 27-29, A-1040 Vienna, Austria.* Monte Carlo transport simulations call for effective methods to calculate the free flight duration and to choose the scattering mechanism and the state after scattering. We propose a representation of the valence bands using an expansion into a series of spherical harmonics that is capable of resolving details of the band structure both at the center and at the boundary of

the Brillouin zone. The basic intention of our method is to simplify the calculation of the integrated scattering probability. Assume that the energy-wave-vector relationship is given in polar coordinates: $\varepsilon = E(k,\Omega)$. Here, ε is the energy of the hole, k the magnitude of the wave vector, and Ω denotes (θ,ϕ). We now introduce a coordinate transformation *(k,* $\Omega) \rightarrow (\varepsilon,\Omega)$, which transforms k to ε and lets Ω unchanged: $k = K(\varepsilon,\Omega)$. For any given Ω the function K is defined to be the inverse of the function E. The function K can be interpreted to describe the shape of an equi-energy surface in **k**-space. Inversion of a function is possible only in an interval where the function is monotonous. By inspection of the full band structure one finds that both the heavy hole and the split-off bands can entirely be represented by such functions K. Above a hole energy of *Ex(3.04eV)* inversion of the light hole band is no longer unique. In this work, we represent the function K as a series of sperical harmonics.

$$K_b(\varepsilon,\Omega)^3 = \frac{3}{4\pi}\sum_{l=0}^{\infty}\sum_{m=0}^{l} a_{lm}^{b}(\varepsilon)P_l^m(\cos\theta)T_m(\cos\phi),$$

b=H,L,SO. (1).

Derivation of the scattering rates is considerably eased by taking the third power of K as the function to be expanded. For symmetry reasons non-vanishing coefficients only exist for even values of l and m being a multible of 4. With (1) a set of functions $a_{lm}^{b}(\varepsilon)$ contains the whole band structure information. The essential advantage of the sperical harmonic expansion of the valence band is the resulting representations of the total scattering rates and of the distribution of the scattering angle. Our transport model accounts for three different scattering mechanisms, namely acoustic deformation potential (ADP) scattering in the elastic approximation, optical deformation potential (ODP) scattering and ionized impurity scattering (ION) in the Brooks and Herring formalism. The angular distribution functions of the solid angle after scattering are also given by spherical harmonics series. The rejection technique is used to choose the after scattering state. The free flight time is calculated by a self-scattering method. The functions $a_{lm}^{b}(\varepsilon)$ are represented numerically by means of a finite elemente method. The free parameters of the series are determined by a variational approach. The number of harmonics was made a function of energy ranging from l_{max} = 20 at lower energies to l_{max} = 60 at higher energies. In this work the steady-state hole transport in silicon has been simulated using the expansion (1) for the heavy and light hole bands up to a hole energy of E_{hole} = *3.04eV.* The split-off band has been neglected. Figure (1) shows the numerical band structure compared with the series representation. The numerical band structure has been computed by a nonlocal empirical pseudopotential method. Figure (2) depicts the resulting drift velocities in comparison to measured data and Figure (3) the simulated average hole energy, both as a function of the electric field applied in characteristic directions.

P32. An Improved Ionized Impurity Scattering Model for Monte Carlo Calculations, *G. Kaiblinger-Grujin and H. Kosina, Institute for Microelectronics, Vienna Technical University, Gusshausstrasse 27-29, A-1040 Vienna, Austria.* We have developed a physically based ionized impurity scattering model including the following corrections to the standard Brooks-Herring model. First, momentum dependent screening of impuritites by conduction electrons is taken into account assuming degenerate statistics. Second, the effect of multi-ion-scattering is included. Dynamical screening is described by a function of both the tranferred momentum q and the Fermi level [1]. Unfortunately, this function is represented by an integral which cannot be solved analytically. We approximated this integral by an analytical expression which has exactly the same behavior as the original integral for large q and is a very good approximation for small q for arbitrary degeneration. The advantage of this approach is that we are able to get a closed form for the scattering rate without changing the physics of the underlying problem. With higher doping, the average distance between tango impurities becomes smaller and the neighboring ion potentials overlap appreciably, so that the single-site-model for ionized impurity scattering breaks down. Therefore it is necessary to consider scattering processes at two ion potentials simultaneously. Equally charged pairs of impurities scatter up to twice as effectivly than monopoles [2]. The well-known problem of very large scattering rates at small angles is commonly solved by using a method after Ridley [3], which essentially cuts off the scattering rates at small impact parameters. As Ridley's method makes the agreement of theory and experiment even worse, we generalized this method in that we allow arbitrary filter functions. The

filter function, which cuts off large values of the impact parameter, is chosen such that the mobility remains unchanged. Comparing our results with experimental data it can be noticed that our impurity scattering model improves the agreement between theory and experimental data significantly and that it is therefore more suitable for Monte Carlo calculations than the classical Brooks-Herring model. Despite the greater complexity our model doesn't consume much more CPU time. The new model represents a rather good trade-off between an exact theory and an accurate approximation that is applicable for simulation of semiconductor devices.

[1] W.-Y. Chung and D.K. Ferry, "Dynamic Screening for Ionized Impurity Scattering in Degenerate Semiconductors," Solid-State Electron., Vol. 31, no. 9, pp. 1369-1374, 1988.
[2] J. Meyer and F. Bartoli, "Effect of coherent multi-ion interference on ionized-impurity scattering in semiconductors," Physical Review B, Vol. 30, no. 2, pp. 1026-1029, 1983.
[3] B. Ridley, "Reconciliation of the Conwell-Weisskopf and Brooks-Herring formulae for Charged-Impurity Scattering in Semiconductors: Third-Body Interference," J. Phys. C: Solid-State Phys., Vol. 10, pp. 1589-1593, 1977.

P33. Simulation of Electron Transport in Strained Si/SiGe Heterostructures, *Mahbub Rashed. W.-K. Shih, S. Jallepalli, R. Zaman, T.J.T. Kwan*, and C. M. Maziar, Microelectronics Research Center, The University of Texas at Austin; *Los Alamos National Laboratory, New Mexico.* Scaling of silicon MOSFET channel lengths to achieve increases in speed and drive current has pushed the limit of gate length towards 0.1 μm. An alternate approach for drive current enhancement is to increase the mobility of the charge carriers in the channel. Recent reports have suggested that electron mobility is enhanced when electrons flow in a strained-Si channel pseudomorphically grown on relaxed (001) $Si_{1-x}Ge_x$ [1,2,3]. The enhancement of mobility in strained-Si is due to both the suppression of intervalley scattering and the lower effective mass due to the valley splitting of the six-fold degeneracy of the silicon conduction band minima. This lifting of degeneracy results in an upward shift of the four transverse valleys and lowering of the two longitudinal valleys (in energy). In this work electron transport in strained $Si/Si_{1-x}Ge_x$ heterostructures is studied using a both a bulk Monte Carlo (MC) tool and one developed for 2D systems. The MC simulator SLAPSHOT [4] has been modified and enhanced to investigate electron transport in strained Si/SiGe systems. The bulk MC simulator is based on a multiband analytical model representing the features of a realistic energy bandstructure. The scattering rate computation is based on a non-local pseudopotential bandstructure. Recent results of semi-empirical pseudopotential bandstructure calculations show that, to first order, biaxial strain yields changes in only the relative energy and not the shape of the valleys [3]. Therefore, in our work, effective masses and nonparabolicities of different valleys are assumed to be unaffected by the strain. Fig. 1 shows the velocity-field characteristics of strained and unstrained silicon for different directions of the field. Figs. 2 and 3 illustrate the velocity-field characteristics at 300 K and 77 K for several mole fractions of relaxed $Si_{1-x}Ge_x$. Low field mobility is enhanced by about 80% at 300 K and by 35% at 77 K, as compared to bulk silicon. The higher mobility observed at room temperature is due to greater suppression of intervalley phonons as phonon scattering increases with temperature. While bulk simulation ignores the quantization effect in the transport, the nature of transport in the inversion layer requires consideration of these effects. The subband structure is calculated by applying the formalism based on the effectivemass approximation with bulk non-parabolic E(**K**) relation, as described in detail in [5] for the case of Si MOSFETs. Scattering of the 2D electrons due to bulk phonons and surface roughness is included. The formalism developed by Price [6] has been adopted for the phonon scattering rate calculation. Ionized impurity scattering, being important only in the presence of large interface charge density or when the channel is weakly inverted, is ignored. Surface roughness scattering is simply modeled with the formalism of Cheng et. al.[7]. A long channel strained Si nMOS structure with uniform substrate doping concentration and zero source-drain bias is simulated. At each gate bias, a two dimensional potential profile for the device is obtained by solving drift-diffusion (DD) and Poisson equations. Since a uniform inversion layer is assumed, a slice along the depth is selected at the middle of the channel. One dimensional Schrödinger and Poisson equations are then solved self-consistantly for the slice in order to calculate subband structures in the strained silicon channel. This calculation is followed by a single particle MC simulation, where a single particle is launched according to

the density-of-states (DOS) weighted equilibrium distribution. Fig. 4 shows the electron concentrations in the strained channel for different gate bias conditions. The enhancement of effective electron mobility in strained silicon channel nMOS structures, as compared to conventional silicon nMOSFETs, is presented. Fig. 5 shows the improved mobility in strained Si nMOS as compared to silicon nMOS structure. Agreement between calculated and experimental [9] enhancement of effective mobility is shown in Fig 6. This agreement is sufficiently encouraging that this tool will be used for preliminarv evaluation and analvsis of $Si/Si_{1-x}Ge_x$ based devices.

[1] K. Ismail et al., Appl. Phys. Lett. 58, 2117, 1991.
[2] Y.J. Mii et al., Appl. Phys. Lett. 59, 1611, 1991.
[3] T. Vogelsang et al., Appl. Phys. Lett. 63, 186, 1993.
[4] X.L. Wang et al., J. Appl. Phys. 73. 3339, 1993.
[5] Shih et al., Proceed. of UGIM Symp., May 17-18, 1995.
[6] P.J. Price, Anls. Phys. 133, 217, 1981.
[7] Y.C. Cheng, Surf. Sci. 27, 663, 1971.
[8] G. Yeap, Ph.D Dissertation, UT-Austin, 1995.
[9] J. Welser et al., 373, IEDM-1994.

P34. A New Concept for Solving The Boltzmann Transport Equation in Ultra-fast Transient Situations, *Ming-C. Cheng, Department of Electrical Engineering, University of New Orleans, New Orleans, Louisiana 70148.* It was proposed that evolution scales of *f(k),* which obeys the Boltzmann transport equation, can be characterized by relaxation times. This concept illustrated in Fig. 1 is based on the fact that the kinetic distribution function, *f(k),* can be described by the infinite set of moments (i.e., hydrodynamic parameters); or $f(k) = f(k,n,\bar{k},\bar{\varepsilon},\bar{k}^3,\bar{k}^4,....)$. The axis in Fig. 1 represents the temporal scale of evolution for *f(k)* corresponding to the scales of moments. In semiconductor, $\tau_n > \tau_\varepsilon > \tau_m$, and the characteristic times of higher-order moments are assumed to be smaller than τ_m. Information in *f(k),* after a drastic change in field, described by the smaller-scale moments tends to vanish in a shorter time. As shown in Fig. 1, *f(k)* tends to evolve through $f_m(k,n,\bar{\varepsilon},\bar{k})$ (a τ_m-scale hydro-kinetic distribution) and $f_\varepsilon(k,n,\bar{\varepsilon})$ (a τ_ε-scale hydro-kinetic distribution), and eventually into a quasi-equilibrium distribution, $f_\varepsilon(k,n)$. In fast transient situations, $f\varepsilon$ or f_m can be chosen to describe *f.* The approach to $f\varepsilon$ has been introduced in Ref. 1. In the present study, evolution of the hydro-kinetic distribution from f_m to $f\varepsilon$ is assumed to be a relaxation process described by $\bar{\varepsilon},\bar{k}$, and the change in field. The process can be performed numerically. Results for electrons in Si < 100> subjected to an ultra-fast step field are illustrated in Figs.2-4 where a two-valley model is used. Figs. 3 and 4 clearly show that $f\varepsilon$ responds to the change in field more slowly than *f* and f_m during the velocity overshoot interval where the distribution function is strongly influenced by the velocity relaxation. The velocity dependence is not included in the τ_ε-scale distribution, $f\varepsilon$. Inclusion of the velocity relaxation in f_m significantly improves the accuracy of the hydro-kinetic distribution, as illustrated in Figs. 3 and 4 where *f* and f_m evolve closely. Calculations for the evolution take only about 10 seconds on a 486/33 PC for a single-valley band model and 25 seconds for a 2-valley model. The computational model for the evolution will be presented.

[1] Ming-C. Cheng and Rambabu Chennupati, *J. Phys. D,* 28, 160 (1995).

TA1. Recent Advances in Device Simulation Using Standard Transport Models, *Giorgio Baccarani, Massimo Rudan and Martino Lorenzini, Dipartimento di Elettronica, Informatica e Sistemistica, Viale Risorgimento, 2-40136 Bologna, Italy.* Numerical simulation of semiconductor devices has reached a mature development stage. Two-and three-dimensional simulation codes are increasingly being used both for a better understanding of device behavior and for design purposes. Furthermore, commercial tools

featuring a friendly user interface and sophisticated simulation environments are currently made available to interested users. Yet, it is fair to say that a number of unsolved practical and theoretical problems still exist which make it difficult to achieve an accurate prediction of the device performance. Such problems range from structure definition to mesh generation in 3-D; also, discretization techniques and numerical stability are still far from satisfactory and some specific physical models turn out to be very hard to quantitatively predict. In this paper. we address some the above problems from an engineering standpoint and, whenever possible, indicate desirable research areas waiting for new solutions. Some of the above limitations are listed below.

- When devices are inherently three-dimensional, a realistic definition of the device structure turns out to be very hard to achieve with the necessary accuracy in both device morphology and impurity profiles;
- Automatic mesh generation in 3-D is still a very challenging task. This is due to the constraints imposed by the sensitivity of the numerical solutions to the quality and size of the geometrical elements, and by the need of heavy mesh refinement whenever rapidly-varying functions are to be accurately determined;
- The most popular discretization scheme, which is based on finite boxes, is based on the assumption of a spatially uniform current density along the element sides. Such an assumption is actually correct only when the current density *is* parallel (or perpendicular) to the element side, but fails when the current flows in a slanting direction with respect to them. The problem is especially severe at the drain end of the channel in MOSFETs, where impact ionization occurs under saturation conditions;
- The electric field is known with poorer accuracy than the electric potential, as the former is basically obtained as a difference between close potential values. As a result, all field-dependent physical effects, such as impact ionization, band-to-band and trap-assisted tunneling, Pool-Frenkel enhanced emission rates and Fowler-Nordheim tunneling across the oxide turn out to be affected by relatively-large errors;
- Hot carrier injection into the gate oxide, which is the dominant mechanism for the programming of EPROM and flash EEPROM cells, is very hard to reliably predict as *the* technology changes. This is due to the extreme sensitivity of the energy distribution function at large energies upon the physical model (band structure and scattering mechanisms).

This paper addresses the above limitations, and discusses new solutions and perspectives to overcome them.

TA2. An Efficient Solution Scheme for the Spherical Harmonics Expansion of the Boltzmann Transport Equation Applied to Two-Dimensional Devices, *Maria Christina Vecchi[1], Jan Mohring[2], and Massimo Rudan[1], [1] Dipartimento di Elettronica, Universitá di Bologna, Viale Risorgimento 2, 40136 Bologna, Italy. [2] Universität Kaiserslautern, FB Mathematik, E. Schrödingerstrasse, D-67663 Kaiserslauter, Germany.* In recent years the SHE of the *BTE* has been successfully tested in a wide range of problems in the field of electron transport simulation [1, 2]. Thanks to the assumption of spherically-symmetric bands, the differential equation in energv and space can be transformed into a differential equation in space, and a difference equation in energy [3]. This allows one to connect to each point in space only those nodes in energy coupled via the scattering operator. On the other hand, a detailed knowledge of the distribution function at low energies is necessary to correctly compute its averages (namely concentration, mean energy. mean velocity, etc.). Because of this, several solutions on grids displaced in the energy domain have to be carried out. We propose here a new scheme that improves the solution at low energies, keeping the desired accuracy in the calculation of the mean quantities while saving a significant amount of CPU-time. This is important in view of the applications of the method, since the typical number of nodes to be used in the combined space-energy domain is in the range of 10^4-10^5. Solution Method: The SHE method in steady state provides the second-order difference-differential equation [3]

$$\frac{\partial}{\partial r_i}\left[\tau_1 g u_g^2 \frac{\partial f_0}{\partial r_i}\right] + 3c_{op} g\{g^+[N_{op}^+ f_0^+ - N_{op} f_0] - g^-[N_{op}^+ f_0 - N_{op} f_0^-]\} = 0, \qquad (1)$$

in the unknown distribution function f_0. The equation is solved in a three-dimensional domain (x, y, *H) with* boundaries defined in space by the boundaries of the device and in energy by $H_{min} = -q\varphi(x,y)$) and $H_{max} = E_{max} - q\varphi(x,y)$, where E_{max} is the maximum energy of the band system. A prismatic mesh with

triangular elements in the (x, y) plane is adopted. The nodes at constant total energy H are uniformly spaced in energy by intervals $\Delta H = \hbar\omega_{op}/n$, with n integer. Thanks to the absence in (1) of partial derivatives with respect to H each node is connected along the H direction only to the nodes at $(x, y, H \pm \hbar\omega_{op})$ via the phonon scattering operator. The resulting algebraic system is thus decomposed in n decoupled subsystems. In the solution scheme we present here, eqn. (1) is solved in the full energy domain $[H_{min}, H_{max}]$ only once, while several additional solutions are computed in the reduced energy domain $[H_{min}, m\,x\,H_{op}]$, where $H_{op} = \hbar\omega_{op} - q\varphi(x, y)$. The terms in eqn. (1) which are external to $[H_{min}, m\,x\,H_{op}]$ are expressed by interpolating the values previously computed on the full domain. By letting m = 10 one can express the values of the distribution function outside the domain by an interpolation scheme that maintains the linearity of the system; conversely, to compute the local solution with m = 1 one has to resort to a more sophisticated interpolation scheme. It should be added that, in addition to the loss of linearity of the system, a local solution scheme with m = 1 does not allow one to correctly compute the currents in the device because of the early truncation of the solution domain. We present here, for the case m = 10, the comparison of the results of this solution scheme (consisting of 1 full solution and 9 local solutions) with those of a full solution computed on 10 grids in $[H_{min}, H_{max}]$. The test device is a 2D-MOS transistor with effective channel length 0.25mm. Figs. 1 and 2 present the comparison of the electron concentrations and the normalized electron mean energies along a section of the device parallel to the si-siO_2 interface, and Fig. 3 compares the drain currents. For comparison the current computed by HYDRO-HFIELDS [4], using a mobility model consistent with SHE, is also reported in Fig. 3. In conclusion, the scheme based on the solution of n subsystems displaced in the full-energy domain can be replaced without loss of accuracy by a scheme which considers a single complete solution and (n—1) local solutions in the interval $[H_{min}, m\,x\,H_{op}]$. Thanks to its structure, the new method is intrinsically more efficient. In the example shown here, a reduction factor of about 5 in the CPU-time has been achieved.

[1] N. Goldsman, L. Henrickson, J. Frey, Solid-St. Electr., Vol. 34. No. 4, p. 389, 1991.

[2] A. Gnudi, D. Ventura, G. Baccarani, F. Odeh, Solid-St. Electr., Vol. 34, No. 4, 1993V

[3] D. Ventura, A. Gnudi, G. Baccarani, F. Odeh, Appl. Math. Lett., Vol. 5, no. 3, p. 85-90, 1992.

[4] A. Forghieri, R. Guerrieri, P. Ciampolini, A. Gnudi, M. Rudan, G. Baccarani, IEEE Trans. on CAD, Vol. 7, No. 2, pp. 231-242, 1988.

TA3. Brownian Approach to the Simulation of Small Semiconductor Devices, *C.R. Arokianathan, A. Asenov*, and J.H. Davies, Nanoelectronics Research Centre, Department of Electronics and Electrical Engineering, University of Glasgow, Glasgow,G12-8QQ, UK.* In the small size current and future generation semiconductor devices the discrete nature of the electric charge emerge. There are only a few hundred impurity atoms and approximately the same number of carriers in a typical 0.1 x 0.1 x 0.1 μm^3 device. The random distribution and statistical fluctuation in the number of impurity atoms can produce variations in device characteristics that hamper large-scale integration. Variations in the subthreshold characteristics and threshold voltages in sub-micron MOSFETs caused by random fluctuations in the local impurity distributions have been clearly demonstrated in simple 3D drift-diffusion simulations [1]. The trapping and detrapping of individual carriers on randomly distributed defect states, whose pattern is unique in any device, gives rise to random telegraph noise. Individual carriers can induce modulations in the potential distribution that can significantly affect the blocking characteristics of the barrier at the source-channel junction of FETs. Furthermore, averaged scattering rates are simply inappropriate in devices with countable number of impurities and carriers, and the impurity and carrier-carrier scattering must be treated as interaction between individual charges [2]. All these effects indicate that the detailed distribution of the impurities and the individual motion of the carriers must be considered in the simulation of the semiconductor devices below the 0.1μm limit. A correct treatment of discrete charges and their interaction in a simulation requires 3D solution of Poisson's equation with fine-grain discretization. This in turn requires large computational resources. A suitable method to treat the carrier dynamics must therefore be developed to reduce the computational burden as much as possible. The need to consider the discrete nature of carriers favours methods which follow the motion of individual particles over those which rely on the solution of partial differential equations. Here we report on a new simple approach to the particle

device simulation based on Brownian dynamics and the Langevin equation. It satisfies the above needs where the fullblown Monte Carlo method is not necessary or too expensive. Apart from its simplicity our method may be particularly useful for isolating and studding some specific aspects of the carrier dynamics related to the "atomistic" nature of carriers and impurities. It is more transparent than the Monte Carlo technique in distinguishing the effects due to the discrete nature of particles and their interaction with impurities, because these effects are not obscured by structure arising from the scattering rates. It can be also used for *ab-initio* noise simulations. First we will discuss the relation between our new method and those currently in use for simulation of semiconductor device including drift-diffusion, hydrodynamic, Monte Carlo and Cellular Automaton. This will be followed by a formal description of the Langevin theory and its discrete time approximation. The truncation error and the convergence of the discrete time approximation are studied in details. The practical implementation of the Brownian dynamics approach will be described further. Two modifications of the Brownian simulation technique have been developed, based on randomly fluctuating velocity and random displacement. Several possibilities for the choice of the magnitude of the Wiener process, describing both the velocity and the displacement fluctuation, which lead to a correct Einstein relation will be presented. Special attention is also paid to the realistic modeling of the ohmic contacts. First we have tested the Brownian approach in a bulk material simulation where it predicts correctly the carrier temperature and the diffusion coefficient. The approach has also been tested in a simulation of a p-n junction diode. The results of this test are in excellent agreement both with the ideal diode equation and with the drift-diffusion results obtained from the commercial simulator MEDICI (Fig. 1). The potential across the diode obtained from the Brownian simulation at different applied voltages is given in Fig. 2. The approach will be further applied for simulation of a simplified MESFET with random distribution of impurities (Fig.3). The potential distribution in the middle of such device when both the carriers and the impurities are "atomistically" treated is given in Fig. 4.

[1] H.-S. Wong and Y. Taur, Proc. IEDM, 29.2.1-29.2.4 (1995).
[2] D.K. Ferry, A.M. Kriman and M.J. Kann, Comp. Phys. Com. 67, 119-134 (1991).

TA4. Non-Local Impact Ionization Effects of Hot Carriers in Polar Semiconductor Devices, *P. Lugli, C. Cianci, A. Di Carlo, and D. Meglio, Dipartimento di Ingegneria Elettronica, Universitá di Roma "Tor Vergata", 00133 Roma, Italy.* We have performed a Monte Carlo study of GaAs/GaAlAs and InP/InGaAs Heterojunction Bipolar Transistors under near-breakdown conditions. The good agreement of the calculated values of the multiplication factor with available experimental measurements allows us to point out the fundamental role of the dead space effects in the impact ionization phenomena occurring in the collector. A first consequence of our finding is the impossibility to extract physical ionization coefficients from the measured multiplication factors if such non-local effects connected to the dead space are not accounted for. Thus, all experimentally-deduced ionization coefficients present in the literature for polar materials do not have a general character as they have been derived from essentially local models. Such coefficients are intrinsically dependent on the specific structure used for the measurement. As a matter of example, we will show that the use of the generally accepted ionization coefficients measured by Bulmann, et al., in GaAs photodiodes does not lead to the measured multiplication factor of GaAs HBTs. We have, therefore, developed a non-local "delay" model which includes all basic physical features of the ionization process as extracted from Monte Carlo simulations. The delay model has been implemented in a standard drift-diffusion approach, thus providing a fast and reliable device modelling tool which produces very well the HBT experimental data. Our model has allowed us to design a general procedure for the extraction of physical ionization coefficients from the multiplication factor of a variety of different structures.

P35. Monte Carlo and Hydrodynamical Simulation of a One Dimensional n^+—n—n^+ Silicon Diode, *O. Muscato[1], M.V. Fischetti[2], and R.M. Pidatella[1], [1]Dipartimento di Matematica,Viale Andrea Doria, 95125 Catania, Italy. [2]I.B.M. Research Division, T.J. Watson Reseach Center, P.O. Box 218, Yorktown Heights, New York 10598.* Hydrodynamical models are currently used in simulating charge carrier transport in semiconductor devices in order to describe high-field phenomena such as hot electrons, impact ionization, etc. Hydrodynamical models are derived from the moment equations of the Boltzmann transport equation

(BTE) by making suitable assumptions on the closure of the infinite hierarchy and by modeling the RHS's of the moment equations (i.e. the production terms). The most popular hydrodynamical model is the one introduced by Bloetekjaer [1] and subsequently widely investigated by Baccarani and Wordeman [2], in which the closure is achieved by using the Fourier law with the Wiedemann-Franz expression for the heat conductivity: such a model leads to serious difficulties when compared with results arising from a direct numerical simulation of the BTE [3]. Recently Anile, Muscato and Pennisi [4],[5] proposed an improved hydrodynamical model in which the closure is achieved by exploiting the entropy principle [6], and the production terms are modeled as relaxation terms consistently with the Onsager Reciprocity Principle [7]. In order to test such a model, we simulate the stationary electron flow in the n^+—n—n^+ submicron diode, which mimics the channel in a MOSFET device [8]. The system is discretized by using finite differences and the 1-D box method. The solution of the resulting non-linear system is obtained by Newton's method with the Bank and Rose [9] damping. In such a model the relaxation times for energy, momentum, energy flow, shear (appearing in the production terms) are determined by using the Monte Carlo code *Damocles*™ *[10]*: we also obtained the macroscopic quantities (average energy, velocity, density, etc.), which are compared with those obtained by the hydrodynamical model.

[1] K. Blotekjaer, IEEE Trans. on Electron Devices, ED-17, 38, (1970).
[2] G. Baccarani, M.R. Wordeman, Solid-State Electronics 29, 970, (1982).
[3] M.A. Stettler, M.A. Alam, M.S. Lundstrom, IEEE Trans. on Electron Devices ED-40, 733, (1993).
[4] A.M. Anile, S. Pennisi, Physical Review B 46, 13186, (1992).
[5] A.M. Anile, O. Muscato, to appear in Physical Review B (1995).
[6] I. Muller and T. Ruggeri, Extended Thermodynamics, (Springer-Verlag, Berlin, 1993).
[7] L. Onsager, Phys. Rev. 37, 405, (1931).
[8] C.L. Gardner, J.W. Jerome, D.J. Rose, IEEE Comp.-Aided Design 8, 501, (1989).
[9] R.E. Bank, D.J. Rose, Num. Math 37, 279 (1981).
[10] M.V. Fischetti, S. Laux, Phys. Rev. B 48, 2244, (1993).

P36. A New Self-Consistent 2D Device Simulator Based on Deterministic Solution of the Boltzmann, Poisson and Hole-Continuity Equations, *Wenchao Liang, Neil Goldsman and Isaak Mayergoyz, University of Maryland, Dept. of Electrical Engineering, College Park, MD 20742.* We report on a new 2D simulation tool which, to our knowledge, for the first time performs actual 2D device modeling by deterministic, self-consistent solution of the Boltzmann Transport Equation for electrons, the Hole-Current Continuity Equation and the Poisson Equation. The method has the following additional attributes: (i) It employs the first 2 bands of the transport model of [1], and thereby is virtually equivalent, from a physical point of view, to performing 2-D self-consistent spherical band MC simulations. (ii) The solution directly gives the electron distribution function, electrostatic potential, and the hole concentration for the entire 2-D device. Average quantities such as electron concentration and electron temperature are obtained directly from the integration of the distribution function. Impact ionization and substrate current, as well as I-V characteristics, are also calculated directly from the distribution function. (iii)The method has the advantage of being significantly faster than MC simulations and does not have statistical noise. The method provides more information than the hydrodynamic approach, and does not use empirical mobility models. (iv) The self-consistent, 2D BTE simulator has been adapted to model both 2D conventional MOSFET's and SOI MOSFET's. Tractable Formulation of the BTE: We use the generalized spherical harmonic approach to transform the BTE from a 5-dimensional differential-integral equation to a 3-dimensional system of differential-difference equations which is tractable for numerical evaluation[2]. With this approach, the momentum distribution function is expressed in terms of an infinite series of spherical harmonics. By taking advantage of the recurrence and orthogonal relationships between spherical harmonics, we derive a system of equations for the expansion coefficients to arbitrarily high order. This system is then truncated after the 4th spherical harmonic, and solved numerically. Numerical Approach: We developed a Scharfetter-Gummel (SG) type discretization for the BTE, and use the standard SG discretization on the hole-continuity equation. Each equation in the discretized system is thereby well-conditioned. We overcome memory constraints of the 3D BTE (2D real space, ID energy space) by solving

the discretized BTE with a fixed point iteration method. The overall system is solved using a Gummel type decoupled method.

[1] C. Fiegna and E. Sangiorgi, IEEE Trans. on Electron Devices, Vol . 40, no. 3, pp. 619-627, 1993.
[2] K A Hennacy, Y.-J. Wu, N. Goldsman, and 1. D. Mayergoyz, Solid-State Electronics, 1995, Accepted for publication.

P37. Self-Consistent Solution of the Poisson and the Multi Band Boltzmann Equations in Silicon, *Surinder P. Singh, Neil Goldsman, and Isaak D. Mayergoyz, University of Maryland, Dept. of Electrical Engineering, College Park, MD 20742.* The spherical harmonic approach for solving the BTE, which represents a compromise method in between hydro-dynamic modeling and full zone Monte Carlo (MC) simulation, is gaining more acceptance [1,2]. In this work we have developed a new numerical technique to self-consistently solve the multi-band BTE and Poisson equation and thereby obtain the distribution function for energies greater than 3eV. The multi-band band structure is from [3], which was developed for computationally efficient multi-band MC. The novel aspects of the numerical solution include a Scharfetter-Gummel type discretization on a boundary fitted coordinates (BFC) grid such as those used in computational fluid dynamics (CFD) [4]. The previous solutions [2] have used an orthogonal grid, but the numerical solution is more amenable on a BFC grid, which, to the authors knowledge, is being used for the first time in semiconductor device simulation. The analytical model consists of the BTE for each band k (k = 1,2,3,4), and Poisson equation. The dimensionality of the BTE is reduced by projecting it on a spherical harmonics basis in **k** space, $f(r,k) = \Sigma_{l,m} f_l^m(r,k)\,Y_l^m(\theta,\phi)$ where, $k = |k|, \theta$ is the polar angle, and ϕ is the azimuthal angle. By substitution the expansion into the BTE, and applying the orthogonality of Y_l^m and changing variables $f_0^0(x,\varepsilon)$ to $F_0^0(x,H) = f_0^0(x,H+q\phi)$ we get [2]: $\frac{\tilde{\upsilon}}{3\lambda}\left\{\frac{\partial}{\partial x}\left(r\tilde{\upsilon}\lambda\frac{\partial F_0^0}{\partial x}\right)\right\}+\left[\frac{\partial F_0^0}{\partial t}\right]_{ib} = 0$ (1). Four coupled BTE of this form can be written using the band structure from [3]. Reduction in computational effort is achieved by combining two BTE's for the lower bands into one, indexed by (I), and the other two BTE's for the upper bands into another, indexed by [II]. We have to solve the Poisson equation along with the BTE, eq. (1). The BTE is defined on a curvilinear region bounded by real space x = 0, L_x and $H = -q\phi(x), \varepsilon_{\max,(I)} - q\phi(x)$. Since the boundaries of the solution domain are not orthogonal we resort to a BFC grid which conforms to this boundary and perform interpolations when writing the finite difference approximations of the derivatives [4]. There are three main advantages of BFC, (i) the grid can be made selectively dense in ε, (ii) boundary condition at band maxima is directly specifiable (iii) during self consistent calculations the grid remains the same. The equations are discretized by finite differences, and using Scharfetter-Gummel type discretization of equation (1). The individual equations are solved using a fixed point SOR approach while the overall system is solved self consistently with a decoupled Gummel-type scheme. The approach was tested on a n^+ - n - n^+ device structure.

[1] H. Lin, N. Goldsman, I.D. Mayergoyz, Solid-State Electron., 35(6), 769, 1992.
[2] A. Gnudi, D. Ventura, G. Baccarani, IEEE Trans. on CAD, 12(11), 1706, 1993.
[3] R. Brunetti and C. Jacoboni, F. Venturi, E. Sangiorgi, and B. Ricco, Solid-State Electron., 32(12), 1663, 1989.
[4] J.F. Thompson, Z.U.A. Warsi, J. Comp. Phys., 47, 1, 1982.

P38. Hot-Carrier Reliability of MOSFET Isolation Oxides Using 3-D Hydrodynamic Simulation, *Daniel C. Kerr, Wenchao Liang, Isaak D. Mayergoyz, and Neil Goldsman, Department of Electrical Engineering, University of Maryland, College Park, MD 20742.* Hot-carrier reliability is a major factor in the design of advanced CMOS processes. The isolation oxide is subject to mechanical stress and field boron penetration, which makes it more susceptible to hot-carrier damage than the high-quality gate oxide.

Greater oxide damage at the channel edges causes the current path to redistribute, influencing the hot-carrier lifetime. Experimental studies have difficulty resolving the location of oxide degradation. Estimates of hot-carrier lifetime from substrate current or threshold voltage shift measurements may be inaccurate due to the 3-D redistribution of the current path, which changes the rate of degradation. Existing numerical studies have used 2-D simulation. This paper announces a new, 3-D hydrodynamic T-CAD tool which can predict the detailed accumulation of interface and oxide traps over time and their influence on the hot-carrier lifetime. SIMaster solves the hydrodynamic model equations formulated in terms of new state variables especially tailored for the equation- and space-decoupled fixed-point iteration technique[1,2]. The gate current, interface state generation, and oxide trap generation are computed based on an electron distribution function fit to the average electron energy at successive time steps (Fig. 1). This model has been successfully used to model MOSFET reliability as well as EPROM and FLASH cell programming [3]. The model has been applied to a 0.25 μrn LOCOS-isolated MOSFET (Fig. 2). The stress condition was $V_D = 4.5V$, $V_G = 5.5V$ for a stress time $T_s = 10^6$s. The electron temperature in a 2-D slice at the center of the channel is shown in Fig. 3. The electron temperature in a slice immediately beneath the gate oxide is shown in Fig. 4. Fig. 5 shows the doping concentration, electron concentration, and electron temperature in the channel. The computed interface and oxide traps for each time step are shown in Fig. 6, which is a line across the center of the channel.

[1] D. C. Kerr and 1. D. Mayergoyz, "Simulation of Semiconductor Devices using the Fixed-Point Iteration Method on 3-D Unstructured Meshes," to appear, 1995.
[2] W. Liang, D. C. Kerr, N. Goldsman, and 1. D. Mayergoyz, "Hydrodynamic device Sirnulation using New State variables tailored for a block Gummel iterative approach," to appear, 1995.
[3] J. Z. Peng, Q. Lin, P. Fang, M. Kwan, S. Longcor, and J. Lien. "Accurate Simulation of EPROM Hot-Carrier Induced Degradation using Physics-Based Interface and Oxide Charge Generation Models," International Reliability Physics Symposiurn, pp. 154-160, 1994.

P39. 3-D Device Simulation Using Intelligent Solution Method Control, *Daniel C. Kerr and Isaak D. Mayergoyz, Department of Electrical Engineering, University of Maryland, College Park, MD 20742.* Numerical simulation of semiconductor devices requires the solution of a large, nonlinear, coupled system of discrete equations. The discretized variables of the model equations (Poisson. electron and hole current-continuity, *etc.)* are coupled both in equation space and in real space (see Fig. 1). Several solution methods which treat the coupling differently have been extensively developed: full-coupled (Newton), decoupled in equation space (Gummel), and decoupled both in equation and real space (fixed-point or Jacobi iteration) (see Fig. I(a)). Each solution method can be explained by using Fig. l(b). The Newton method includes all the coupling in equation and real space. The Newton method gathers together the variables from all the equations at all mesh points into one large matrix equation and solves it iteratively. The Gummel method gathers up the variables at all mesh points for each equation into different matrix equations and solves them iteratively. The fixed-point method doesn't use matrices at all. Instead, a single equation is solved and iterations are performed over all mesh points and all equations. Finally, the point-Newton method takes the variables for all the equations at only one mesh point into a small matrix and iterates over all mesh points. Each of these methods has its strengths and weaknesses for different simulation problems. For Newton's method, the advantage is a quadratic rate of convergence; disadvantages are it requires a good initial guess (not globally convergent) and a large computer memory. Gummel's method reduces the computer memory requirements, but this method will slow or fail for tightly coupled equations (high bias conditions). The fixed-point iteration method is globally convergent, not memory intensive, and inherently parallel; however, it suffers the problems of Gummel's method and slow convergence when the mesh points are tightly coupled. The new solution algorithm is illustrated in Fig. 2. After an initial guess is calculated, the degree of equation and space coupling between discretized variables is calculated, and the mesh points are partitioned into groups. The best available solver is applied to each group, and the iteration is over the groups. This approach avoids the weaknesses of each solver by matching its strengths to a narrowly tailored problem. The degree of equation coupling is measured by deviation from charge neutrality or inversion. For example, in a MOSFET, this assigns the channel region to equation-space

coupled solvers. The substrate points are quasi-neutral, so they are assigned to equation-space decoupled solvers. The degree of space coupling is measured by mesh nonuniformity and by strong current flows. Thus, the channel region will be solved using Newton's method, the depletion regions surrounding the source and drain will be solved using Gummel's method, and the rest by the fixed-point iteration method. This efficient and intelligent partitioning saves CPU time compared to any single method alone. This selective coupling approach has been integrated into the general 3-D device simulation program SIMAsTER [1]. Newton's method can be applied to very large meshes on engineering workstations by restricting it to the critical coupled points, which speed improvements over other methods. Rates of convergence and solution times will be given. and compared to standard simulation programs (PISCES-II).

Supported by the Semiconductor Research Corporation contract SJ-377.

[l] D.C. Kerr and 1. D. Mayergoyz, to appear, 1995.

P40. 3D Parallel Monte Carlo Simulation of GaAs MESFETs, *S. Pennathur, Can K. Sandalci, Cetin K. Koc, and S.M. Goodnick, Department of Electrical and Computer Engineering, Oregon State University, Corvallis, OR 97331.* We have investigated three-dimensional (3D) effects in sub-micron GaAs MESFETs using a parallel Monte Carlo device simulator, PMC-3D [1]. The parallel algorithm couples a standard Monte Carlo particle simulator for the Boltzmann equation with a 3D Poisson solver using spatial decomposition of the device domain onto separate processors. The 3D Poisson equation is solved iteratively in parallel using a red-black coloring scheme for up to one million grid points on distributed memory multiprocessor machines. For realistic 3D device structures, we find that the main performance bottleneck is the Poisson solver rather than the Monte Carlo particle simulator for the parallel successive overrelaxation (SOR) scheme employed in [1]. Thus parallel multigrid algorithms are studied and compared to the previous SOR implementation. The frequency dependent small signal parameters of a MESFET device have been studied as a test case of the 3D algorithm. Parameters such as the transconductance and output impedance are calculated through frequency domain analysis of the transient current response to small electrode voltage steps. The scaling properties of the small signal parameters have been simulated for both the gate width in the third dimension as well as the gate length. Deviations from the ideal linear scaling of the device gain with lateral scaling of the gate width are found associated with the 3D field and particle distribution in the structure.

[1] U.A. Ranawake, C. Huster, P.M. Lenders, and S.M. Goodnick, *IEEE Trans. on CAD,* Vol. 13, No. 6, 712 (1994).

P 41. Hydrodynamic Simulations: The Forced Notched Oscillator, and Channel Geometry in the MESFET, *Gui-Qiang Chen and Joseph Jerome, Department of Mathematics, Northwestern University, Evanston, IL 60208; Chi-Wang Shu, Division of Applied Mathematics, Brown University, Providence, RI 02912.* We introduce a novel two carrier hydrodynamic model, which has the capability of incorporating higher dimensional geometric effects into a one dimensional model, if symmetry is present. This abstract presents two special cases of the model, the first of which will be illustrated on the following two pages through simulations. For the GaAs device in the notched oscillator circuit, considered by the authors of [3], the model reduces to that first considered by Blotekjaer in [1], as a two valley hydrodynamic moment model. However, the critical form of the couplings is not discussed in [1], and is studied in detail here. We do not employ the actual circuit, but use an analogue sinusoidal forcing term for the bias at the drain, closely correlated to the resonant frequency of the circuit, which can be computed by analytical methods. We find that our concentration curves, illustrated for both valleys ($1=\Gamma$, $2=L$), share the structural features of [3], where the curves were computed by Monte-Carlo simulation. It is also apparent that the coupling threshold in the energy equation for the Γ valley is crucial for the inter-valley transfer between the carriers. We have performed simulations for different coupling thresholds with different results (not shown in the abstract). In fact, it is simply inadequate information about the couplings which limits the valleys to two in this modeling. We acknowledge with gratitude the extremely helpful advice of Umberto Ravaioli

for this part of the work. If the one carrier MESFET channel is geometrically idealized by a nozzle configuration, the model reduces to a one dimensional perturbed hydrodynamic model (one carrier). The perturbation is a geometric source term, proportional to the derivative of the cross sectional area of the channel. It has been found in transonic nozzle flow that this term assumes an important role in predicting possible shock structure, and we study its role in semiconductor modeling. Our algorithms are extensions of those described in [2].

[1] K. Blotekjaer, Transport equations for electrons in two-valley semiconductors, IEEE Trans. Electron Devices ED-17 (1970) 38-47.
[2] J.W. Jerome and C.-W. Shu, Energy models for one-carrier transport in semiconductor devices, in IMA Volumes in Mathematics and Its Applications. Vol.59, W. Coughran, J. Cole, P. Lloyd and J. White, eds., Springer-Verlag 1994 pp. 185-207.
[3] U. Ravaioli, C.H. Lee and M.B. Patil, AIonte Carlo simulation of microwave devices, manuscript.

P42. Transient Analysis of Silicon Devices Using the Hydrodynamic Model, *Luigi Colalongo, Marina Valdinoci, Antonio Gnudi, and Massimo Rudan, Dipartimento di Elettronica, Universitá, di Bologna, Viale Risorgimento 2, 40136 Bologna, Italy.* The analysis of the switching behaviour of submicron devices brings about the necessity of extending the solution of the Hydrodynamic Model to the transient case. The implementation of such model has been carried out and a few examples of simulation are presented here, showing the velocity-overshoot of a ballistic diode and the temperature spread in the drain region of a realistic MOS device. The Hydrodynamic Model (HD) in the transient case reads [1]:

$$
\begin{aligned}
&-\mathrm{div}(\varepsilon_s grad\varphi) = q(p - n + N_D^+ - N_A^-),\\
&\partial n/\partial t - div(J_n/q) = -U,\\
&\partial p/\partial t + div(J_p/q) = U, \quad (1)\\
&\partial(n\omega_n)/\partial t + div\left[-k_n gradT_n - (5/2)k_B T_n J_n/q\right] = \mathrm{E}\bullet J_n - \omega_n U - n(\omega_n - \omega_{bo})\tau_{\omega n}, \quad (2)\\
&\partial(p\omega_p)/\partial t + div\left[-k_p gradT_p + (5/2)k_B T_p J_p/q\right] = \mathrm{E}\bullet J_p - \omega_p U - p(\omega_p - \omega_{po})/\tau_{\omega p}, \quad (3)
\end{aligned}
$$

where $J_n = qD_n grad n + \theta\mu_n n\, grad(k_B T_n/q - \varphi)$, $J_p = -qD_p gradp + q\mu_p grad(k_B T_p/q - \varphi)$, T, τ_p, τ_ω are the temperature, momentum-relaxation time, and energy-relaxation time of the carriers, and $\omega = (1/2)m\upsilon^2 + (3/2)k_B T$ is the average kinetic energy. The remaining symbols have the usual meaning. This set of equations is discretized in space using the so-called Box *Integration Method.* The time derivatives are discretized using the Gear method which is an *A*-stable, *L*-stable method for stiff differential equations. The discretization yields at each time step a system of $5N$ algebraic equations, where N is the size of the discretization grid [1]. The system of non-linear equations is solved using the following scheme: first, the system of Poisson, electron- and hole-continuity equations is solved by a coupled Newton method, then the temperature is updated solving the energy-balance equations for electrons and holes. The external loop is repeated until the global convergence is reached, and the whole procedure is repeated at each time step. The solution scheme depicted above is easier to implement than the full Newton method coupling all equations; it has proven very stable and, supplemented with a quadratic projection algorithm, rather fast as well. The term $\mathrm{E}\bullet J$ is treated by the vectorial identity $\mathrm{E}\bullet J = -div(\varphi J) + \varphi div(J)$ [3], this leading to $\sum_{i\neq j} J_{ij}(\varphi_i + \varphi_j)/2$. This expression is easy to handle as the time dependence is not explicit: therefore, in the transient case there is no need to account for the time derivatives in div(J) and div(φJ). The simulations have been carried out using a two-dimensional version of the device-analysis program HFIELDS [1], supplemented with the method described above, first on a 0.5 μm, n^+-n-n^+ ballistic diode having a 0.35 μm n-region. The diode is initially at equilibrium, then it is biased by a linear ramp which brings the voltage drop between the contacts from 0 to 2 V in 1 psec; the voltage on this contact remains at 2 V for 1 μsec after the end of the ramp. It is worth noting that the duration of the ramp is about one order

of magnitude larger than the carrier momentum-relaxation time; for this reason the terms $\partial J/\partial t$ are dropped from the transport equations. On the contrary, the time derivatives are retained in (2,3) because the carrier energy-relaxation times are larger [2]. In any case the ramp is slow enough to allow for the steady-state approximation leading to Poisson's equation. Fig. 1 shows the normalized temperature at two different times 1 psec and 1 μsec. The first one is of the same order as $\tau\omega$ and corresponds to the instant at which the ramp reaches 2 V; at t = 1 μsec the transient is extinguished. The figure exhibits the delay in the temperature growth due to the time derivatives in (2,3). In Fig. 2 a velocity overshoot is observed at t = 1 psec, due to the fact that the momentum-relaxation time is smaller by about one order of magnitude than the energy-relaxation time. Because of this, the velocity increase is considerably faster than that of energy, as is seen in Figs. 1 and 2. As the carrier temperature grows, the velocity overshoot becomes less important. The features of the momentum and energy-relaxation times are reflected into the mobility model used in the HD equations, $\mu(\omega) = \mu_o / \left[1 + \alpha(\omega - \omega_o)\right] \alpha = \mu_o / (q\tau_\omega \upsilon_{sat}^2)$: in the first time intervals ($t < \tau_\omega$), while the temperature is still growing the mobility is in fact larger than in steady-state conditions. Figs. 3 and 4 show the electron concentration and the electric field, respectively, at the same time intervals and at equilibrium. Next, more simulations have been carried out on a realistic n-type, 0.8 μm channel MOS transistor. The source and gate voltages were set at 0 and 1 V, respectively. Starting from equilibrium, the drain voltage was first brought from 0 to 3 V using a 1-psec linear ramp, then kept at 3 V for 1 μsec. Figs. 5 and 6 show the normalized temperature at t = 1 psec, i.e., when the ramp reaches 3 V and, respectively, at the end of the transient. In the direction of the channel the results are qualitatively similar to those of the previous case: the temperature peak is initially localized in the channel region while, after the end of the ramp, it starts spreading to eventually reach the steady-state profile of Fig. 6. In addition, thanks to the two-dimensional analysis, the spread of the energy from the surface to the bulk is also evident in the figure.

[1] A. Forghieri et al., IEEE Transactions on Computer-Aided *Design,* Vol. 7, No. 2, 1988, pp. 231-242.
[2] G. Baccarani and M. Worderman, Solid-State Electronics, *Vol.* 28, No. 4, 1985, pp 407-416.
[3] A. Gnudi and F. Odeh, Proc. SISDEP, Vol. 3, Bologna, 1988, pp. 387-390.

P43. Numerical Simulation of Thermal Behavior in a Trench Emitter Insulated Gate Bipolar Transistor (IGBT), *L.Sabesan, P. Mawby, M.S. Towers, K. Board, P. Waind*, Department of Electrical & Electronic Engineering, University of Wales Swansea, Singleton Park, Swansea SA2 8PP, UK.; * GEC-Plessey Semiconductors, Carhome Road, Lincoln, LN1 1SG, UK.* The modelling of thermal effects in an IGBT structure is presented. The semiconductor equations are solved in two dimensions with physical effects such as carrier-carrier scattering mobility and SRH and Auger recombination included. I-V characteristics, carrier concentrations and temperature profiles have been investigated. Among the various power Bipolar and MOS transistors the IGBT provides better performance with respect to low on-resistance and low gate drive requirements. Further, IGBTs offer better high-temperature forward conduction characteristics by being less sensitive to temperature variation in comparison to other power devices [2,3]. This feature makes the device attractive for applications in which high ambient temperatures may be encountered. The main drawback in the device is its tendency to latchup at high current levels. This limits the operation of the device within a range determined by various structural and material parameters. In order to overcome this, a new device structure, the trench emitter configuration, has been considered and is reported here. The schematic structure of the device is shown in figure 1. This structure is seen to be slightly different from conventional IGBT structures shown in references [3-8]. In order to eliminate the possibility of punch-through in the device, a buffer layer has been introduced between the substrate and the n-base region. The thick lightly doped epitaxial layer is necessary to support high voltages in the forward blocking mode. However, it also contributes to a large on-state resistance. This paper analyses the dependence of the operating characteristics and the internal carrier distributions on the ambient temperature under isothermal conditions and considers the effects of Joule heating and recombination in the non-isothermal case. The simulations were carried out using the 2-D Swansea University Device Simulator (SUDS). The resulting spatial current density, electric field and recombination effects in the device were used to calculate the heat dissipation distribution. The heat

equation was then solved to provide the temperature profile self consistently. The temperature dependence of thermal conductivity in silicon was also considered in the calculation. The low on-resistance essential in all power devices is achieved in IGBTs through high injection of electrons and holes into the n-base drift region thereby causing conductivity modulation. The simulated output characteristics are shown in figure 2, together with measured results. As can be seen a very good qualitative and quantitative agreement has been obtained. Figure 3 shows the influence of ambient temperature on the output characteristics at a gate bias of 15 V under simple isothermal conditions. This shows the voltage drop increasing with temperature due to the increase of resistance from 0.01 ohm at 300K to 0.03 ohm at 500K. The change, however is relatively small compared to that in MOSFET [2]. Similar findings were observed in measurements and reported in references [2],[3]. Figure 4 shows the effect of temperature variation on the distribution of carrier concentration through a vertical cut at x = 10 microns with biases of 15 V on the gate and SV on the anode. Reduction in electron and hole concentrations can be seen with increasing temperature. Any increase in temperature severely reduces the mobility of the carriers, more significantly in the drift region. Figure 5 shows the effect of temperature variation on the hole mobility through the same vertical cut with the same biases as stated for figure 4. This is the dominant mechanism for the reduction of current at higher temperatures. The temperature distribution throughout the domain caused by self heating is shown in figure 6. A small hot spot can be seen near the gate-emitter region. This is caused mainly by high Joule heating due to locally increased electric field and current density.

This work is supported by EPSRC and is a part of a LINK PEDDS scheme.

[1] S. Selberherr, Analysis of semiconductor devices, 2nd Edn., Wiley, New York (1981).
[2] B. Jayanth Baliga, 'Temperature Behaviour of Insulated Gate Transistor Characteristics', Solid State Electronics, Vol.28, pp 289-297 (1985).
[3] B. Jayant Baliga, 'Modern Power Devices', 1st Edn., John Wiley & Sons, Canada (1987).
[4] K. Board, Z.-R. Hu,'New Latch-Up-Free IGBT with Low On-Resistance', Electronics Letters, Vol.29, 18, pp. 1664-1666, 2nd September 1993.
[5] J. Zeng, P. A. Mawby, M. S. Towers, K Board and Z.-R. Hu, 'Design of IGBTs for Latch-Up Free Operation', Solid-State Electronics,Vol.37, 8, pp. 1471-1475 (1994).
[6] Johnny K.O. Sin and Satyen Mukherjee, 'Analysis and Characterization of the segmented Anode LIGBT', IEEE Transactions on Electron Devices, Vol. 40, 7, pp. 1300-1305, July 1993.
[7] Di-Son Kuo and Chenming Hu, 'Optimization of Epitaxial Layers for Power Bipolar-Mos Transistor', IEEE Electron Devices Letters, vol. EDL-7, 9, pp 510-512, September 1986.
[8] K. Heumann and M. Quenum, 'Second Breakdown and Latch-Up Behaviour of IGBTs', EPE Conference, Brighton, UK. 13-16.9.1993.

P44. Monte Carlo Simulation of a Submicron MOSFET Including Inversion Layer Quantization, *J.B.Roldán, F.Gámiz, J.A.López-Villanueva and J.E.Carceller, Departamento Electrónica y Tecnología Computadores, Universidad de Granada, 18071 Granada, Spain.* A simulation of a submicron MOSFET by Monte Carlo method including inversion layer quantization has been done. The simulator has been applied to the study of electron transport in normal operation conditions. The device is divided into a convenient number N of smaller channels (μchannels) of unknown length. The difference between the pseudofermi levels is fixed in the extremes of each μchannel. The one-dimensional Poisson and Schrödinger equations are then self-consistenly solved in each of these points. The length of each μchannel is iteratively calculated by imposing the current continuity along the MOSFET channel. Both drift and diffusion components are taken into account in a modified charged sheet model in order to evaluate the drain current. The resultant potential distribution is used as the starting point to iteratively solve the two-dimensional Poisson equation. Following, both the current and length of each μchannel are again calculated. This procedure is repeated until a convergence criteria is reached. An adaptive grid is used along the channel. In each point, the electron scattering rates, and the longitudinal electric field are evaluated. To proceed in the Monte Carlo simulation, a great number of electrons are introduced, one by one, in the channel from the source. Then, they move towards the drain drifted by the longitudinal electric field, undergoing phonon, Coulomb and surface-roughness scattering. Different electron transport

properties are calculated from the mean time each electron spends in every grid zone. Some results for a 0.2μm channel length MOSFET are shown in the attached figures.

TA5. Analysis of Anomalous-Negative Differential Resistance in Diode Breakdown Simulation Using Carrier Temperature Dependent Impact Ionization, *Edwin C. Kan, Zhiping Yu and Robert W. Dutton, AEL 201, Stanford University, Stanford, CA 94305.* In recent years, the drift-diffusion (DD) model has been extended to the energy transport (ET) model and the hydrodynamic (HD) model to account for the elevated average energy in the carrier systems at high fields. Inclusion of electron and hole temperatures as state variables allows transport coefficients such as mobility and impact ionization rate as functions of the carrier temperatures instead of the local electric field to remove the thermal equilibrium approximation [1]. However, this new parametrization of the transport coefficients has received controversial criticisms. Although much success has been achieved in fitting specific experiment measurements, especially in MOSFET substrate current cases (e.g., [2]), it has also been established that the distribution function, in particular the tail part that determines the impact ionization and MOSFET gate current, is not well characterized by the carrier concentration and average energy alone [3, 4]. Nevertheless, if the impact ionization rates are chosen as functions of the carrier temperatures, for the first time we have observed an anomalous negative differential resistance (NDR) in a simple pn junction breakdown simulation. Mechanisms that cause this NDR are analyzed below. The reverse-bias diode IV curves using field and energy dependencies for the mobility μ and the impact ionization rate *a* are shown in Fig. 1. The simulation is performed by PISCES-2ET with curve tracing techniques [5] to capture NDR. The DD model with *a(F)* does not have any NDR region and the breakdown voltage is close to the measured data. At the onset of breakdown, which is highlighted in Fig. 2, the ET model with $a(T_c)$ and $\mu(T_c)$ already shows a small NDR, while the ET model with $a(T_c)$ and $\mu(F)$ does not. This is due to the cooling mechanism of impact ionization [6] that gives a positive feedback for enhancement of $\mu(Tc)$, since asymptotically μT_c^{-1} for velocity saturation. This small NDR will disappear if $\mu(F)$ is used or the cooling mechanism is not accounted for in the carrier energy balance equation. In addition, significant NDR in the high current region appears in both ET models as long as both $a_n(T_n)$ *and* $a_p(T_p)$ are used. This NDR cannot be attributed to the previous cooling mechanism since the feedback is removed ill the case of $\mu(F)$, but is possibly caused by the Joule-heat feedback to the carrier temperature or the dislocated $a_n(T_n)$ and $a_p(T_p)$. *As* can be seen in Fig. 3, in the depletion region the peaks of T_n *and* T_p are offset by a small distance [6]. The multiplication factor *M* defined by the ratio of outgoing and incoming electron (or hole) currents in the depletion region can be expressed as [7]:

$$1-\frac{1}{M}=\int_0^W \alpha_n \exp\left[-\int_x^W(\alpha_n-\alpha_p)dx'\right]dx \qquad (1)$$

If $\alpha_n(x)\equiv\alpha_p(x)$, the breakdown condition as $M\rightarrow\infty$ is simply $\int_0^W\alpha=1$ and no NDR is possible. However, if $\alpha_n(x)\neq\alpha_p(x)$, the reverse breakdown current is affected by the convolution of α_n and α_p, and NDR can exist based for different T_n and T_p profiles. More details will be presented at the conference. Besides, it can be observed that the breakdown voltage predicted by $\alpha(T_c)$ is much larger than that by *a(F)[9].* This can be understood from two aspects. First, when only one carrier is considered (as in nin cases of Fig. 4), the generation rate calculated by $a(T_c)$ is smaller than *a(F)* due to the latent effect from *dF/dx* (note that in the bulk case, $\alpha(T_c)\equiv\alpha(F)$ by definition). Second, if the peaks of a_n and a_p are dislocated, the integral in (1) will be damped when $a_n > a_p$ (similar calculations hold for holes too).

[1] B. Meinerzhagen and W.L. Engl, IEEE Trans. Electron Devices, Vol. 35, No. 5, pp. 689-697, May 1988.

[2] J.W. Slotboom, et.al., IEDM Tech. Dig., 1991, p. 127.

[3] S. Ramaswamy and T. Tang, IEEE Trans. Electron Devices, Vol. 41, No. 1, pp. 76-83, Jan. 1994.

[4] J.-G. Ahn, et.al., IEEE Electron Dev. Lett., Vol. 15, No. 9, pp. 348-350, Sept. 1994.

[5] Z. Yu, D. Chen, L.L. So and R.W. Dutton, PESCES-2ET Manual, Stanford University, 1994.

[6] W. Quade, M. Rudan and E. Schöll, IEEE Trans. CAD, Vol. 10, pp. 1287-1294.

[7] S.M. Sze, Physics of Semiconductor Devices, 2nd Ed., New York: John Wiley, 1981, Chap. 2.

[8] H.J. Peifer, B. Mainerzhagen, R. Thoma and W.L. Engl, in IEDM Tech. Dig., pp. 131-134, 1991.
[9] Y. Apanovich, et.al., Proc. 3rd Intl. Workshop Comp. Elec., Portland, May 1994.

TA6. Statistical Enhancement of Terminal Current Estimation for Monte Carlo Device Simulation, *P.D. Yoder, U. Krumbein, K. Gärtner, and W. Fichtner, Swiss Federal Institute of Technology, Integrated Systems Laboratory, Gloriastrasse 35, CH-8092 Zürich, Switzerland.* To account for capacitative effects and to improve upon the poor convergence properties of the particle counting method, terminal current estimators may be devised which make use of information about all particles within a given device. One such formalism was developed by Shockley [1] and Ramo [2], relating the currents induced on an arbitrary number of terminals to the motion of charges in multiple dimensions. For use in semiconductor device simulation, this approach has several drawbacks. We present theory and applications of a new generalized domain integration technique for Monte Carlo simulation, which in contrast 1) accelerates convergence by minimizing the terminal current estimator variances, 2) is valid for time-dependent or steady-state calculations, 3) differentiates between electron, hole and displacement currents, and 4) reduces to the Ramo-Shockley theorem as a special use. Simulated charge density and velocity information, such as shown in Fig. 1, is integrated against a special weighting function throughout the domain for each bias condition, to obtain I-V curves like the one shown in Fig. 2. Figure 2 also demonstrates the accelerated convergence rates for source, drain and substrate currents which may be achieved with this technique. Finally, we show how this method may be applied to "window"-type Monte Carlo simulation.

[1] W. Shockley, "Currents to Conductors Induced by a Moving Point Charge," Journal of Applied Physics, Vol. 9, pp. 635-636, 1938.
[2] S. Ramo, "Currents Induced by Electron Motion," Proceedings of the IRE, Vol. 27, pp. 584-585, 1939.

TA7. New Approach to Hot Electron Effects in Si-MOSFETs Based on an Evolutionary Algorithm Using a Monte Carlo-Like Mutation Operator, *J. Jakumeit, U. Ravaioli, K. Hess, Beckman Institute, University of Illinois, Urbana, IL 61801.* A new approach to study gate and substrate current in Si-MOSFETs is introduced, which is based on a mixture of evolutionary optimization algorithms and Monte Carlo technique. The goal is to develop an algorithm for the investigation of hot electron effects in Si-MOSFETs, which is less complex and computationally expensive than a full band Monte Carlo program, yet gives more precise information than lucky electron or electron temperature models and can thus be used as a mediator between precise theory and experimental results. To achieve this goal, use is made of an evolutionary optimization algorithm EA [1] to search for electron distribution functions *f(E, x),* which fit a given substrate current I_{sub}^{goal} .I_{sub}^{goal} will usually be an experimental result. The EA searches for the correct *f(E,x)* by starting from a set of initial guesses for *f(E,x).* In each iteration new guesses are created by modifying the old guesses with help of a Monte Carlo-like mutation operator. From the old and new guesses a new set of distribution functions is selected by simulated annealing-like selection criteria. In this way the set of distribution functions converges towards an appropriate solution. The algorithm stops, if I_{sub} calculated from *f(E, x)* lies within 0.1% of I_{sub}^{goal}. The results of this new approach are distribution functions for the region of interest in terms of gate and substrate current, which can be compared to results of a full band Monte Carlo method with enhancement of the high energy tail of the distribution. If I_{sub}^{goal} is not consistent with the physical model inside the mutation operator, the algorithm does not converge or gives unphysical results. An important advantage of the EA is that even very simplified mutation operators will drive the search for the distribution function in the correct direction. The use of a goal function such as I_{sub}^{goal} (*f(E,* x)) guarantees a reasonable estimate particulary for the portion of the distribution function that is responsible for I_{sub}^{goal}. The energy distribution obtained in this way can then be used to assess the validity of simpler models (e.g. electron temperature) and can also be directly compared to results of full band Monte Carlo simualtions. First results indicate that this method can also be used to derive relationships between gate and substrate currents, that are superior to the ones derived from electron temperature and

lucky electron models. Our new method may therefore bridge the gap between these simplified models and full band approaches for considerations of hot electron effects on device reliability.

[1] J. Jakumeit, Appl. Phys. Lett. 66, 1995, p. 1812.

WA1. Absorbing Boundary Conditions for Quantum Evolution Equations, *Anton Arnold, Department of Mathematics, Purdue University, West Lafayette, IN.* When numerically solving a whole-space evolution problem, the computation has to be confined to a finite domain by introducing artificial boundary conditions. Numerically transparent or absorbing boundary conditions (ABC) have first been derived by Engquist & Majda for hyperbolic systems by requiring that outgoing waves can leave the computational domain without being reflected back in. This talk will be concerned with the construction, analysis, and discretization of ABC's for the (transient) Schrödinger equation and the (relaxation-time) Wigner equation. Under the assumption of a homogeneous medium (i.e. constant potential) outside of the computational domain one can derive a transparent BC for the Schrödinger equation. In ID it relates the normal space derivative of the wave function at the boundary to its fractial (1/2) time derivative, which can be written as a memory term involving the past evolution. In 2D the transparent BC is also non-local in space. For numerical efficiency, it therefore has to be approximated by an ABC that is at least local in space. When using the Crank-Nicolson scheme for the Schrödinger equation we will discuss an accurate discretization of this BC, which is constructed as an ABC for the discrete problem. We will analyze the numerical stability of this BC and present numerical tests. An extended model, formulated on the level of density matrices, allows to prescribe incoming wave packets at the contacts in combination with absorbing the outgoing waves. In the classical limit (h -> 0) this BC corresponds to an inflow BC for a kinetic equation. Finally we will discuss ABC's for the Wigner equation. Such BC's have been used for the numerical simulation of resonant tunneling diodes via the relaxation-time Wigner-Poisson equation. Most of these studies focused on the steady state behavior of the device for an applied voltage. The known ABC's for the Wigner equation, however, are only valid for short-time transient calculations and do not guarantee the convergence towards the correct quantum steady state. We will present and analyze the long-time modifications of these ABC's for the relaxation-time Wigner equation that are appropriate for the convergence to the steady state.

WA2. Modeling Nonlinear and Chaotic Dynamics in Semiconductor Device Structures, *Eckehard Schöll, Institut für Theoretische Physik, Technische Universität Berlin, Hardenbergstr. 36, 10623 Berlin, Germany.* Semiconductors represent complex nonlinear dynamic systems whose electrical transport properties may exhibit a variety of instabilities [1-3]. They often involve switching behavior, self-generated regular or chaotic current oscillations, current filamentation and solid-state turbulence. In this paper we review the modeling and simulation of such instabilities with a special emphasis on recent progress in the application to semiconductor microstructures. Our approach involves combinations of semiclassical Monte Carlo simulations and hydrodynamic balance equations. In the center of interest is the nonlinear spatio-temporal dynamics of the coupled system of charge carriers and electric field. The following model systems are treated in detail: (i) The dynamics of current filaments in the regime of low-temperature impurity breakdown in p-Ge and n-GaAs is studied. The chaotic behavior of laterally travelling filaments in crossed electric and magnetic fields is considered as well as the 2D simulation of the nascence of a filament upon application of a bias voltage [4]. The transport parameters including impact ionization and capture rates are calculated by a single particle Monte Carlo technique, while the spatio-temporal dynamics is obtained self-consistently from the carrier continuity and Maxwell's equations. (ii) Vertical electrical transport in layered semiconductor structures like the heterostructure hot electron diode (HHED) is considered [5]. Periodic as well as chaotic spatio-temporal spiking of the current is obtained and analyzed with sophisticated tools from nonlinear dynamics. In particular we find long transients of spatio-temporal chaos preceding regular spiking. (iii) Vertical transport in a superlattice is modeled for high fields [6]. Self-generated current oscillations or the formation of stable stationary electric field domains is found. We demonstrate that this behavior is strongly affected by growth-related imperfections and weak disorder.

[1] E. Scholl, Nonequilibrium Phase Transitions in Semiconductors (Springer, Berlin 1987; Russian Translation: Mir, 1991).
[2] M.P. Shaw, V.V. Mitin, E. Scholl, and H.L. Grubin, The Physics of Instabilities in Solid State Electron Devices (Plenum Press, New York 1992).
[3] E. Scholl, Nonlinear Dynamics, Phase Transitions and Chaos in Semiconductors. In: Handbook on Semiconductors, Vol. 1, Ch. 8, 2nd edition, ed. by P.T. Landsberg (Elsevier, Amsterdam 1992).
[4] M. Gaa, R.E. Kunz, E. Scholl, International Conf. Hot Carriers in Semiconductors, Chicago, 1995.
[5] S. Bose, A. Wacker, E. Scholl, Phys. Lett. A 195, 144, 1995.
[6] F. Prengel, A. Wacker, E. Scholl, Phys. Rev. B 50, 1705, 1994.

WA3. Studies of Chaotic Transport of Electrons in Quantum Boxes, *D. K. Ferry and G. Edwards, Department of Electrical Engineering, Arizona State University, Tempe, AZ 85287-5706.* Recent studies of transport through ballistic quantum dot resonators have revealed a complex array of behavior, including the existence of "universal" conductance fluctuations which are presumed to arise not from disorder scattering, but from the chaotic behavior of the underlying classical dynamics [1,2]. In this paper, the results of studies on the classical ballistic transport of carriers, supposedly within a quasi-two-dimensional electron gas, through a 1.0 micron square structure in a magnetic field are presented. The boundary on one side is modified in a manner that both prohibits straightthrough trajectories. The presence of the hard walls, connecting wires, and a magnetic field are thought to combine to introduce chaos in the structures. Results for B=0.01 T are shown in the attached figures. We will also discuss the effects of interelectronic scattering in the fully interacting limit.

Work supported by NEDO under the International Joint Program "Nanostructures and Electron Waves Project".

[1] C.M. Marcus, R.M. Westervelt, P.F. Hopkins, and A.C. Gossard, Phys. Rev. B 48, 2460 (1993).
[2] J.P. Bird, K.Ishibashi, D.K. Ferry, R.Newbury, D.M. Olatana, Y. Ochiai, Y. Aoyagi, and T. Sugano, to be published.

WA4. Simulation of Quantum-Dot Structures in Si/SiO2, *Minhan Chen and Wolfgang Porod; Department of Electrical Engineering, University of Notre Dame, Notre Dame, IN 46556.* We present numerical simulations for the design of gated few-electron quantum dot structures in the Si/SiO2 material system. The motivation for this work is to investigate the feasibility of transferring the emerging technology of quantum dot fabrication from the III-V material system, where it was pioneered over the past few years, to the technologically more important si/siO2 structures. Our main emphasis is on the realization of coupled quantum dot structures, so-called *Quantum Cellular Automata* [1], in silicon. Si appears to be a promising candidate due to the excellent insulating behavior of thin siO_2 films which yields the required crisp gate-control of the potential in the plane of the two-dimensional electron gas at the Si/SiO_2 interface. In our simulations, the confining potential is obtained from the Poisson equation with a Thomas-Fermi charge model. Following our previous work [2,3], the electrostatic potential is obtained both in the semiconductor domain and in the dielectric above. The electronic states in the quantum dot are then obtained from solutions of the axially symmetric Schrödinger equation. We explore various gate configurations and biasing modes. Our simulations show that the number of electrons can be effectively controlled in the few electron regime, especially by the use of separately-biased dual-gate structures.

This work has been supported by the Advanced Research Projects Agency through the Office of Naval Research.

[1] C.S. Lent, P.D. Tougaw, W. Porod, and G.H. Bernstein, Nanotechnology 4, 49 (1993); C.S. Lent, P.D. Tougaw, and W. Porod, Appl. Phys. Lett. 62, 714 (]993); P.D. Tougaw, C.S. Lent, and W. Porod, J. Appl. Phys. 74, 3558 (1993).
[2] M. Chen, W. Porod, and D.J. Kirkner, J. Appl. Phys. 75, 2545 (1994).
[3] M. Chen and W. Porod, J. Appl. Phys. (July, 1995).

WA5. Adiabatic Switching of Quantum Cellular Automata, *Craig S. Lent and P. Douglas Tougaw, Department of Electrical Engineering, University of Notre Dame, Notre Dame, IN 46556.* We have previously proposed a way of using coupled quantum dots to construct digital computing elements. Cells composed of a few quantum dots which are tunneling-coupled are occupied by few electrons. The Coulomb interaction within the cell produces two possible ground states with quite different charge alignment within the cell. The actual ground state is determined by the Coulombic (non-tunneling) interaction with neighboring cells. In this way a cellular-automata-like architecture can be built up. We have shown that the ground state of an inhomogeneous cellular array can be mapped onto the solution of a logical or arithmetic problem using this quantum cellular automata (QCA) approach [1]. Here we will examine the problem of switching such QCA arrays. Abrupt switching has been discussed in the past and relies on intrinsic dissipative processes to relax the array to its new ground state. However, a clocked switching mode with a controlled time-to-solution may be desirable. We consider here switching the array slowly so that it is, at each point in time, in the instantaneous ground state. We will present results of direct time-dependent solutions of the few-electron Schrödinger equation which show that such adiabatic switching is possible. The calculations are enabled by a novel use of operator-overloading methods in Fortran 90. Implications for possible future device architectures using adiabatic QCA arrays are discussed.

[1] P. Douglas Tougaw and Craig S. Lent, J. Appl. Phys. 75, 1818 (1994).

WA6. Analysis of Q_0-Independent Single-Electron Systems, *Alexander N. Korotkov and Konstantin K. Likharev, Department of Physics, State University of New York at Stony Brook, NY 11794-3800.* Fractional background charge Q_0 is a major problem of the applied single-electronics. Most of single-electronic devices suggested so far (see, e.g., Ref. 1) require a definite value of Q_0 with the margins of the order of $\pm 0.1e$. In spite of evidence of relaxation of the background charge in some experiments, conditions of such relaxation are not yet clear. The goal of this work was to analyze in detail two single-electron digital systems which may operate at random values of the background charge. Both systems are using the periodic dependence of the current in the single-electron transistor on the gate voltage, and hence its ability to perform several oscillations, regardless of the background charge, when fed by a gate pulse. These oscillations may be easily sensed using ordinary FET amplifier, located at a relatively small distance L from the SET transistor (for example, for a realistic output SET resistance of $100k\Omega, a \sim 1 - Gb/s$ bandwidth may be provided at $L \leq 100\mu m$). The first system we have considered is a DRAM, were a few-electron charge *(~lOe)* may be written into the initially empty trap [1] by application of the voltage pulse to the trap array. Our results show that room temperature operation and density in excess of 10^{11} bits/cm^2 may be achieved in such RAMs, using ~l-nm nanolithography. The similar principle may be applied to superdense (up to ~10^{12} bit/cm^2) data storage in a layer of ultrafine conducting grains (D~1 nm) separated from the conducting substrate by a ~10-nm-thick insulator. Binary data may be written into the grains as extra few-electron charges, using signal voltage applied to a head (tip) moving close to the surface. Readout of the data may be performed with the same tip carrying the SET/FET transistor pair discussed above. In our report, methods and results of geometrical analysis and numerical simulation of these two systems will be presented in detail.

The work was supported in part by AFOSR and ONR/ARPA.

[1] D.V. Averin and K.K. Likharev, in: Single Charge Tunneling, ed. by H. Grabert and M. Devoret (Plenum, New York, 1992), p. 311.

WA7. Corrections to the Capacitance Between Two Electrodes Due to the Presence of a Quantum Confined System, *M. Macucci, Dipartimento di Ingegneria dell'Informazione, Via Diotisalvi, 2 I-56126 Pisa, Italy; and Karl Hess, Beckman Institute, 405 N Mathews, Urbana, IL 61801.* For structures enclosing low-dimensional systems the classical concept of differential capacitance needs to be augmented with quantum corrections that include the effects of confinement energy. Luryi first approached the problem by deriving the quantum capacitance contribution for the 2D electron gas of an infinite MOS structure. Our aim is to extend this concept to more complex situations, characterized by additional degrees of confinement, and to determine whether quantum corrections may play a significant role in scaled-down classical devices. Our approach is based on the evaluation of the free energy of the combined device plus voltage source system, a method often used in Coulomb Blockade studies. By minimizing the free energy, we can determine the number of electrons in the quantum system (2DEG, quantum dot, etc.) for a given applied voltage and the thresholds for the addition of each electron. A few simple cases can be treated analytically, and we show, as an example, that Luryi's formula can be retrieved. The case of the 2D electron gas is particularly simple, because of the quadratic dependence of the confinement energy on the number of electrons: this makes possible to consider an equivalent circuit including a "quantum capacitor". If further confinement is added such as in the case of a quantum dot, this quadratic dependence disappears, and it is not possible to resort to simple equivalent circuits. A numerical approach, which also allows the study of more realistic models becomes necessary. We solve the Schrödinger and Poisson equations self-consistently in structures with cylindrical symmetry, thus obtaining the electron eigenvalues and eigenfunctions in the quantum dot and the charge induced on the electrodes, from which the free energy and thereby the tunneling thresholds of each electron can be computed. The differential capacitance is finally derived by taking the ratio of the variation of charge induced on the electrodes to that of the bias voltage.

WA8. Simulation of Dissipative Quantum Transport in Electron Distributed Bragg Reflectors, *Leonard F. Register and Karl Hess, Beckman Institute and Coordinated Science Laboratory, University of Illinois at Urbana-Champaign, 61801.* The effects of inelastic scattering on carrier transport through electron distributed Bragg reflectors (electron DBRs)[1,2] is simulated using both "Schrödinger equation (based) Monte Carlo" (SEMC)[3-5] and, more simply, a complex absorbing potential approach to scattering [5]. Analogous to optical DBRs, electron DBRs employ interference among the relatively weak partial reflections of the electron wave function at each heterointerface to achieve an overall high reflectivity. However, inelastic scattering processes in semiconductors limit the phase coherence length of the electron wave function, and, thus, can be expected to limit the reflectivity of electron DBRs. SEMC and the complex "absorbing" potential model allow simulation of such coherence limiting dissipative quantum transport. SEMC is specifically formulated to allow first-principles simulation of dissipative quantum transport and is rigorously quantum mechanical. However, the numerical algorithm has much in common with semiclassical Monte Carlo methods. For carrier-phonon interactions, a set of Schrödinger equations is solved simultaneously (and deterministically) for the carrier, with the individual equations corresponding to the discrete initial or "trunk" state and various final or "branch" states of the phonon system, with energies separated by plus or minus the phonon energy for phonon absorption and emission, respectively. Only the non-local coupling potentials between the trunk and branch states are obtained by Monte Carlo sampling, of (the spatial correlation functions of) the carrier-phonon interactions [3]. In contrast, the use of absorbing potentials within Schrödinger's equation in lieu of the branch states to represent scattering, allows more simple and efficient if less rigorous modeling of the loss of phase coherence [5].

---

[1] F. Capasso, C. Sirtori, J. Faist, D. L. Sivco, Sung-Nee G. Chu and A. Y. Cho, Nature, 358, 13 August 1992.

[2] C. Sirtori, F. Capasso, J. Faist, D. L. Sivco, Sung-Nee G. Chu and A. Y. Cho, Appl. Phys. Lett. 61, (1994).

[3] L. F. Register and K. Hess, Phys. Rev. B 49, 1900 (1994).

[4] K. Hess, L.F. Register and M. Macucci, in Proceedings of the 2nd International Symposium on Quantum Confinement: Physics and Applications, ed. by M. Cahay, S. Bandyopadhyay, J.P. Leburton, A. W. Kleinsasser and M. A. Osman (The Electrochemical Society, 1994) Vol. 94, 17, pp. 3-17.
[5] L.F. Register and K. Hess, to be presented at the Eight International Conference on Superlattices, Microstructures and Microdevices, Cincinnati, August 20-25, 1995.

WPA1. The Coupled Optoelectronic Problems of Quantum Well Laser Operation, *Karl Hess and Matt Grupen, The Beckman Institute, Department of Electrical and Computer Engineering, University of Illinois, 405 N. Mathews Ave., Urbana, IL 61801.* The optical output of a quantum well laser depends on several different physical processes. These include classical carrier transport, mesoscopic transport over a quantum structure, intrasubband scattering, quantum confinement, radiative recombination, and electromagnetic wave guiding. Each process is important to laser operation, and each poses a complex theoretical problem. The different optics and electronics related problems associated with laser operation have been treated separately and independently in great detail. Simulators have been developed to calculate classical transport throughout an entire two-dimensional laser cross section [1]. Other sophisticated codes have been developed to determine the reflection and transmission of carriers incident on a quantum well [2] and the scattering dynamics of bound carriers [3]. Still, other research has been conducted on the band structure within a quantum well and the matrix elements associated with optical transitions [4]. Also, considerable work has been done on the accurate solution of Maxwell's equations in a dielectric wave guide [5] and on emission from a microcavity [6]. However, these separate treatments cannot reveal how these different problems couple and how their interaction affects laser operation. A laser simulator Minilase II has been developed to address all of the aforementioned problems self-consistently and completely coupled within the limits of workstation computational capacity. This paper will describe the ways in which these problems are modeled and the methods used to couple them. It will also present certain results that highlight coupling between different physical processes and which, therefore, can only be obtained through such a self-consistent approach.

---

[1] Z.-M. Li et al., IEEE J. Quantum Electron., 28 (4), p. 792, 1992.
[2] F. Register and K. Hess, Phys. Pev. B. 49 (3), p. 1900, 1994.
[3] L. Rota et al., submitted to Proc. Ninth International Conf. Hot Carriers in Semicon., Chicago, 1995.
[4] M.S. Hybertsen et al., submitted to Proc. SPIE, 2399, San Jose, CA, 1995.
[5] A.T. Galick et al., IEEE Trans. Micro. Tech., 40 (4), p. 699, 1992.
[6] L.F. Register et al., Appl. Phys. Lett., 66 (3), p. 259, 1995.

WPA2. Modeling Light-Extraction Characteristics of Packaged Light-Emitting Diodes, *D. Z.-Y. Ting and T. C. McGill, Thomas J. Watson, Sr. Laboratory of Applied Physics, Mail Stop 128-95, California Institute of Technology, Pasadena, California 91125.* We employ a Monte Carlo ray tracing technique to model light-extraction characteristics of light-emitting diodes. By relaxing restrictive assumptions on photon traversal history, our method improves upon available analytical models for estimating light-extraction efficiencies from bare LED chips, and enhances modeling capabilities by realistically treating the various processes which photons can encounter in a packaged LED. Our method is not only capable of calculating extraction efficiencies, but can also provide extensive statistical information on photon extraction processes, and predict LED spatial emission characteristics. Preliminary results from a sample parametric study indicate that simulations using our method can be performed very rapidly on modern workstations. We expect that, with some refinement, our method could be used as a computer-aided design tool for optimizing light-extraction efficiencies, and for designing LED spatial emission characteristics.

WPA3. Gain Calculation in a Quantum Well Laser Simulator Using an Eight Band k . p Model, *F. Oyafuso, P. Von Allmen, M. Grupen, K. Hess, Beckman Institute, University of Illinois, Urbana, IL 61801.* Gain spectra for a strained-layer $Ga_{.8}In_{.2}As/Al_{.1}Ga_{.9}As$ quantum well laser are calculated using an eight

band **k . p** model. Effects of non-parabolicity of the energy dispersion are entered in a QW laser simulator (MINILASE-II). The **k . p** calculation yields the bandstructure and momentum matrix elements for a superlattice grown along the [001] direction. The calculation works within the envelope function approximation, where the envelope functions are expanded in a plane wave basis. The barrier between the wells of the superlattice is made sufficiently large so that the bound state solutions are expected to match those of a single quantum well. The **k . p** results are then exported to MINILASE-II in the form of a density of states and an energy-dependent averaged momentum matrix element. The matrix elements are averaged over the entire ID mini-band Brillouin zone and the set of in-plane wave vectors corresponding to a given pair of initial and final energies. For each transition energy, many pairs of conduction and valence band states can contribute because of the anisotropy and multivalued nature of the band structure. A broadening factor is introduced within the laser simulator. To reduce computation time, the calculations are coupled to Poisson's equation within MINILASE-II. In other words, a flat band approximation is assumed for the **k . p** calculation, and the resulting density of states is pinned to the lowest subbands calculated within MINILASE-II. Results will be presented for the gain and modulation response using this model for a TE optical field and will be compared with the results obtained from a simple parabolic Kane model with a constant matrix element.

WPB1. Moving Adaptive Unstructured 3-D Meshes in Semiconductor Process Modeling Applications, *Harold Trease, Andrew Kuprat, Denise George, Eldon Linnebur, Los Alamos National Laboratory, and R. Kent Smith, AT+T Bell Laboratories.* The next generation of semiconductor process and device modeling codes will require 3-D mesh capabilities including moving volume and surface grids, adaptive mesh refinement and adaptive mesh smoothing. To illustrate the value of these techniques, a time dependent process simulation model was constructed using analytic functions to return time dependent dopant concentration and time dependent SiO_2 volume and surface velocities . Adaptive mesh refinement and adaptive mesh smoothing techniques were used to resolve the moving boron dopant diffusion front in the Si substrate. The lower SiO_2 surface was modeled as a moving surface grid which advanced through the background grid, converting the polysilicon and silicon in its path to SiO_2. An interesting problem addressed in the moving surface implementation of the oxide expansion was maintaining material interfaces by reapplying the material region definitions at each time step. The expanding volume of SiO_2, in turn, pushed the unreactive nitride mask ahead, requiring that the nitride region be treated as an incompressible volume. The novel adaptive mesh smoothing technique for resolving the evolving dopant concentration in the underlying Si substrate involves minimizing an error functional over the volume mesh. The error functional chosen is the L_2 norm of the gradient of the error between the true dopant concentration and the piecewise linear approximation over the tetrahedral mesh. By minimizing the gradient of the error (rather than just the error) we assure that the mesh is optimal for representing evolving solution gradients. This implies correct mesh alignment with the dopant field as well as high quality tetrahedral shapes. Also implemented is constrained boundary smoothing, wherein the moving SiO_2/Si interface is represented by moving nodes that correctly track the interface motion, and which use their remaining degrees of freedom to minimize the aforementioned error functional. This implies optimal tetrahedral shape and alignment is obtained even in the neighborhood of a moving boundary. At each time step, a topological "reconnection" step assures that no negative coupling coefficients are present in the mesh. The combination of adaptive refinement, adaptive smoothing, and mesh reconnection give excellent front tracking, feature resolution, and grid quality for finite volume/finite element computation.

WPB2. Computational Aspects of Topography Evolution During Low Pressure Deposition and Etch Processes, *Timothy S. Cale, Center for Solid State Electronics Research, Department of Chemical, Bio & Materials Engineering, Arizona State University, Tempe, AZ 85287-6206.* Low pressure deposition and etch steps are common in device fabrication. Transport and reaction at low pressures in micron scale features, where species transport through the vacuum is essentially collisionless, is well modeled by the 'ballistic transport and reaction model' (BTRM) [1,2]. The integrodifferential equations which represent the BTRM include terms which express how the ballistic species interact with the surface; i.e., adsorb onto,

react with or re-emit from the surface. The solution of the BTRM equations yields the distributions of the fluxes of ballistic species and surface coverages by physisorbed and/or chemisorbed species over the surface. In turn, these yield rates of surface evolution. Surface evolution is performed using the method of characteristics [3]. In order to perform accurate, predictive topography simulation, submodels for the reaction kinetics, ballistic species flux distributions and surface diffusion of adsorbed species must be established. Although simulations of the processing of most device structures require complete three dimensional transport and surface movement algorithms [4], we have focused on structures for which three dimensional transport and two dimensional surface profile evolution is appropriate. Infinitely long trenches or lines and features of circular horizontal cross section (idealized vias or contact holes) fall into this category. These structures are ideal to establish models for species transport and chemical reactions, because film profiles can be experimentally determined using electron microscopy. Models can be developed and validated by comparing simulated and experimental film profiles. These models can then be used with confidence in deposition and etch process simulations for fully three dimensional surfaces. In this paper, I will review 1) the BTRM, 2) the methods used to solve the governing equations of the BTRM, with and without surface diffusion, and 3) the implementation of the method of characteristics for multiple material substrates.

[1] T.S. Cale and G.B. Raupp, J. Vac. Sci. Tech. B8(4), 649(1990).
[2] T.S. Cale and G.B. Raupp, J. Vac. Sci. Tech. B8(6), 1242(1990).
[3] D. Ross, J. Electrochem. Soc. 135(5) 1235 and 1260 (1988).
[4] H. Liao and T.S. Cale, Thin Solid Films 236(1), 352 (1993).

WPB3. Hierarchical Process Simulation for Nanoelectronics, *Robert W. Dutton, Stanford University Center for Integrated Systems, Stanford, CA 94305.* Over a period of more than two decades the field of process simulation for integrated circuits has become established as an essential enabling technology. Over this same period the critical dimensions for devices have steadily moved from the regime of 10 μm to well below 1.0 μm - the most recent technology papers are pushing the limits of 0.1 μm devices. With dielectric layers below 10 nanometers and junction depths below 100 nanometers, it is certainly safe to say that we are now entering the era of nanoelectronics. The focus of this talk will be to look critically at the recent history of developments in process simulation and to consider the opportunities and challenges facing this new era of IC technology development. The following gives an outline of several topics and results to be discussed. Bulk process simulation relates to transformations of the silicon wafer to create the active devices and it continues to pose many challenges both for simulation and characterization. The topics related to ion implantation, thermal diffusion and oxidation will each be considered both in terms of atomic level effects as well as based on the more traditional continuum models. There is a growing need for and emphasis on first-principles modeling of these bulk processing effects, exactly because of the nanometer scale effects and device requirements. Even where continuum modeling can be applied, there are needs to extract model parameters and understand the interdependence In one sense these issues very much parallel those faced in developing the hierarchy of device simulation models; both the similarities and differences will be considered. Simulation of multi-level interconnections, the back-end of the process, has become a major topic of focus and concern. Both the cost and performance of technology is critically impacted by interconnect technology. In contrast to the front-end or bulk processing, the materials and process physics put a very different set of requirements on the simulators--greater emphasis on surfaces and kinetics of deposition and etching. While the development of such back-end simulators is many years behind that of front-end simulators, there are new opportunities to share both atomic-scale modeling techniques and software infrastructure. Examples will be presented that show very exciting progress to fully bridge the hierarchy from atomic through continuum modeling techniques in this area. Finally, the software engineering and other computational issues related to hierarchical process simulation will be considered. Deep software reconfigurability in support of new and changing problems and numerical techniques is needed to ensure both integrity and timely development on software. With the growing computational demands arising from complex physical definition and full 3D treatment, software in the simulation hierarchy needs to exploit possible parallel and scalable techniques including solver libraries and geometry/grid servers. With our experience with parallelization of the device simulation code, it can be projected that effective use of computers with hundreds of processors will achieve performance levels that can support engineering application of a full hierarchy of process modeling capabilities.

WPB4. A Compound Semiconductor Process Simulator and its Application to Mask Dependent Undercut Etching, *Masami Kumagai and Kiyoyuki Yokoyama, NTT Opto-electronics Laboratories, and Satoshi Tazawa, NTT LSI Laboratories.* A process simulator for the compound semiconductor process is developed. This simulator is designed for describing the etching and deposition processes of compound semiconductors. A block diagram of the simulator is given in Figure 1. It consists of three user-interface modules and three calculation modules. The calculation modules, the "Gas Distribution Module", the "Crystal Orientation Module" and the "Surface Reaction Module", determine the time evolution of the etching and deposition processes. The "Gas Distribution Module" and the "Crystal Orientation Module" supplement the "Surface Reaction Module" and enhance its applications. In compound semiconductor processes, especially in optical device processes, crystal orientation dependence plays an important role. Compound semiconductors, such as GaAs or InP, have anions and cations while Si is made of a single atomic species. This binary nature yields a variety of processed profiles including mesa or reverse mesa shape. In the optical device processes, the mesa and the reverse mesa shape formation is very common and thus detailed representations are required for the process simulation. Figures 2a and 2b give the simulated etching profiles for mesa and reverse mesa faces, respectively. Mesa and reverse mesa shape formation is quite sensitive to process conditions. Figures 3a and 3b show the experimental wet etching profiles for an InP substrate with two different mask materials, SiO2 and SiN, respectively. The SiO2 masked InP shows the large undercut etching and the side faces become throughly mesa shaped, while the SiN masked InP gives lesser undercut etching and the mesa shaped portions are significantly shrunk. This etching process was simulated by using the virtual metamorphic layer model, which employs a thin virtual layer between the mask material and the InP substrate and assumes this layer is changed during the mask deposition process. The simulation results are presented in Figs. 4a and 4b. Good agreement between the Fig.3 and Fig. 4 can be seen. The simulation conditions for 4a and 4b are equivalent except for the etching rate of each metamorphic layer. The etching rate of the metamorphic layer under the SiO2 mask (Fig. 4a) is assumed to be five times that of the substrate material, while that under the SiN mask (Fig. 4b) is assumed to be the same as the substrate material. The mask etching rate is taken to be zero. In summary, the process simulator describes the complicated etching processes on compound semiconductors yielding information about the physical properties of the processes as well as the process conditions for the desired processed shapes. Details of the simulation procedures and further results will be presented by an oral presentation.

WPB5. The Combination of Equipment Scale and Feature Scale Models for Chemical Vapor Deposition via a Homogenization Technique, *M. Gobbert*, T.S. Cale#, and C. Ringhofer*, *Department of Mathematics, Arizona State University, Tempe, AZ 85287-1804; #Center for Solid State Electronics Research, Dept. of Chemical, Bio & Materials Engineering, Arizona State University, Tempe, AZ 85287-6206.* The conformality and composition of deposited films on the scale of device features impact device performance and reliability. Variations of these properties along the wafer during processing lead to unwanted variations in device performance. Thus, an acceptable deposition process provides both average values and across wafer uniformity of conformality and composition within process dependent, specified ranges in addition to an acceptable wafer throughout. In recent years, equipment scale models have successfully been used to establish acceptable operating conditions for existing reactors and to design reactors which provide the necessary across wafer uniformity [1]. More generally, feature scale simulations should be coupled with equipment scale simulations in order to ensure acceptable response, i.e., to predict film properties and uniformity as functions of reactor setpoints. In previous studies, reactor scale simulators have been used to provide the boundary conditions (fluxes) for feature scale simulators [2]. This approach assumes that feature scale processes do not influence the local species concentrations at the wafer surface; i.e., increases in the local deposition area due to topography do not affect film properties. If this is not the case, then the predictions of local film properties can be improved upon by using information from the feature scale simulator in the reactor scale simulator. A truly global simulator would solve feature scale and reactor scale models simultaneously and account for local 'loading' effects due to the presence of topography, when appropriate. In this paper, we present a method for combining the vastly different length scales appropriate for equipment and feature scale simulators based on a homogenization

technique from asymptotic analysis. The reactor scale model is coupled to the surface via a near surface region. The near surface region accounts for surface topography using asymptotic analysis to account for the micro structure of the wafer surface. The equations which govern transport and deposition inside the features are solved simultaneously, and the appropriate species fluxes will be included in the boundary conditions of the near surface region, which are in turn will be used as boundary conditions for the equipment scale equations. This model is capable of predicting the effects of feature aspect ratios and feature spacing on film properties. This approach has been validated mathematically and numerically [3]. We explain the model and discuss predictions of our simulator based on the model by analyzing the deposition of silicon dioxide from tetraethoxysilane (TEOS). In particular, we will discuss the effects of pattern density variations on local film thickness uniformity.

[1] D.W. Studiner, J.T. Hillman, R. Aurora and R.F. Foster, in Advanced Metallization for ULSI Applications 1992, T. S. Cale and F. S. Pintchovski, eds., Materials Research Society, 1993. 211.
[2] T.S. Cale, J.-H. Park, T.H. Gandy, G.B. Raupp and M.K. Jain, Chemical Engineering Communications, 119, 197 (1993).
[3] M.K. Gobbert and C.A. Ringhofer, An asymptotic analysis for a model of chemical vapor deposition on a micro structured surface, submitted.

Attendees

Richard Akis
CSSER
Arizona State University
Tempe, AZ 85287-6206

Angelo Anile
Viala A. Doria 6
Citta Universitaria
95125 Catania,
Italy

Clinton Arokianthan
University of Glasgow
Electronics & Electrical Engineering
Glasgow G128QQ,
Scotland

Anton Arnold
TU-Berlin, FB3, MA 6-2
Strasse d. 17 Juni 1.36
D-10623
Berlin, Germany

Kunihiro Asada
Dept. of Electrical Engineering
University of Tokyo
7-3-1 Hongo
Bunkyo-ku, Tokyo 113,
Japan

Giorgio Baccarani
Universita degli Studi di Bologna
Viale Risorgimento 2
40136 Bologna,
Italy

Fuad Badrieh
CSSER
Arizona State University
Tempe, AZ 85287-6206

Nikolai Bannon
ECE Department
Wayne State University
Detroit, MI 48202

John Barker
Dept. of Electronics & Electrical Engr.
University of Glasgow
Glasgow G128QQ,
Scotland

Timothy Cale
Center for Solid State Electronics Research
Arizona State University
Tempe, AZ 85287-6206

Ming-C. Cheng
Dept. of Electrical Engineering
University of New Orleans
New Orleans, LA 70148

Larry Cooper
Office of Naval Research
800 N. Quincy Street
Arlington, VA 22217-5660

Robert Cottle
Silvaco International
4701 Patrick Henry Drive, Bldg. 3
Santa Clara, CA 95054

Hong-Liang Cui
Dept. of Physics
Stevens Institute of Technology
Hoboken, NJ 07030

Robert Dutton
AEL 203, M/C 4055
Stanford University
Stanford, CA 94305-4055

Gerard Edwards
CSSER
Arizona State University
Tempe, AZ 85287-6206

David K. Ferry
Arizona State University
Dept. of Electrical Engr.
Tempe, AZ 85287-5706

Leonardo Fonseca
SUNY at Stony Brook
Dept. of Applied Mathematics
Stony Brook, NY 11794-3600

Gabriele Formicone
CSSER
Arizona State University
Tempe, AZ 85287-6206

Francisco Gamiz
Departamento Electronica
Universidad Granada
18071 Granada, Spain

Denise George
MS B221
Los Alamos National Lab
Los Alamos, NM 87545

Matthias Gobbert
Dept. of Mathematics
Arizona State University
Tempe, AZ 85287-1804

Neil Goldsman
Electrical Engr. Dept.
University of Maryland
College Park, MD 20742

Stephen Goodnick
Dept. of Electrical Engr.
Oregon State University
Corvallis, OR 97331-3211

Anna Grincwajg
CSSER
Arizona State University
Tempe, AZ 85287-6206

Mathew Grupen
Beckman Institute
University of Illinois
405 N. Mathews Ave.
Urbana, IL 61801

Chihiro Hamaguchi
Dept. of Electronic Engr.
University of Osaka
2-1 Yamada-oka
Suita City, Osaka 565
Japan

Henry Harbury
College of Science Computing Facilities
University of Notre Dame
Notre Dame, IN 46556-5675

Karl Hess
Beckman Institute
University of Illinois
405 N. Mathews Ave.
Urbana, IL 61801

Jack Higman
Motorola
3501 Ed Bluestein Blvd.
MD.K-10
Austin, TX 78721

Carl Huster
1285 EE Blvd., Box 249
Purdue University
West Lafayette, IN 47907-1285

Rimon Ikeno
Dept. of Electronics Engr.
University of Tokyo
7-3-1 Hongo, Bunkyo-ku
Tokyo 113, Japan

Jurgen Jakumeit
Beckman Institute
University of Illinois
405 N. Mathews Ave.
Urbana, IL 61801

Antti-Pekka Jauho
MIC, Tech. Univ. of Denmark
Bldg. 345 East
DK-2800 Lyngby,
Denmark

Joseph Jerome
Northwestern University
2033 Sheridan road
Evanston, IL 60208-2730

Gyoyoung Jin
AEL 204, M/C 4055
Stanford University
Stanford, CA 94305-4055

Dejan Jovanovic
Texas Instruments
13588 N. Central Expressway
M/S 124
Dallas, TX 75243

Juan Bautista Roldan
Departamento de Electronica
Avda. Fuente Nueva
Universidad de Granada
18071 Granada, Spain

Goran Kalblinger
Institute fur Microelectronics
Gusshausstrasse 27-29/E36
A-1040 Vienna, Austria

Ahmed Khamayseh
MS B258
Los Alamos National Lab
Los Alamos, NM 84545

Rahim Khoie
Dept. of Electrical Engr.
University of Nevada, Las Vegas
4505 Maryland Parkway
Las Vegas, NV 89154-4026

Gerhard Klimeck
Texas Instruments, Inc.
P.O. Box 655936
M/S 134
Dallas, TX 75265

Can Koman
Phillips Hall, Room 611
George Washington University
801 22nd St. N.W.
Washington, DC 20052

Alexander Korotkov
Dept. of Physics
SUNY at Stony Brook
Stony Brook, NY 11794-3800

Mitsumasa Koyanagi
Tohoku University
Aramaki, Aoba-ku
Sendai 980-77, Japan

Masami Kumagai
NTT Opto-Electronics Lab
3-1, Morinosato Wakamiya
Atsugi, Kanagawa 243-01
Japan

Andrew Kuprat
T-15, MS K717
Los Alamos National Lab
Los Alamos, NM 84545

Roger Lake
Texas Instruments, Inc.
P.O. Box 655936, MS 134
Dallas, TX 75265

Steven Laux
IBM Research
P.O. Box 218
Yorktown Heights, NY 10598

George Lea
National Science Foundation
4201 Wilson Blvd.
Arlington, VA 22230

Craig Lent
Dept. of Electrical Engr.
University of Notre Dame
Notre Dame, IN 46556

Charles Levermore
Dept. of Mathematics
University of Arizona
Tucson, AZ 85721

Kuok Ling
P.O. Box 1663, MS K717
Los Alamos National Lab
Los Alamos, NM 87545

Paolo Lugli
Walter Schottky Institut
am Coulombwall
D-85748 Garching,
Germany

Massimo Macucci
Dipartimento di Ingegneria
del' Informazione
Universita di Pisa
via Diotisalvi, 2
1-56126 Pisa, Italy

Robert Maier
Dept. of Mathematics
University of Arizona
Tucson, AZ 85721

Meyya Meyyappan
SRA, Inc.
P.O. Box 1058
50 Nye Road
Glastonbury, CT 06033

Hiroshi Mizuta
Electron Devices Res. Dept.
Central Research Lab
Hitachi, Ltd.
1-280 Higashi-Koigakubo
Kokubunji, Tokyo 185
Japan

Jan Mohring
FB Mathematik
University Kaiserslautern
Erwin-Schrodinger-Strasse
D-67653 Kaiserslautern,
Germany

Orazio Muscato
Dipartimento di Matematica
University Catania
Viale A. Doria 6
Catania, Italy

Fabiano Oyajuso
Beckman Institute
University of Illinois
405 N. Mathews Ave.
Urbana, IL 61801

Namsee Pamula
Dept. of Electrical Engr.
University of Nevada, Las Vegas
4505 Maryland Parkway
Las Vegas, NV 89154-4026

Joseph Parks
6640 Akers Mill Rd.
Apt. 17B8
Atlanta, GA 30339

Alfredo Piazza
Phillips Hall, Room 616
George Washington University
801 22nd St. N.W.
Washington, DC 20052

Wolfgang Porod
Dept. of Electrical Engr.
University of Notre Dame
Notre Dame, IN 46556

Mahbub Rashed
Electrical & Computer Engr.
MER-2-606G
University of Texas at Austin
Austin, TX 78712-1100

Umberto Ravaioli
Beckman Institute
University of Illinois
405 N. Mathews Ave.
Urbana, IL 61801

Leonard Register
Beckman Institute
University of Illinois
405 N. Mathews Ave.
Urbana, IL 61801

Salvatore Rinaudo
Co. Ri. M.Me.
Stradale Primosole, 50
985121 Catania,
Italy

Massimo Rudan
University of Bologna
V. Risorgimento 2
40138 Bologna,
Italy

Barbara Sanborn
CSSER
Arizona State University
Tempe, AZ 85287-6206

Nobuyuki Sano
NTT LSI Labs
3-1 Morinosato, Wakamiya
Atsugi, Kanagawa 243-01
Japan

Eckehard Scholl
Inst. F. Theor. Physics,
TU Berlin
Hardenbergstr. 36
10623 Berlin,
Germany

Hai Shao
Computer Science Dept.
Duke University
Box 90124
Durham, NC 27708

Wei-Kai Shih
Elec. & Computer Engr.
MER-2-606G
Univ. of Texas at Austin
Austin, TX 78712-1100

P. Kent Smith
AT&T Bell Labs
600 Mountain Avenue
Murray Hill, NJ 07974

Paul Sotirelis
Texas Instruments, Inc.
13588 N. Central Expressway
MS 134
Dallas, TX 75265

J. P. Sun
EECS Dept.
University of Michigan
Ann Arbor, MI 48109-2122

Ting-Wei Tang
Dept. of ECE
University of Massachusetts
Amherst, MA 01002

Prabaharan Thanikasalam
Dept. of Electrical Engr.
Arizona State University
Tempe, AZ 85287-5706

David Ting
Dept. of Physics
National Tsing Hua University
Hsinchu, Taiwan

Harold Trease
MS B265
Los Alamos National Lab
Los Alamos, NM 87544

Sujeeth Udipi
CSSER
Arizona State University
Tempe, AZ 85287-6206

Dragica Vasileska
CSSER
Arizona State University
Tempe, AZ 85287-6206

Rame Venkatasubramanian
Dept. of Electrical Engr.
University of Nevada, Las Vegas
4505 Maryland Parkway
Las Vegas, NV 89154-4026

Christoph Wasshuber
Institute fur Microelectronics
Gusshausstrasse 27-29/E360
D-1040 Vienna,
Austria

Douglas Yoder
ETH Integrated Systems Lab
Gloriastr. 35
8092 Zurich,
Switzerland